GENETIC EPISTASIS BETWEEN *TRPC6* MUTATION AND NEPHRIN POLYMORPHISMS IN HEREDITARY FOCAL SEGMENTAL GLOMERULOSCLEROSIS

SUN ZI JIN

B.Sc., Shandong Agricultural University

M.Sc., South China Agricultural University

A THESIS SUBMITTED

FOR THE DEGREE OF DOCTOR OF PHILOSOPHY

DEPARTMENT OF PAEDIATRICS

NATIONAL UNIVERSITY OF SINGAPORE

2013

THIS THESIS IS DEDICATED TO:

MY FAMILY MEMBERS FOR THEIR SUPPORT

AND UNDERSTANDING

DECLARATION

I hereby declare that this thesis is my original work and it has been written by me in its entirety. I have duly acknowledged all the sources of information which have been used in the thesis.

This thesis has also not been submitted for any degree in any university previously.

_____

SUN ZI JIN
7 August 2013

ACKNOWLEDGEMENTS

I would like to express my sincere gratitude to my supervisor Professor Yap Hui Kim for giving me the opportunity to pursue my postgraduate studies in the Department of Paediatrics. I am deeply indebted for her invaluable advice, continuous encouragement and inspiration throughout these years.

I would like to thank Assistant Professor Ng Kar Hui for her technical suggestions and devoted efforts in proofreading my manuscripts.

I would like to thank my co-supervisor Dr Liao Ping from National Neuroscience Institute (NNI) for his expert advice on my electrophysiology studies.

My deep appreciation also goes to Professor Soong Tuck Wah from Department of Physiology (NUS) for his invaluable advice and support when I was doing experiments in his laboratory.

In addition, my sincere thanks to all my laboratory members for their help, especially Ng Jun Li, Chan Chang Yien, Lauretta Low, Seah Ching Ching, Liang Ai Wei. Special thanks to Dr Zhang Yaochun for his help on biotinylation assay and Co-IP studies. Thanks for all the friendly and nice people from Prof Soong Tuck Wah's lab.

Last but not least, I would like to extend my appreciation to my family for their continuous support and encouragement.

This work was supported by a research grant from the National Medical Research Council, Singapore (Grant Number: NMRC EDG07nov033 and NMRC/1236/2009from 2009)

TABLE OF CONTENTS

SUMMARY

Focal segmental glomerulosclerosis (FSGS) is the most common cause of therapy-resistant nephrotic syndrome in children worldwide. Transient Receptor Potential Cation Channel, subfamily C, member 6 (*TRPC6*) is a calcium channel which interacts with nephrin (*NPHS1*) and podocin (*NPHS2*) in podocytes. Mutations in *TRPC6* cause familial FSGS. The primary aim of this thesis is to investigate the function of a novel *TRPC6* mutation identified in an index family with hereditary FSGS, as well as the interactions between this *TRPC6* mutation and polymorphisms identified in other podocyte genes, namely *NPHS1* and *NPHS2*. Chapter 1 is a comprehensive literature review on our current understanding of nephrotic syndrome, FSGS and their pathogenesis, as well as the structure, function and regulation of *TRPC6*. Chapter 2 is the "Materials & Methods" section which outlines the principles of all the experimental procedures used in this study. The complete protocols of some experimental procedures are described in detail in the "Appendix" section. In chapter 3, we screened for podocyte gene variants in the index family, as well as in patients with sporadic steroid-resistant or steroid-dependent nephrotic syndrome or FSGS, and validated these in healthy controls. We identified a novel mutation p.R68W and a polymorphism c.-254C>G in *TRPC6* gene in the Singapore Chinese index family. Meanwhile, we found two *NPHS1* polymorphisms, c.294C>T and c.2289C>T, and one *NPHS2* polymorphism c.954T>C which segregated with renal disease. In chapter 4, we examined the function of the novel *TRPC6* mutation p.R68W through whole-cell patch clamp method. We confirmed it is a gain-of-function mutation. In addition, we showed that this mutation enhanced its surface expression by biotinylation assay. In chapter 5, we explored the effects of *NPHS1* and *NPHS2* polymorphisms on *TRPC6* activity by co-transfection of the variants into cells and measurement of the *TRPC6* currents. We showed that wild-type *NPHS1* and *NPHS2* down-

regulate *TRPC6* activity; whereas the presence of *NPHS1* polymorphism c.294C>T resulted in the loss of this down-regulation activity. The other polymorphisms did not alter *TRPC6* currents. We showed that the polymorphisms, including *NPHS1* c.294C>T, did not alter physical binding between *TRPC6* and *NPHS1* as shown by our co-IP studies. Chapter 6 is a follow-up study focusing on the mechanism of action of the *NPHS1* polymorphism *c.294C>T*. Our results showed this synonymous polymorphism decreased nephrin protein expression. We further proved via real-time PCR that this decreased protein expression was caused by decreased mRNA stability. Chapter 7 is an overall summary and conclusion of this study.

LIST OF ABBREVIATIONS

AA	Arachidonic acid
ACTN4	Alpha actinin 4
ANK	Ankyrin-like repeats
APS	Ammonium persulphate
BSA	Bovine serum albumin
CaM	Calmodulin
CD2AP	CD2-associated proteins
cDNA	Complementary deoxyribonucleic acid
CNF	Congenital nephrotic syndrome of the Finnish type
CNI	Calcineurin inhibitors
CNS	Congenital nephrotic syndrome
Co-IP	Co-immunoprecipitation
Cp	Crossing point
CsA	Cyclosporine A
C-terminus	Carboxyl-terminus
DAG	Diacylglycerol
DAGK	DAG kinase
ddH_2O	Double distilled water
DEPC	Diethyl pyrocarbonate
DMEM	Dulbecco's Modified Eagle Medium
DMS	Diffuse mesangial sclerosis
DNA	Deoxyribonucleic acid
dNTPs	Deoxynucleotide triphosphates

E.coli	*Escherichia coli*
EDTA	Ethylenediaminetetraacetic
ESE	Exon splicing enhancer
ESRD	End stage renal disease
ESS	Exon splicing silencer
F-actin	Filamentous actin
FBS	Foetal bovine serum
FGS	Focal global sclerosis
FMPGN	Focal mesangial proliferative glomerulonephritis
FSGS	Focal segmental glomerulosclerosis
GBM	Glomerular basement membrane
gDNA	Genomic DNA
GFP	Green fluorescence protein
GN	Glomerulonephritis
HBSS	Hanks' Balanced Salt solution
HEK	Human embryonic kidney
HEPES	*N*-2-hyroxyethylpiperazine-*N*'2-ethanesulponic acid
HRM	High resolution melting
IFN	Interferon
Ig	Immunoglobulin
IgAN	IgA nephropathy
IP_3	Inositol 1,4,5-triphosphate
IQGAP-1	IQ motif–containing GTPase-activating protein 1
ISKDC	International Study of Kidney Diseases in Children
kb	Kilo base pairs (nucleotide)

LB	Luria-Bertani
M1 mAChR	M1 muscarinic acetylcholine receptors
MCNS	Minimal change nephrotic syndrome
M-MLV	Moloney murine leukemia virus
MPGN	Membranoproliferative glomerulonephritis
mRNA	Messenger ribonucleic acid
NEPH1	Nephrin homolog 1
NS	Nephrotic Syndrome
N-terminus	Amino-terminus
nt	Nucleotides
NUH	National University Hospital of Singapore
OAG	1-oleoyl-2-acetyl-sn-glycerol
OD	Optical density
p	p-value
P-cadherin	Proto-cadherin
PAGE	Polyacrylamide gel electrophoresis
PBS	Phosphate buffered saline
PCR	Polymerase chain reaction
PI3K	Phosphoinositide 3-OH kinase
PLC	Phospholipase C
PKC	Protein kinase C
PMA	Phorbol-12-myristoyl-13-acetate
RNA	Ribonucleic acid
RT	Reverse transcription
RT-PCR	Reverse transcription – polymerase chain reaction

SD	Slit diaphragm
SDS	Sodium dodecylsulphate
SDNS	Steroid dependent nephrotic syndrome
SGVP	Singapore Genome Variation Project
SH2	Src homology 2
SNP	Single nucleotide polymorphism
SRNS	Steroid-resistant nephrotic syndrome
SSNS	Steroid-sensitive nephrotic syndrome
suPAR	Serum soluble urokinase plasminogen activator receptor
TALENs	Transcription activator-like effector nucleases
TBE	Tris borate EDTA
TBS	Tris buffered saline
TE	Tris-EDTA
T_m	Melting temperature
TEMED	Tetramethylethylenediamine
TRP	Transient receptor potential
TRP6	Transient receptor potential cation channel, subfamily C, member 6
UTR	Untranslated region
VGCC	Voltage-gated Ca^{2+} channels
WT	Wild-type
WT-1	Wilms' tumor - 1
ZO-1	Zonula occludens-1

LIST OF TABLES

LIST OF FIGURES

LIST OF APPENDIECS

LIST OF PUBLICATIONS AND CONFERENCE ABSTRACTS

ORAL PRESENTATION

1. SUN*, Z J, P LIAO, K H NG, J L NG, T W Soong, Isaac LIU and H K Yap, "Successful renal transplant from donor with *TRPC6* mutation may be explained by interactions between *TRPC6* and nephrin single nucleotide polymorphisms". *The YLL SoM-Graduate Scientific Congress 2011 Abstract book* (2011)

2. NG*, K H, Z J SUN, P LIAO, J L NG, T W Soong and H K Yap, "A novel *TRPC6* gain-of-function mutation may cause focal segmental glomerulosclerosis through altered interactions with podocin and nephrin". *4th Scientific Meeting of Advanced Specialty Trainees in Nephrology* (Invited paper) (2009) (Tan Tock Seng Hospital, Singapore)

POSTER PRESENTATION

3. Liu*, I, SY Tay, K H NG, J L NG, Z J SUN, S S Chong and H K Yap, "A Novel Mutation in *TRPC6* is Associated with Autosomal Dominant Focal Segmental Glomerulosclerosis (AD FSGS)". *Annals of the Academy of Medicine Singapore* (2007).

4. SUN*, Z J, J L NG, K H NG, Ping Liao, Isaac Liu, T W Soong and H K Yap, "NEPHRIN SINGLE NUCLEOTIDE POLYMORPHISMS PARTICIPATE FOCAL SEGMENTAL GLOMERULORSCLEROSIS CAUSED BY *TRPC6* MUTATION". *YLLSoM 2nd Annual Graduate Scientific Congress*: 77, P040 (2012)

5. SUN*, Z J, P LIAO, K H NG, J L NG, I Liu, T W Soong and H K Yap, "A novel *TRPC6* gain-of-function mutation may cause focal segmental glomerulosclerosis through altered interactions with podocin and nephrin". *NHG Annual Scientific Congress* (2009)

PUBLISHED PAPER

6. Ng K H, Z J Sun, Ping Liao, Y C Zhang, J L NG, Isaac Liu, P H Tan, S S Chong, Y H Chan, J J Liu, Sonia Davila, C K Heng, T W Soong, HK Yap, " Successful renal Transplant from Donor with *TRPC6* Mutation explained by Genetic Epistasis between *TRPC6* mutation and *NPHS1* Polymorphisms" (submitted)

CHAPTER 1 INTRODUCTION

1.1 Nephrotic Syndrome

1.1.1 Definition of Nephrotic Syndrome

Nephrotic syndrome is characterized by generalised edema, nephrotic-range proteinuria, hypoalbuminemia (serum albumin <25g/L), and hyperlipidemia. Nephrotic-range proteinuria has been defined as urinary protein excretion ≥3 g/day/1.73m^2 or a spot urinary protein: creatinine ratio ≥0.2 g/mmol (Yap and Lau 2008).

The unifying pathomechanism of nephrotic syndrome involves structural and functional defects in the glomerular filtration barrier, resulting in its inability to restrict urinary loss of protein.

1.1.2 Classification and Etiologies of Nephrotic Syndrome

Nephrotic syndrome may be primary or secondary. Primary nephrotic syndrome can be classified based on histology (Table 1-1). The commonest cause of primary nephrotic syndrome in children is minimal change nephrotic syndrome (MCNS). MCNS frequently occurs between 18 months and 4 years of age (Zhu *et al.* 2009). By definition, there are no abnormalities of kidney biopsy specimens on light microscopy, but effacement of the podocyte foot processes can be seen on electron microscopy (van den Berg *et al.* 2004).

Other causes of primary nephrotic syndrome include focal segmental glomerulosclerosis, mesangial proliferative glomerolonephritis (GN) and membranoproliferative GN. Secondary nephrotic syndrome may be due to systemic diseases (eg. lupus), drugs, viruses and physical agents (Table 1-1).

Table 1-1 Common Causes of Primary and Secondary Nephrotic Syndrome

Primary Nephrotic Syndrome (75%)

- Minimal change nephrotic syndrome- the most common cause in children (Filler *et al.* 2003)
- Focal segmental glomerulosclerosis- the most common cause of idiopathic nephrotic syndrome in adults (Kitiyakara *et al.* 2003)
- Membranous GN
- Membranoproliferative GN
- Mesangioproliferative GN
- Immunotactoid and fibrillary GN

Secondary /Systemic Nephrotic Syndrome (25%)

- Diabetes mellitus, systemic lupus erythematosus, amyloidosis, HIV-associated nephropathy
- Drugs: gold, penicillamine, probenecid, street heroin, captopril, NSAIDs
- Infections: bacterial endocarditis, hepatitis B, shunt infections, syphilis, malaria, hepatic schistosomiasis
- Malignancy: multiple myeloma, light chain deposition disease, Hodgkin's and other lymphomas, leukemia, carcinoma of breast or gastrointestinal tract

Children with primary nephrotic syndrome are often empirically treated with a course of steroids. Nephrotic syndrome can also be classified based on their responses to steroid treatment as steroid-sensitive nephrotic syndrome (SSNS) or steroid-resistent nephrotic syndrome (SRNS). Within the steroid-sensitive group, some patients are dependent on chronic steroids to prevent recurrent relapses, and therefore have steroid-dependent nephrotic syndrome (SDNS). A proportion of these have frequent relapses, and are classified as frequent-relapsing nephrotic syndrome (FRNS) (Denis F. Geary and Schaefer. 2008). Up to 70% of children with MCNS have multiple relapses. Half of these patients will require long-term steroid therapy or cytotoxic drugs, and they may suffer from their adverse effects such as short stature, cataracts and malignancy.

1.1.3 Epidemiology of Nephrotic Syndrome

Primary nephrotic syndrome accounts for 75% of all cases in children (Table 1-1). Among them, the three most common diseases, minimal change nephrotic syndrome (MCNS), focal segmental glomerulosclerosis (FSGS) and membranous glomerulonephritis (GN), account for 58.4% of all cases (Nasir. *et al.* 2012). FSGS consistently accounts for 36-39% of all cases in children, adults, and the elderly (Nair *et al.* 2004).

The reported incidence of nephrotic syndrome in children is estimated at 2 to 7 cases per 100,000 per year, and this is about 15 times higher than adults (Hogg *et al.* 2000). There is a male preponderance among young children at a male : female ratio of 2:1, whereas in older people, both sexes are equally affected (Denis F. Geary and Schaefer. 2008). In addition, epidemiology appears to differ according to geographic and racial differences. For example, the prevalence of MCNS, mesangioproliferative GN, and membranous glomerulonephritis are distinctly different in Thailand, China and Italy (Kirdpon *et al.* 1989; Huang *et al.* 2001; Gesualdo *et al.* 2004). Even within a country, the epidemiology among various races or ethnicity differs. For example, the prevalence of the different histological types of nephrotic symdrome differs among the blacks, Indians, and mixed race children in South Africa (Bhimma *et al.* 1997).

1.2 Focal Segmental Glomerulosclerosis (FSGS)

FSGS is a histological diagnosis in which sclerosis occurs in some, but not all, glomeruli (focal), and the sclerosis affects a portion of, but not the entire glomerular tuft (segmental) (Figure 1-1). The unscarred glomeruli may appear normal, but glomerular enlargement is characteristic of primary FSGS in both adults and children (Nyberg *et al.* 1994; Suzuki *et al.* 1994). FSGS affects initially the glomerulus, followed by the tubulointerstitium and renal

vessels (Meyrier 2005). FSGS is characterized clinically by nephrotic syndrome and is often steroid-resistant. In addition, a significant proportion of these patients go on to develop renal failure (Thomas *et al.* 2006).

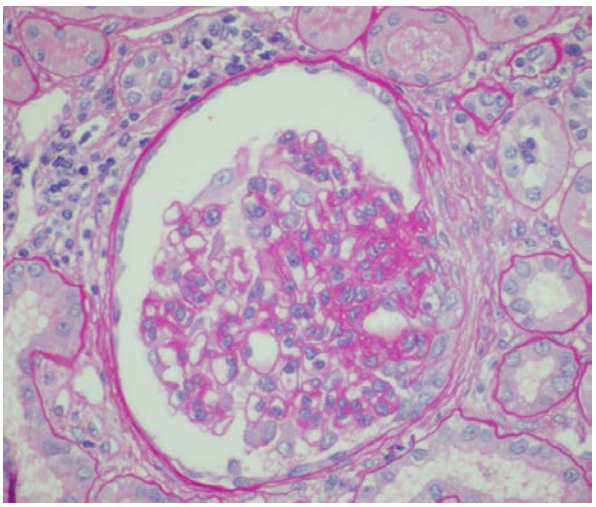

Figure 1-1 Focal Segmental Glomerulosclerosis.

Light microscopy of a human kidney showing a glomerulus with a dense segmental scar adherent to the Bowman's capsule.

1.2.1 Classification of FSGS

FSGS, like nephrotic syndrome, can be divided into primary (idiopathic) FSGS and secondary FSGS. Primary FSGS is a clinicopathologic diagnosis. The pathologic diagnosis requires a glomerular lesion that falls within the morphologic spectrum of FSGS, and there must be no evidence of an antecedent glomerulonephritis (Jennette *et al.* 2007). Secondary FSGS may be caused by drugs, viruses, immunologic diseases and physical agents. This etiologic diversity emphasizes that FSGS is a nonspecific pattern of glomerular injury. The secondary forms of FSGS may be divided into those in which podocyte injury is the main inciting factor and those caused by other mechanisms (Rennke and Klein 1989).

Five histological variants of FSGS have been described: collapsing, cellular, tip lesion, perihilar and not-otherwise-specified (NOS) (D'Agati 2003; Thomas *et al.* 2006) (Table 1-2). Some of these histological subtypes are more commonly associated with specific etiologies. For example, perihilar forms of FSGS are more common in adaptive FSGS associated with obesity, reflux nephropathy or hypertensive nephrosclerosis (D'Agati *et al.* 2011).

Table 1-2 Histologic Variants of FSGS

Type	**Defining features**
FSGS, not otherwise specified(NOS)	Discrete segmental sclerosis
FSGS, perihilar variant	Perihilar sclerosis and hyalinosis
FSGS, cellular variant	Endocapillary hypercellularity
FSGS, tip variant	Sclerosis at tubular pole with adhesion at tubular lumen/neck
FSGS, collapsing variant (Collapsing glomerulopathy)	Segmental or global collapse and podocyte hypertrophy

1.2.2 Epidemiology of FSGS

FSGS is the most common glomerular disease in adults worldwide. In children, it is the second most common glomerular disease after MCNS. The proportion of nephrotic patients with FSGS varies from 10% to 78% in different countries and geographic regions. The prevalence of FSGS in African American adults with nephrotic syndrome is among the highest in the world (56% to 78%) (Eddy and Symons 2003; Mollet *et al.* 2009). In contrast,

about 20% of Caucasian adult patients in the United States and Europe with nephrotic syndrome have FSGS (Haas *et al.* 1995; Korbet *et al.* 1996; Haas *et al.* 1997).

FSGS is the most common cause of therapy-resistant nephrotic syndrome in children worldwide. In children, FSGS accounts for 63–73% of patients with SRNS (Ruf *et al.* 2004; Gbadegesin *et al.* 2007). In adults, approximately 30–50% patients with FSGS do not respond to steroid therapy. About 30-40% of patients with FSGS progress to end-stage renal disease (ESRD) within ten years of diagnosis (Cattran and Rao 1998; Mekahli *et al.* 2009). The proportion of ESRD attributed by FSGS has increased more than 10-fold over the past two decades (Srivastava *et al.* 1999; Kitiyakara *et al.* 2004), especially in African Americans. FSGS now accounts for 12.2% of incident pediatric patients with ESRD in the United States (Kitiyakara *et al.* 2003; Kitiyakara *et al.* 2004; 2012).

1.2.3 Clinical Course and Prognosis of FSGS

FSGS is distinguished clinically from MCNS by significantly poorer responses to steroid therapy, hematuria, hypertension and renal insufficiency (Habib 1973). FSGS is the most common cause of therapy-resistant nephrotic syndrome in children worldwide. The initial empirical treatment of primary nephrotic syndrome in children consists of prednisolone 60 mg/day per $1.73m^2$ (up to 80 mg/day) given for 4 weeks, followed by 40 mg/day per $1.73m^2$ (up to 60 mg/day) given every other day for 4 weeks, and then tapered off over the next 4 weeks. A multicentre International Study of Kidney Diseases in Children (ISKDC) study performed on more than 521 children with idiopathic NS revealed that approximately 80% of children with idiopathic nephrotic syndrome respond to steroid therapy. Interestingly, 93% of these steroid-responsive children had MCNS and only 30% of them had FSGS (Orsini and

Boscherini 1961; ISKDC 1981). The complete remission rate for children with primary FSGS using this treatment protocol is between 20 and 25% (Korbet *et al.* 1994)(24,26). Indeed, the initial response to steroid therapy is an important FSGS prognostic indicator. Those with steroid-resistant FSGS are more likely to progress to ESRD.

The severity of proteinuria at presentation is most often used to predict the clinical course in FSGS. The presence of nephrotic-range proteinuria (>3 to 3.5 g/24 h) has consistently been associated with a poor outcome in primary FSGS, with 50% of patients reaching (ESRD) within 6 to 8 years (Beaufils *et al.* 1978; Cameron *et al.* 1978; Korbet *et al.* 1994; Rydel *et al.* 1995). An additional clinical feature with prognostic significance is the serum creatinine level at presentation. A serum creatinine of >1.3 mg/dL is associated with significantly poorer renal survival regardless of the severity of proteinuria (Korbet 1998).

1.2.4 Pathogenesis of FSGS

The precise pathogenesis of FSGS remains incompletely understood. Generally speaking, FSGS stems from relative or absolute podocyte depletion or changes to its functional integrity. Broadly speaking, this podocyte damage in primary FSGS may be divided into two causes: genetic mutations involving podocyte-related genes (genetic FSGS) and circulating immune factors (immune FSGS). For secondary FSGS, humoral factors or hemodynamic injury from hyperfiltration of the glomeruli, or immune-mediated injury from systemic immunologic diseases are some of the factors that can cause damage to the podocytes.

Podocyte injury

FSGS is now widely accepted as a disease caused by podocyte damage (D'Agati 2008). The clinical signatures of podocyte injury include proteinuria and glomerular scarring, leading to reduced kidney function (Shankland and Pollak 2011). Podocytes in FSGS undergo cell

injury and loss of functional integrity and structural stability. This has been shown in renal biopsy studies in patients with primary FSGS (Schwartz and Korbet 1993), recurrent FSGS in transplants (Verani and Hawkins 1986; Korbet *et al.* 1988), and HIV-associated FSGS (Cohen and Nast 1988). For example, in collapsing glomerulopathy and HIV-associated nephropathy, loss of mature podocyte differentiation markers (WT-1, CALLA, C3b receptor, GLEPP-1, podocalyxin, and synaptopodin) and increased podocyte proliferation have been demonstrated (Barisoni *et al.* 1999).

The decrease in the number of podocytes, as the initiating factor in FSGS, results in the inability of podocytes to completely cover the glomerular capillaries. This then leads to the formation of synechiae or adhesions between the glomerular capillaries and the Bowman's capsule. The filtrate from the capillaries in the tuft adhesion then enters the interstitium instead of into Bowman's space. This misdirected filtration finally leads to progression of segmental injury, tubular degeneration, and interstitial fibrosis (Gbadegesin *et al.* 2011).

Genetics

Studies of familial FSGS have demonstrated mutations in podocyte proteins that are critical in forming and maintaining the glomerular filtration barrier. Mutations in podocyte genes, like *NPHS1* (nephrin), *NPHS2* (podocin), *CD2AP*, *ACTN4* (α-actinin 4) (Pollak 2003), and *TRPC6* (Reiser *et al.* 2005; Winn *et al.* 2005) have been implicated in glomerular disease in human beings. The fact that mutations in these genes are disease-causing suggests that these molecules are necessary for glomerular function, and the integrity of the podocyte and its slit diaphragm complex (Jennette *et al.* 2007).

Humoral factors

The response to immunosuppressive drugs in FSGS patients is powerful circumstantial evidence in favor of a pathogenetic role of the immune system. Humoral factors are discussed below in three categories: immunoglobulins, non-immunoglobulin lymphocyte products, and the circulating factors identified in patients with recurrent FSGS.

Immunoglobulins The lesions of FSGS may contain immunoglobulins (principally IgM), complement components, and other serum proteins. It was found that the distribution of immunopathology in FSGS is also focal and segmental (Tejani *et al.* 1983; Faubert and Porush 1997; Conlon *et al.* 1999). The deposits, usually IgM in combination with C3, conform to the sclerotic segment without an obvious granular or linear pattern (Faubert and Porush 1997). Similar deposits in glomerular scars in non–immune-mediated diseases such as hypertension, diabetes, and secondary FSGS of diverse causes suggest that the immunoglobulins are nonspecifically trapped in glomerular scars (Jennette *et al.* 2007). In experimental animals, antibodies against podocyte antigens cause accelerated glomerular sclerosis and FSGS (Gubler 2003), but these proteins have not been identified as antigenic targets in primary FSGS, and there is no clinical or experimental evidence to support a direct role for antibodies in the pathogenesis of primary FSGS in human beings.

Cytokines and Growth Factors Studies in biopsies from patients with FSGS have shown impairment of cell-mediated immunity (Matsumoto *et al.* 1983; Matsumoto *et al.* 1988), activation of the fibrogenic TGF-β/Smad signal transduction pathway in podocytes (Schachter *et al.* 2000; Schiffer *et al.* 2002; Kim *et al.* 2003), and up-regulation of fibrogenic PDGFR-β and βFGF in a segmental glomerular distribution and in the interstitium (Stein-

Oakley *et al.* 1997). Experimental studies in the remnant kidney and other models of glomerulosclerosis have implicated a number of cytokines and growth factors in the pathogenesis of glomerular scarring and progression of renal disease (Schiffer *et al.* 2001; Choi *et al.* 2003; Fogo 2003). These studies along with the presence of elevated levels of cytokines in the peripheral blood of patients with FSGS support a mechanism by which injured glomeruli progress to fibrous scars. However, there is no evidence that cytokines or growth factors initiate glomerular injury in primary FSGS in human beings.

Circulating Factor The pathogenicity of circulating factors was demonstrated in experimental animals: serum or plasma from patients with recurrent FSGS could increase glomerular permeability (P_{alb}) of glomeruli isolated from normal rats and that plasmapheresis decreased the serum activity of P_{alb} (Savin *et al.* 1996). Injection of whole serum from patients with collapsing glomerulopathy into mice led to the mice developing glomerular enlargement, focal segmental and global collapse, podocyte hypertrophy and diffuse foot process effacement (Avila-Casado Mdel *et al.* 2004). Coward et al showed that plasma from nephrotic FSGS patients caused redistribution of slit diaphragm proteins, such as nephrin, podocin, CD2AP and actin, from the cell membranes of cultured human podocytes to a diffuse cytoplasmic distribution (Coward *et al.* 2005).

Recent research identified soluble urokinase plasminogen activator receptor (suPAR) as a possible circulating factor. Serum suPAR was elevated in patients with primary FSGS and it can activate podocyte β3 integrin, leading to FSGS pathology (Shankland and Pollak 2011; Wei *et al.* 2011). The rapid recovery of allograft function after retransplantation also supports the theory (Gallon *et al.* 2012). However, suPAR is not a specific marker for idiopathic FSGS

and it does not reliably predict response to treatment (Maas *et al.* 2012). Therefore, it is believed that there are other FSGS circulating factors that are yet to be identified.

Hemodynamic injury

Glomerular hemodynamic changes are implicated in the pathogenesis of FSGS through studies in both animal models and humans. The increase in glomerular capillary pressure is important in generating pathologic changes. For example, animals who have undergone subtotal nephrectomy (remnant kidney model) develop segmental glomerular scars, proteinuria, and progressive renal disease. This is accomplished in part by elevation of the transcapillary pressure gradient resulting in compensatory hyperfiltration (Hostetter *et al.* 1981), supporting the primary role for glomerular capillary hypertension in the pathogenesis of progressive glomerular disease (Hostetter 2003). Angiotensin-converting enzyme inhibitors and aldosterone receptor blockers that lower intraglomerular capillary pressure therefore have been shown to prevent the progression of FSGS as they reduce glomerular hypertension (Korbet 2003).

Glomerular hypertrophy

Shea et al first suggested that glomerular hypertrophy preceded the development of sclerosis in the model of renal ablation (Shea *et al.* 1978). Several studies that were designed to separate the effects of hypertrophy from hemodynamic injury in the remnant kidney model concluded that glomerular hypertrophy was necessary for glomerular sclerosis to occur (Fries *et al.* 1989; Yoshida *et al.* 1989). Furthermore, patients with minimal change disease and enlarged glomeruli were more likely to develop FSGS on a second biopsy, suggesting that hypertrophy is a factor in the pathogenesis of FSGS (Fogo *et al.* 1990). However, when

glomerular hypertrophy in the remnant kidney model is separated from the effects of hypertension in rats genetically resistant to the development of hypertension, the animals do not develop progressive glomerular injury or nephron loss (Bidani *et al.* 1990; Schwartz and Bidani 1993).

1.3 Pathophysiology of the Glomerular Podocyte

1.3.1 The Glomerular Filtration Barrier

The glomerulus located within the Bowman's capsule at the kidney cortex is the main filter of the nephron. Blood flows through the glomerular capillaries where it is filtered by pressure. The glomerulus is a twisted mass of capillaries consisting of four cell types: endothelial cells, mesangial cells, parietal epithelial cells and visceral epithelial cells which are known as podocytes (Figure 1.2). The glycocalyx-coated fenestrated endothelial cells form a porous layer and are in direct contact with blood, restricting cell passage across the capillary wall and play a minor role in restriction of macromolecular transport (Jennette *et al.* 2007). The mesangial cells reside within the central axial supporting mesangial matrix and together with matrix constitute the mesangium. The parietal epithelial cells line the epithelium of the Bowman’s capsule facing the urinary space while the podocytes line the visceral epithelium of the urinary space. The fenestrated endothelium, the glomerular basement membrane (GBM) and the podocytes together form the filtration barrier in the glomerulus. This limits the outflow of large molecules, including albumin, from the blood capillaries to the urinary space.

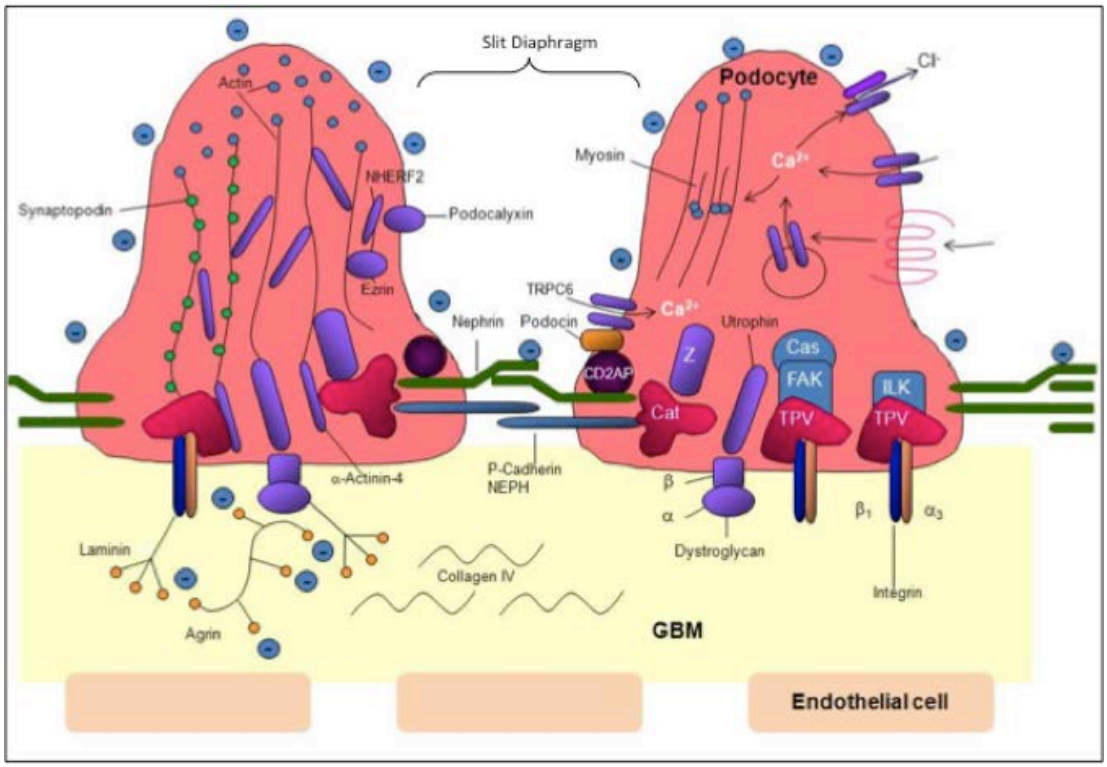

Figure 1-2 The Glomerular Filtration Barrier.

Two podocyte foot processes, the glomerular basement membrane (GBM) and the porous capillary endothelium. The slit diaphragm connects the podocyte foot processes. The slit diaphragm-associated molecules include nephrin, podocin, *CD2AP*, *TRPC6* and *NEPH*. The GBM is composed of the collagen type IV, laminin and heparan sulphate proteoglycan agrin. Integrins are heterodimeric transmembrance receptors which specifically connect the TVP complex (talin, vinculin and paxillin) to laminin. The α and β dystroglycans connect utrophin to agrin. (Adapted from: Kriz, W. 2005. *TRPC6* - a new podocyte gene involved in focal segmental glomerulosclerosis. *Trends Mol Med*, 11, 527-30 (Kriz 2005))

1.3.2 Structure and Function of the Podocyte

Podocytes are highly specialized and terminally differentiated epithelial cells that line the outer surface of the GBM. They serve to maintain the glomerular architecture and bar the egress of plasma-derived proteins through the slit diaphragm (Haraldsson *et al.* 2008; Meyrier 2011). Podocytes are made up of three morphological and functionally different segments, the cell body (CB), the major processes (MP), and the foot processes (FP). The cell body containing nucleus and other major organelles such as rough endoplasmic reticulum is usually located within a valley created by the reflection of adjacent capillary loops. The

major processes extend from the cell bodies and participate in cell trafficking. The foot processes are derived from the splitting of the major processes and consist of an actin cytoskeleton which is linked to the GBM in focal contacts. They form a tight interdigitating network with their neighbouring podocyte foot processes through a continuous membrane-like structure known as the slit diaphragm (SD) (Mundel and Kriz 1995). The foot processes are dynamic structures that can respond to changing hydrostatic pressures and other environmental factors by continuous reorganization of their cytoskeletons (Kim *et al.* 2003; Reiser *et al.* 2005; Winn *et al.* 2005).

1.3.3 The Slit Diaphragm

The slit diaphragm (SD) is a modified adherens junction that connects adjacent podocyte foot processes to form a tight interdigitating network. The role of the SD is to maintain the structure of the foot processes and regulate the selectivity of the glomerular filtration barrier (Figure 1-2). It shares some typical morphological features with an adherens junction, such as wide intercellular gap and presence of a central dense line in grazing sections (Reiser *et al.* 2000). The three-dimensional molecular architecture of the SD observed under electron microscopy revealed that it is made up of a convoluted network of irregularly shaped pores emanating from a central dense region (Wartiovaara *et al.* 2004).

Several molecules associated with the SD have been identified. The first reported molecule was *ZO-1*, which is located at the point of insertion of the SD (Schnabel *et al.* 1990). Nephrin and P-cadherin are the main protein components of the SD (Patrakka *et al.* 2000; Reiser *et al.* 2000). Other SD molecules include podocin, Neph 1, *FAT*, *TRPC6* (will be discussed in section 1.4) and CD2-associated proteins (*CD2AP*) linked to the actin cytoskeleton (Reiser *et al.* 2000; Schwarz *et al.* 2001).

Table 1-3 Common genes implicated in inherited nephrotic syndrome/FSGS

Name	Associated disorder	Chromosomal location	Pattern of inheritance	Clinical features	Structure/function	References
Nephrin	Congenital nephrotic syndrome of the Finnish type	19q13	AR	Massive proteinuria in utero with high mortality rate	Transmembrane adhesion protein localizes to lipid rafts within the slit diaphragm of the podocyte	(Kestila *et al.* 1994; Kestila *et al.* 1998; Lenkkeri *et al.* 1999)
Podocin	Steroid resistant nephrotic syndrome	1q25–31	AR	Proteinuria between 3 months and 5 years of age with rapid progression to ESRD	Structural protein that recruits nephrin and CD2AP to lipid rafts in the slit diaphragm	(Fuchshuber *et al.* 1995)
Alpha-actinin 4	Hereditary FSGS	19q13	AD	Adult onset FSGS with variable age of onset, severity, and progression to ESRD	Actin-binding protein that binds actin to the cell membrane of the podocyte	(Kim *et al.* 2003)
Transient Receptor Potential Cation channel 6	Hereditary FSGS	11q21–22	AD	High grade proteinuria in 3rd to 4th decade with ESRD in 60% within 10 years of diagnosis	Relatively non-selective cation channel that associates with nephrin, podocin, and CD2AP at the slit diaphragm	(Winn *et al.* 2005)
CD2-associated protein	FSGS	6p12	Haplo-insufficiency	FSGS	Scaffold protein that interacts with the cytoplasmic domain of nephrin	(Kim *et al.* 2003)
APOL1	FSGS	22q13.1	AD	strong association with FSGS and HIVAN among African Americans.		(Papeta *et al.* 2011)
INF2	FSGS	14q32-33	AD	FSGS	a member of the formin family of actin regulating proteins	(Brown *et al.* 2010)

1.3.4 Genes Implicated in FSGS

Recent studies in hereditary forms of nephrotic syndrome had led to the identification of several podocyte genes and this has increased our understanding of podocyte biology. To date, all causative genes found in hereditary FSGS are located to the podocyte and many of them are found in the SD. This further confirms the importance of the SD in the function of podocytes. The podocyte-related genes involved in inherited nephrotic syndrome or FSGS are listed below (Table 1-3).

Nephrin

Human nephrin is encoded by the *NPHS1* gene which consists of 1241 amino acids and is located on chromosome 19 (location: 19q13.1). It is a transmembrane protein with 29 exons (Gene Bank Accession Number: NM_004646). Nephrin is detected in the kidney, different regions of the brain and in the pancreatic β-cells. Within the kidney, nephrin is exclusively expressed in podocytes and predominantly localized to the SD (Kestila *et al.* 1998; Putaala *et al.* 2001). It has an N-terminal signal peptide, followed by an extracellular domain containing eight immunoglobulin motifs, a fibronectin type III-like domain, a single transmembrane domain and a cytosolic C-terminal domain (Kestila *et al.* 1998).

Nephrin plays a crucial role in the glomerular filtration barrier by acting as a signalling hub. The nephrin cytoplasmic domain can be phosphorylated by the Src family kinase Fyn (Verma *et al.* 2003), and signals from the phosphorylated nephrin go on to initiate a cascade of effectors that activate different intracellular pathways (Huber and Benzing 2005). For example, phosphorylated nephrin inactivates pro-apoptotic factor Bad (Huber *et al.* 2003) and leads to anti-apoptotic signals (Asanuma *et al.* 2007). Nephrin maintains homophilic and

heterophilic cis and trans interactions with neph family proteins (Neph1, Neph2 and Neph3) (Gerke *et al.* 2003) and therefore also provides stability to the SD.

Mutations in human nephrin gene cause congenital nephrotic syndrome of the Finnish type (CNF). This autosomal recessive disease is the most severe form of nephrotic syndrome characterized by massive proteinuria in utero and nephrosis at birth (Kestila *et al.* 1998). To date, over 50 nephrin mutations have been reported including deletions, insertions, splice-site, nonsense and missense mutations (Lenkkeri *et al.* 1999; Beltcheva *et al.* 2001). On the other hand, reduced nephrin expression was shown in patients with primary or acquired nephrotic syndrome, independent from the initial pathogenic mechanism (Huh *et al.* 2002; Doublier *et al.* 2003). Animal experiments showed that nephrin knockout mice had no slit diaphragms and died at birth with massive proteinuria (Putaala *et al.* 2001).

Podocin

Podocin, encoded by *NPHS2* gene, is a member of the stomatin protein family with a short amino terminal domain, a transmembrane region, and a cytosolic carboxy terminal domain forming a hairpin like structure (Boute *et al.* 2000). It has 383 amino acids mapped to human chromosome 1q25-31 (Gene Bank Accession Number: BC029141). Podocin is exclusively expressed in podocytes of the developing and mature glomeruli. It is predicted to form a membrane-associated hairpin-like structure with the N- and C-terminal domains facing the cytosolic side of the SD (Roselli *et al.* 2002). Mutations of the podocin gene were first identified in patients with autosomal recessive steroid-resistant nephrotic syndrome (Boute *et al.* 2000). $NPHS2^{-/-}$ knockout mice developed proteinuria during the antenatal period and died a few days after birth from renal failure caused by massive proteinuria. Electron

microscopy revealed extensive effacement of podocyte foot processes and the lack of a slit diaphragm in the remaining foot process junctions (Roselli et al, 2004). On the other hand, the inactivation of podocin in the mature kidney of mice led to a different phenotype. These mice had progressive renal disease and showed the features of NS, such as hyperlipidemia, hypertension and renal insufficiency (Mollet *et al.* 2009).

In patients with FSGS not related to podocin mutations, the expression of podocin was decreased or absent in 74% of the cases. Those with sufficient podocin expression tended to have a better prognosis that those without podocin expression (Horinouchi *et al.* 2003).

Podocin forms homo-oligomers and associates with the lipid rafts (Schwarz *et al.* 2001). It binds to the cytoplasmic tail of nephrin. This interaction is mediated by the C-terminal domain of podocin (Huber *et al.* 2001) and is increased with the phosphorylation of nephrin (Li *et al.* 2004). Podocin acts as a scaffolding protein that mediates nephrin recruitment into the specialized microdomains of the plasma membranes. It provides nephrin with a specialized lipid environment which is necessary for nephrin signal transduction (Huber *et al.* 2003). Podocin has been found to increase the efficiency of nephrin signalling without the recruitment of other signalling molecules (Huber *et al.* 2001).

NEPH1

Neph1, structurally related to nephrin, is a type I transmembrane protein of the immunoglobulin superfamily. It interacts in a cis-fashion in the plane of the membrane via the cytoplasmic domain (Gerke *et al.* 2003; Liu *et al.* 2003). NEPH1 is widely expressed in

numerous cell types, including podocytes, where it localizes to the insertion site of the SD. The extracellular region of Neph1 contains five immunoglobulin-like repeats, followed by a transmembrane domain and a cytoplasmic domain consisting of 198 to 235 amino acids (Sellin *et al.* 2003). Nephrin, podocin, and Neph1 form a protein complex that functions as a transmembrane receptor to mediate signal transduction. Loss of any one of these receptor components, either in patients carrying an inherited genetic mutation or in experimental gene-targeted mice, causes proteinuria and effacement of podocyte foot processes (Kestila *et al.* 1998; Boute *et al.* 2000; Donoviel *et al.* 2001; Garg *et al.* 2007). Further studies showed that its phosphorylation and interaction with nephrin play a functional role in maintaining podocyte structure and function (Garg *et al.* 2007). Knockout studies in mice suggested that, similar to nephrin, the genetic deletion of Neph1 results in a podocyte effacement phenotype with proteinuria and early postnatal death (Donoviel *et al.* 2001).

CD2AP

CD2-associated protein (*CD2AP*) (MIM *607832) is an adapter molecule which interacts with filamentous actin and a variety of cell membrane proteins through multiple actin binding sites. It is an 80kDa cytoplasmic protein mapped to chromosome 6p12.3. *CD2AP* contains three Src homology 3 (SH3) domains in its NH2-terminal region, a proline-rich region in the midregion, and a coiled-coil domain and actin-binding sites in the COOH terminus (Dustin *et al.* 1998; Kirsch *et al.* 1999; Lehtonen *et al.* 2000).

CD2AP plays a critical role in maintaining the integrity of the glomerular filtration barrier. It is originally identified as a ligand for the T-cell-adhesion protein CD2. In the kidney, it is expressed primarily in glomerular podocytes at the cytoplasmic face of the SD domain. It

directly interacts with podocin and nephrin at its C-terminal region (Schwarz *et al.* 2001; Shih *et al.* 2001) and participates in their signalling pathways (Mao *et al.* 2006). Both nephrin and *CD2AP* interact with the p85 regulatory subunit of phosphoinositide 3-OH kinase (PI3K), recruit PI3K to the plasma membrane, and, together with podocin, stimulate PI3K-dependent AKT signalling in podocytes (Huber *et al.* 2003). Animal experiments showed that lack of the glomerular expression of *CD2AP* in animals produces mesangial cell proliferation with extracellular matrix deposition, glomerulosclerosis and extensive foot-process effacements. *CD2AP*$^{-/-}$ mice developed severe nephrotic syndrome and died of massive proteinuria shortly after birth (Shih *et al.* 1999). Recent study from 80 Italian patients with idiopathic nephrotic syndrome showed that *CD2AP* mutations may alter the composition of the SD by modifying the interaction with CD2 in lymphocytes (Gigante *et al.* 2009).

PLCε1

Phospholipase C epsilon 1 (PLCε1), a family member of phosphoinositide-specific phospholipase C (PLC), is expressed predominantly in the cell bodies of podocytes (Hinkes *et al.* 2006). PLC proteins are typically characterised by the two phospholipase catalytic domains (PLC_X and PLC_Y) and Ca^{2+} lipid binding domain (C2 domain) (Boyer *et al.* 2010). They play essential roles in the coupling of G-protein coupled receptors by catalysing the hydrolysis of polyphosphoinositides such as phosphatidylinositol-4,5-bisphosphate to generate the second messengers inositol 1,4,5-triphosphate (IP3) and diacylglycerol (DAG) (Wing *et al.* 2003). IP3 releases calcium from intracellular storage and the elevated calcium level leads to a series of signalling cascades. DAG activates protein kinase C, which in turn modulates the activity of many proteins by phosphorylation.

In addition to conserved PLC domains, PLCε1 contains one RasGEF domain and two C-terminal Ras-binding (RA) domains, RA1 and RA2 (Boyer *et al.* 2010), which may serve as an activator and an effector of small GTPases (Zhou and Hildebrandt 2009). PLCε1 knockdown zebrafish has been shown to have pathological features of nephrotic syndrome, namely foot process effacement and severe disorganization of SD. The absence of PLCε1 has been found to be associated with a significant reduction in nephrin expression and arrest the development of glomerulus at the capillary loop stage (Hinkes *et al.* 2006). In humans, *PLCε1* mutations are frequently found in familial and sporadic diffuse mesangial sclerosis (DMS) cases. They were also detected in a non-negligible proportion of familial FSGS cases, but no clear genotype–phenotype correlation was present (Boyer *et al.* 2010).

α-Actinin-4

α-actinin-4 (*ACTN4*) is an actin-binding protein which is widely expressed in a number of human tissues, most notably glomerular podocytes (Kaplan *et al.* 2000). *ACTN4* binds actin in the cell cytoskeleton, contributes to cell structure, regulates cell motility and interacts with GBM molecules (Honda *et al.* 1998; Shao *et al.* 2010).

ACTN4-deficient mice have severely damaged podocytes and progressive kidney disease. Their podocytes have increased fluidity and altered cell motility and adhesion (Kos *et al.* 2003). Transgenic mice with an *ACTN4* mutation expressed in a podocyte-specific manner also developed significant albuminuria, as well as down-regulation of nephrin gene and protein expression in the kidney (Michaud *et al*, 2003). These studies confirmed that *ACTN4* is important for podocyte function. In humans, mutations of *ACTN4* gene were associated with an autosomal dominant form of FSGS. (Kaplan *et al.* 2000; Aucella *et al.* 2005; Weins

et al. 2005). Most mutations led to increased actin binding by *ACTN4* with subsequent abnormal formation of actin aggregates (Komatsuda *et al.* 2003; Yao *et al.* 2004; Michaud *et al.* 2006). However, this form of familial FSGS is rare in the general population (Bostrom *et al.* 2012).

INF2

Besides *ACTN4* and *TRPC6*, *INF2* gene is the third gene that is found to cause autosomal dominant FSGS recently (Brown *et al.* 2010). *INF2* encodes inverted formin-2, which is a member of actin-regulating proteins that accelerate actin filament assembly (Faix and Grosse 2006). Formins govern several dynamic events that require remodeling of the actin cytoskeleton such as cell polarity, cell and tissue morphogenesis and cytokinesis (Goode and Eck 2007). *INF2* is an actin-binding protein widely expressed in actin-rich area, like podocyte. It has the unique ability to accelerate both polymerization and depolymerization of actin (Brown *et al.* 2010).

INF2 is currently shown to be a major cause of autosomal dominant FSGS, explaining almost one fifth of the cases (Boyer *et al.* 2011), whereas *ACTN4* and *TRPC6* account for approximately 4% and 6% of familial FSGS respectively (Weins *et al.* 2005; Heeringa *et al.* 2009; Santin *et al.* 2009). All of the FSGS-associated *INF2* mutations identified to date are localized to the N-terminal diaphanous inhibitory domain (DID) of the protein, a region that interacts with the C-terminal diaphanous autoregulatory domain (DAD), thereby competing for actin monomer binding and inhibiting depolymerisation (Boyer *et al.* 2011). Interestingly, no mutation in DAD has been identified, suggesting DID, and not DAD, has a critical role for *INF2* function. Disease-causing *INF2* mutations therefore may have a defect in actin-mediated podocyte structural maintenance and repair (Boyer *et al.* 2011).

Synaptopodin

Synaptopodin belongs to a class of proline-rich actin-associated proteins and has a key role in regulating the actin-based shape and motility of podocyte foot processes. Synaptopodin binds to α-actinin-4, regulating its actin-bundling activity, and to *CD2AP* (Huber *et al.* 2006). Synaptopodin inhibits filopodia formation downstream of the small GTPase Cdc42 while promoting formation of contractile actin stress fibers by blocking the degradation of RhoA (Asanuma *et al.* 2006; Yanagida-Asanuma *et al.* 2007). Interest in the role of synaptopodin in podocytes has increased since it was found that the anti-proteinuric effects of cyclosporin (a calcineurin inhibitor) were due to inhibitions of the calcineurin-mediated dephosphorylation and subsequent degradation of synaptopodin, resulting in stabilization of the podocyte actin cytoskeleton and thereby protection from proteinuria (Faul *et al.* 2008).

The latest identified genes involved in FSGS in the past two years include *Arhgap24* and *MYO1E*. In addition, mammalian target of rapamycin (mTOR) and soluble urokinase receptor (suPAR) have been shown to play important roles in the pathogenesis of FSGS.

Arhgap24

Podocytes under physiological conditions might exhibit a rather stationary phenotype, and this is mainly due to upregulated RhoA and downregulated Cdc42/Rac1 activity (Zhu *et al.* 2011). Under stress and in pathophysiological situations, the podocytes may shift to a more migratory phenotype, characterized by an increase in Cdc42/Rac1 activity (Zhu *et al.* 2011). Using a combined approach of podocyte cell culture and genetic studies, Shaw et al. identified *Arhgap24*, which is a reported Rac1-inactivating GAP, as a highly podocyte-specific protein. Loss-of-function mutations of the *Arhgap24* gene was found in FSGS

patients. Furthermore, the expression of its transcript significantly increases with podocyte differentiation, suggesting that podocytes shift to a more stationary phenotype when they become highly differentiated (Akilesh *et al.* 2011).

MYO1E

MYO1E encodes Myosin-1e protein, and is recently identified to be linked to childhood-onset steroid-resistant form of FSGS (Mele *et al.* 2011). *MYO1E* is highly enriched in human podocytes, and the two identified mutations (A159P and Y695X) were linked with decreased motility of human podocytes and mislocalized expression of the *MYO1E* protein in vitro (Mele *et al.* 2011). This underlines how sensitive podocytes react to unbalanced cytoskeletal homeostasis leading to FSGS development and also implicates Myo1e as a novel human gene causing FSGS and regulating podocyte motility.

mTOR

Mammalian target of rapamycin (mTOR) is an evolutionarily conserved protein kinase regulating many essential cellular processes including translation, transcription and autophagy (Schell and Huber 2012). mTOR is a central regulator of podocyte function. In glomerular diseases such as diabetic nephropathy, mTOR is persistently hyper-activated and this ultimately causes podocyte loss, glomerulosclerosis and disease progression (Godel *et al.* 2011; Inoki *et al.* 2011). mTORC1, one of the two mTOR complexes, is sensitive to rapamycin and consists of multiple components including Raptor. It centrally regulates the podocyte growth, hypertrophy and de-differentiation.

suPAR

A soluble and circulating factor has been assumed for a long time since it has been observed that close to 30% of transplanted FSGS cases reoccur in the transplanted graft (Ponticelli and Glassock 2010). The identification of this soluble factor had remained elusive. Reiser et al. suggested soluble form of urokinase receptor (suPAR) might be the circulating factor (Wei *et al.* 2008). This was based on the finding that suPAR was not only elevated in the serum of two thirds of FSGS patients, but also correlated with the risk of FSGS recurrence after transplantation. Mechanistically, the authors showed that increased levels of suPAR resulted in beta-3 integrin activation in human podocytes (Wei *et al.* 2011).

1.4 *TRPC6* Channels

Transient Receptor Potential Cation Channel 6 (*TRPC6*) is a member of the transient receptor potential (TRP) superfamily of cation-selective ion channels, which are involved in numerous fundamental cell functions and are considered to play important roles in the pathophysiology of many diseases. The discovery in 2005 that mutations in *TRPC6* channels cause familial FSGS underscored the potential importance of Ca^{2+} dynamics for podocyte function and opened an entirely new line of investigation (Reiser *et al.* 2005; Winn *et al.* 2005). An overview of the TRP channels, specifically the *TRPC6* channels, is given below..

1.4.1 TRP Channels

Channel proteins are important for the survival and function of every cell, and Ca^{2+} permeable channels are particularly important since Ca^{2+} is not only a charge carrier but is also one of the most important second messengers (Minke 2010). TRP cation channels mediate the flux of Na^{+} and Ca^{2+} across the plasma membrane and into the cytoplasm (Berridge *et al.* 2003). TRP channels were first discovered in 1969 due to a mutation in the Drosophila photoreceptor, which resulted in inhibited Ca^{2+} permeability and sensitivity to light (Cosens and Manning 1969; Putney 1977). Two decades later, this *TRP* gene was cloned (Montell and Rubin 1989) and was shown to encode a Ca^{2+}-permeable cation channel (Hardie and Minke 1992). To date, more than 50 *TRP* channels are found in many organisms including yeast, worms, insects, fish, and mammals (Petersen *et al.* 1995; Wes *et al.* 1995). These have diverse functions and share structural similarities with *Drosophila TRP* channels.

1.4.1.1 TRP Classification

Unlike most ion channels, *TRP* channels are identified by their homology rather than by

ligand function or selectivity. This is because their functions are disparate and often unknown. Based on sequence homology, *TRP* channels are commonly subdivided into 7 subfamilies: *TRPC* (Canonical, *TRPC1-TRPC7*), *TRPV* (Vanilloid, *TRPV1-TRPV6*), *TRPM* (Melastatin, *TRPM1-TRPM8*), *TRPP* (Polycystin, *TRPP1-TRPP3*), *TRPML* (Mucolipin, *TRPML1-TRPML3*), *TRPA* (Ankyrin, *TRPA1*), and *TRPN* (no mechanoreceptor potential C, *NOMPC*) (Montell 2005; Voets *et al.* 2005) (Table 1-4). Except for *TRPN*, all of the subfamilies can be found in mammals.

Table 1-4 The Seven Subfamilies of *TRP* Channels

	Fly	Worm	Fish	Mouse	Human
TRPC	3	3	8	7	6
TRPV	2	5	4	6	6
TRPM	1	4	6	8	8
TRPA	4	2	1	1	1
TRPP	4	1	2	3	3
TRPML	1	1	4	3	3
TRPN	1	1	-	-	-
Total	16	17	25	28	27

Adapted from (Flockerzi 2007).

1.4.1.2 TRP Structure and Permeability

TRP channel proteins are evolutionally conserved. All *TRP* proteins have four identical or similar subunits with six putative transmembrane domains (S1-S6) and cytosolic N- and C-terminal tails tetramerize to form a functional channel (Figure 1-3) (Hoenderop *et al.* 2003). S5, S6 and the connecting pore loop form the central cation-conducting pore (Voets *et al.* 2004), whereas S1–S4 and the extremely long cytoplasmic N- and C-terminal parts are thought to contain the regulatory domains that control channel gating (Voets *et al.* 2005).

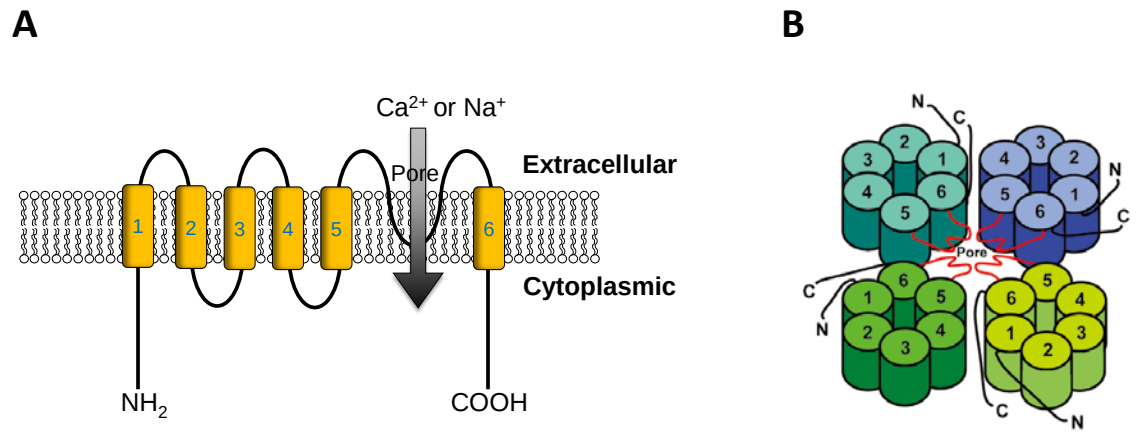

Figure 1-3 Predicted structure of *TRP* and topology of *TRP* channels.

Panel A shows the putative structure of a *TRP* channel. It has 6 transmembrane helices (S1-S6) with a putative pore region between S5 and S6. Panel B shows the proposed tetrameric channel structure. A *TRP* channel is composed of hetero or homo tetrameric *TRP* molecules. *Adapted from (Watanabe et al. 2009).*

The degree of similarity in amino acid sequences among members within one subfamily is up to more than 90%. Within the cytoplasmic domains, some structural motifs have been identified by sequence comparisons. These include ankyrin repeat domains, a coiled-coil domain (Schindl and Romanin, 2007), and the so-called '*TRP* domain', which is a highly conserved stretch of ~25 amino acids in the C-terminal region close to S6. The *TRP* domain is found in all mammalian *TRP* subfamilies except *TRPA* and *TRPP* (Montell 2005; Ramsey *et al.* 2006). In addition, amino acid sequences forming the pore are strongly conserved across different *TRP* subfamilies (Montell, 2005). S5, S6 and the *TRP* domain are similar even in distinct *TRP* channels (Ramsey et al., 2006).

TRP channels represent a new class of Ca^{2+} permeable channels, not belonging to traditional voltage gated and ligand gated channels. Although they have six transmembrane segments, and the pore region loop, which is typical of voltage gated channels, the positively charge residues in S4 are replaced with uncharged amino acid residues (Phillips *et al.* 1992). In

addition, mammalian *TRP*s, like *TRPV1*, bind specific "ligands" such as capsaicin (Caterina *et al.* 1997), but this channel is not considered as a typical ligand gated channel (Bohlen *et al.* 2010).

All *TRP* channels are permeable to cations except *TRPM4* and *TRPM5* channels, which are impermeable to Ca^{2+}. The permeability ratios PCa/PNa for these channels vary considerably, ranging from 0.1 to >100, and *TRPV5* and *TRPV6* are two highly Ca^{2+} permeable channels (Owsianik et al., 2006a).

1.4.1.3 TRP Channel Regulation and Activation

TRP channels participate in a diversity of functions in all excitable and nonexcitable cells. Many *TRP*s have been found to participate in sensory transduction pathways, including thermosensation, mechanosensation, taste perception, perception of pungent compounds, pheromone sensing and osmolarity regulation (Montell 2001; Minke and Cook 2002; Clapham 2003; Julius 2005; Nilius and Mahieu 2006; Nishida *et al.* 2006). Regulation of *TRP* channels includes: (1) posttranslational modifications such as phosphorylation, glycosylation and nitrosylation; (2) protein-protein interactions implying actors like calmodulin (CaM), IP3R, stromal interacting molecule (STIM) and Orai proteins; (3) lipid interactions such as PIP2 and cholesterol; and (4) trafficking (TU 2009; Zhu 2011).

.

Several activation mechanisms have been established for *TRP* channels, including receptor activation, ligand activation, direct activation as well as indirect activity, or activation by calcium store depletion.

1) *Receptor activation.* This is the most likely mechanism for *TRPC* channels and the Drosophila photoreceptor *TRP*. All mammalian *TRPC* channels can be activated by G

protein–coupled receptors (GPCRs). GPCRs and receptor tyrosine kinases can modulate *TRP* channel activity through activation of phospholipases C (PLCs). PLCs catalyze the hydrolysis of phosphatidylinositol 4,5-bisphosphate (PIP_2) into diacylglycerol (DAG) and inositol 1,4,5-triphosphate (IP_3). IP_3 in turn activates the IP_3 receptor (IP_3R), causing release of Ca^{2+} from an intracellular Ca^{2+}-containing compartment which is part of the endoplasmic reticulum (ER). Downstream of receptor activation, *TRP* channels are activated by one of the following mechanisms: (1) the decreased level of PIP_2; (2) the production of DAG; or (3) the release of Ca^{2+} from internal stores of the ER induced by IP_3 binding to IP_3R.

2) Ligands activation. Various ligands can activate *TRP* Channels. Ligands that activate *TRP* channels may be broadly classified as: (a) exogenous small organic molecules such as 2-aminoethyoxydiphenyl borane (2-APB), capsaicin, menthol and hyperforin; (b) endogenous lipid and lipid metabolites, such as phosphoinositides, DAG, eicosanoids and anandamide; (c) purine nucleotides and their metabolites such as ADP-ribose and βNAD^+; (d) inorganic molecules and ions such as Ca^{2+}, La^{3+}, Zn^{2+} and H_2O_2 (Zhang *et al.* 2002; Venkatachalam *et al.* 2003; Zhu 2005).

3) Direct activation. The putative direct activators include temperature, mechanical stimuli, conformational coupling with other proteins such as STIM1 (stromal interacting molecule 1 or IP3R, channel phosphorylation, osmolarity and pH (Clapham 2003; Maroto *et al.* 2005).

4) Activation by calcium store depletion. For a long time, there has been a debate concerning the molecular identity of the store operated channels (SOC). Store-operated Ca^{2+} entry (SOCE), also called capacitative Ca^{2+} entry (CCE), refers to a phenomenon in which the depletion of intracellular Ca^{2+} stores (primarily the ER) leads to the activation of plasma

membrane Ca^{2+}-permeable channels. Ca^{2+} entering through SOC can be pumped into the stores and thus permit their replenishment (Putney, 1986; Parekh and Putney, 2005). Although some *TRPC* (see Section 1.1.5) may participate in SOCE, they exhibit biophysical properties distinct from SOC. For example, *TRPC* channels underline non-selective cation currents which stand in contrast with the highly Ca2+-selective SOC currents like *I*CRAC (calcium release-activated current), (Putney, 2007a). The exact contribution of *TRPC* in SOCE remains currently debated.

It is worth mentioning that some *TRP* channels may have several modes of activation and function as polymodal sensors, integrating many of the signals mentioned above.

1.4.1.4 TRPC Subfamily

TRPC channels comprise a family of nonselective Ca^{2+}-permeable cation channels that are ubiquitously expressed, forming homomeric and heteromeric cation channels (Tai *et al.* 2009). Based on sequence and functional characteristics, the seven *TRPC* channels, *TRPC*1-7, can be subdivided into three groups: *TRPC1*/4/5, *TRPC2*, and *TRPC3*/6/7.

TRPC1, the first mammalian *TRP* protein reported, is widely expressed in many tissues and thought to from heteromeric channels with *TRPC*4 and/or *TRPC5* (Wes *et al.* 1995). *TRPC*4 and *TRPC5* are believed to form homomeric channels. When expressed together, *TRPC1*, 4, and 5 form nonselective cation channels that are activated by G_q signaling through a phospholipase Cβ1 (PLCβ1) pathway (Plant and Schaefer 2005). Mice lacking *TRPC*4 have defects in agonist-induced vasoregulation and lung microvascular permeability (Freichel *et al.* 2001; Tiruppathi *et al.* 2002). Growth factor stimulates rapid translocation of *TRPC5* into the plasma membrane from vesicles located near the plasma membrane (Jung *et al.* 2003).

TRPC3, *TRPC6* and *TRPC7* proteins share 75% identity, and are highly expressed in smooth and cardiac muscle cells. They have relatively low selectivity for Ca^{2+} over Na^{+}, and are sensitive to the intracellular concentration of Ca^{2+} ($[Ca^{2+}]_i$). These channels are activated by a receptor-mediated pathway involving DAG and are important in vascular and airway smooth muscle (Hofmann *et al.* 1999). Channels formed by *TRPC3* or *TRPC6* are also regulated by N-linked glycosylation and Ca/CaM (Dietrich *et al.* 2003). *TRPC3* is activated by phosphorylation by PKG (Kwan *et al.* 2004). *TRPC6* is phosphorylated by the Src family of tyrosine kinases (Vazquez *et al.* 2004).

TRPC2 shares roughly 30% sequence homology with *TRPC3*/6/7. *TRPC2* full-length messenger RNA (mRNA) is expressed in mouse and rat tissues. Its rat orthologue encodes an important sensor localized to neuronal microvilli in the vomeronasal organ (Liman *et al.* 1999). *TRPC2*-deficient mice display abnormal mating behaviour, consistent with a role for this channelin pheromone signalling (Stowers *et al.* 2002). However, *TRPC2* is a pseudogene in humans (Ramsey *et al.* 2006).

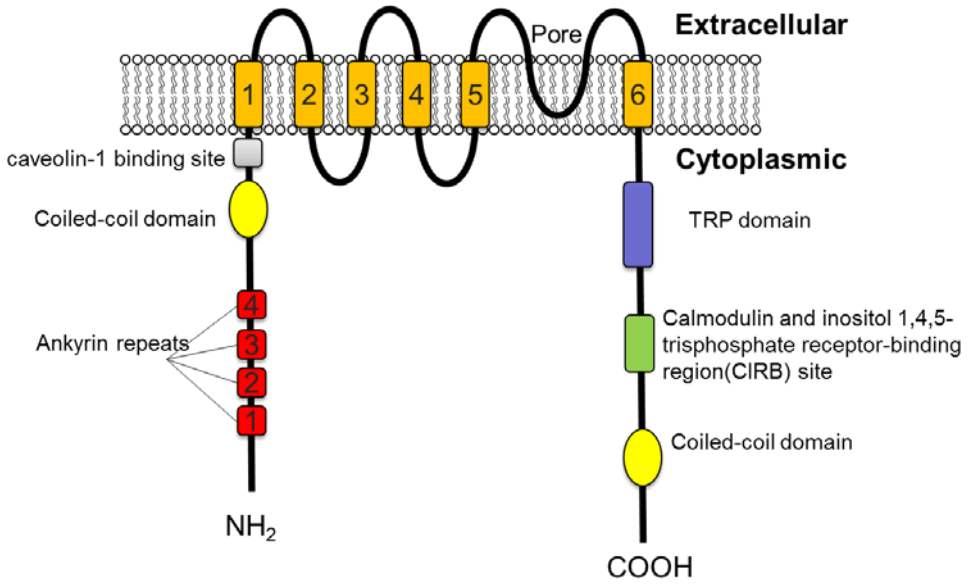

Figure 1-4 Structure of *TRPC6* Channels.

The structural elements of *TRPC6* channels include cytoplasmic N- and C-termini, six transmembrane helices (S1-S6), a putative pore region located between S5 and S6, four N-terminal ankyrin-like repeats (ANK1-4), caveolin-1 binding site, and the C-terminal TRP domain CIRB domain.

1.4.2 *TRPC6* Structure and Expression

TRPC6 displays common structural features of the TRP superfamily（Figure 1-4): cytoplasmic N- and C-termini, six transmembrane helices (S1-S6) and a putative pore region located between S5 and S6. *TRPC6* also possesses features of the *TRPC* subfamily. For example, It contains four N-terminal ankyrin-like repeats (ANK1-4) (Venkatachalam and Montell 2007), a N-terminal caveolin-1 binding site (Vazquez et al., 2004), C-terminal highly conserved regions of TRP domain including TRP box 1 (Glu-Trp-Lys-Phe-Ala-Arg or EWKFAR) and TRP box 2 (a proline-rich motif) (Montell 2005; Venkatachalam and Montell 2007) and the Calmodulin and IP3R-binding (CIRB) site (Zhu 2005). The ankyrin repeats consist of 30-34 amino acid residues. They are common protein-protein interaction motifs thought to be important in protein function, perhaps signifying association with the cytoskeleton (Montell 2005). There are two coiled-coil (CC) domains in each of the cytosolic

N- and C-termini, which are ubiquitous protein motifs that are commonly used to control oligomerisation (Vazquez *et al.* 2004).

TRPC6 is expressed in numerous tissues enriched with smooth muscle cells including brain, lung, stomach, colon, kidney, as well as in immune and blood cells (Dietrich and Gudermann 2007). Specifically, in the kidney, *TRPC6* is expressed in the podocyte cell body, major processes, and foot processes in the vicinity of the SD (Reiser *et al.* 2005). Despite its abundance, the exact physiological role of *TRPC6* has not been fully elucidated.

.

1.4.3 *TRPC6* Biophysical Properties

TRPC6 channels mediate the flux of Na^+ and Ca^{2+} across the plasma membrane and into the cytoplasm, showing a dual inward and outward rectification at negative potentials and positive potentials receptively. The current-voltage relationship displays an S-shaped curve. The relative ion permeability PCa/PNa of *TRPC6* channels is around 5 (Hofmann *et al.* 1999; Inoue *et al.* 2001). The Na^+ entry via *TRPC6* induces a depolarization which in turn activates other channels, like voltage-gated Ca^{2+} channels (VGCC) (Soboloff *et al.* 2005).

In human embryonic kidney (HEK)-293 cells stably expressing *TRPC6,* Ca^{2+}, in the presence of extracellular Na^+, contributes poorly (~4%) to the whole-cell currents (Estacion et al., 2004). It is concluded that in cells with a high input resistance, the primary effect of *TRPC6* activation is to depolarize (due to the entry of Na^+), limiting Ca^{2+} entry via *TRPC6* but facilitating Ca^{2+} entry via VGCC. In cells with a large inward-rectifier current or expressing Ca^{2+}-activated K^+ channels to hold the membrane potential negative, receptor-mediated activation of *TRPC6* permits a sustained Ca^{2+} influx pathway (Estacion et al., 2004). *TRPC6*

channels assemble into homo- and heterotetramers with other TRPC subfamily members (Hofmann *et al.* 2002; Strubing *et al.* 2003; Bandyopadhyay *et al.* 2005).

1.4.4 Activation of *TRPC6* Channels

TRPC6, like other TRP channels, can be activated by receptor stimulation, store depletion (Liao *et al.* 2008; Jardin *et al.* 2009), mechanosensation (Spassova *et al.* 2006; Inoue *et al.* 2009), and diacylglycerol (DAG) and related lipids.

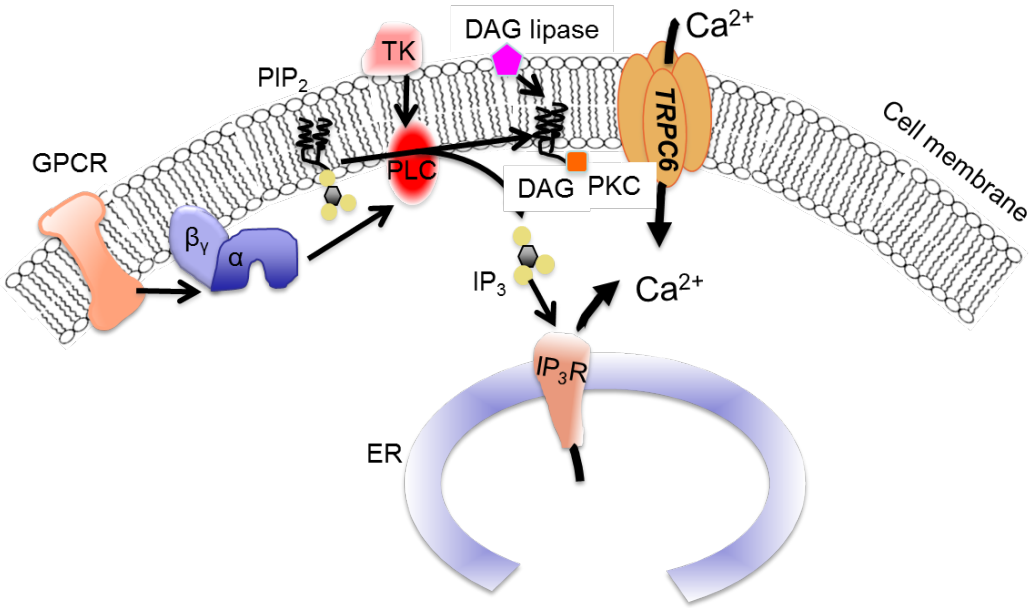

Figure 1-5 *TRPC6* activation and signal transduction.

A G protein–coupled receptor (for example, muscarinic M1 acetylcholine receptor) catalyses G protein nucleotide exchange to form active G_{α} and $G_{\beta\gamma}$ subunits, in turn activating PLC_{β}. Alternatively, tyrosine kinase (TK) receptors can also activate PLC_{γ}. PLC hydrolyses an abundant membrane component, PIP_2, into DAG and IP_3. The soluble IP_3 activates the IP_3R on the endoplasmic reticulum to release intracellular Ca^{2+}, which is inherently a localized second messenger and *TRPC6* channels are activated. The *TRPC6* channels can also be activated by decreased level of PIP_2 or the production of DAG. Adapted from (Clapham 2003).

The activation of *TRPC6* channels through receptor stimulation is well studied (Abramowitz and Birnbaumer 2009). Among them, the most well-studied receptor is the G protein–coupled receptor (GPCR). Stimulated GPCRs or tyrosine kinase (TK) receptors will activate phospholipases C (PLC) signaling pathway as shown in figure 1-5. The activated PLC catalyzes the hydrolysis of phosphatidylinositol 4,5-bisphosphate (PIP_2) into DAG and inositol 1,4,5-triphosphate (IP_3). DAG can be metabolized by the DAG lipase to yield poly-unsaturated fatty acids (PUFA) such as arachidonic acid (AA) and linolenic acid, which can then activate or modulate a wide range of ion channels, including *Drosophila* TRP and TRPL (Chyb *et al.* 1999), TRPV4 (Watanabe *et al.* 2003), TRPM5 (Oike *et al.* 2006) and *TRPC6* (Basora et al., 2003). Another PIP_2 product, IP_3, in turn activates the IP_3 receptor on the endoplasmic reticulum to release intracellular Ca^{2+}, which is inherently a localized second messenger, and *TRPC6* channels are then activated.

In addition, *TRPC6* channels can also be activated by cytokine receptor, like interleukin-1. The activation of interleukin-1 receptor also generates DAG, followed by *TRPC6* activation (Beskina *et al.* 2007). In summary, downstream from receptor activation, *TRPC6* channels are activated by one of the following mechanisms: (1) the decreased level of PIP_2; (2) the production of DAG; or (3) the release of Ca^{2+} from internal stores of the endoplasmic reticulum (ER). It is worth to mention that DAG alone may not fully account for the activation of *TRPC6*, and other receptor-mediated events may act synergistically with DAG to stimulate channel activity (Estacion *et al.* 2004).

1.4.5 Regulation of *TRPC6* Channels

TRPC6 channels are mainly regulated by phosphorylation. Src family protein-tyrosine kinases (PTKs), like Fyn, can modulate *TRPC6* channel activity via tyrosine phosphorylation, causing an increase in DAG-evoked *TRPC6* activation in excised patches (Hisatsune *et al.* 2004). This in turn causes alterations in the dynamics of the cytoskeleton.

Protein kinase C (PKC) has controversial effects on *TRPC6* channel regulation. DAG is the physiological activator of PKC while DAG kinase (DAGK) phosphorylates DAG to form phosphatidic acid. Previous studies show that *TRPC6* channel activities are not affected by upregulation or downregulation of PKC (Hofmann *et al.* 1999; Inoue *et al.* 2001). However, some studies show the involvement of PKC in *TRPC6* inactivation. By activating PKC, phorbol-12-myristoyl-13-acetate (PMA), one PKC activator, blocks the activation of *TRPC6* by DAG and carbachol (Zhang and Saffen 2001). Interestingly, a later study shows a differential effect of PKC activation on DAG- and carbachol-induced *TRPC6* currents: PMA has no significant effect on DAG-activated currents whereas it essentially eliminates the regulation by receptor stimulation (Estacion *et al.* 2004). Currently, it is well accepted that *TRPC6* can be regulated by the formation of a multiprotein complex centered on *TRPC6* containing PKC and M1 muscarinic acetylcholine receptors (M1 mAChRs), and this can be initiated by carbachol (Kim and Saffen 2005).

In addition, calcium is also known to influence the activity of *TRPC6* channels through the action of calmodulin (CaM), a small soluble Ca^{2+}-binding protein that is involved in the regulation of many cellular functions including channel activity (Saimi and Kung 2002). CaM binds to the highly conserved CIRB site of *TRPC6* (Tang *et al.* 2001), at where it competes with IP3R in a Ca^{2+}-dependent manner since CaM only binds to the CIRB site in the presence of Ca^{2+}. In some cases, CaM binding to the CIRB site can prevent *TRPC*

channels from being activated, whereas the displacement of CaM by activated IP3R or the inhibition by CaM antagonists activate the channels (Kwon *et al.* 2007). On the contrary, several studies show that CaM binding to *TRPC6* is necessary for its activation. CaM inhibitors like calmidazolium and trifluoperazine, which dissociate CaM from *TRPC6*, inhibit *TRPC6* activity in HEK-293 cells (Boulay 2002; Shi *et al.* 2004).

1.4.6 *TRPC6* and its Podocyte Binding Partners

TRPC6 interacts with a number of different podocyte proteins, including scaffolding molecules, signaling proteins, cytoskeletal elements, and other types of ion channels (Dryer and Reiser 2010). Recent research has implicated as many as 24 podocyte genes in primary nephrotic syndrome or FSGS (McCarthy *et al.* 2013). It is well-known that *TRPC6* interacts with nephrin and podocin and these interactions may be central to the physiological function of these channels at the SD.

Podocin was shown to regulate the activity of *TRPC6* in a cholesterol-dependent manner, and Huber and coworkers have proposed that podocin binds sterols and alters the local lipid environment surrounding the channel molecule, thereby facilitating the ability of *TRPC6* to respond directly to deformation of the plasma membrane (Huber *et al.* 2006).

TRPC6 interactions with nephrin near the SD may underlie regulation of gating and trafficking of these channels (Huber and Benzing 2005; Verma *et al.* 2006). Functional interactions between these proteins may serve to monitor the integrity of the filtration apparatus in podocytes to sense mechanical stimuli and to trigger Ca^2 signaling cascades that could alter cytoskeletal dynamics (Kriz *et al.* 1994; Kriz *et al.* 1995; Kriz *et al.* 1996). For example, engagement of the ectodomains of nephrin results in localized activation of Src

family tyrosine kinases (Verma *et al.* 2006). Moreover, the absence of nephrin as shown in neonatal nephrin$^{-/-}$ mice led to increased expression of *TRPC6* in podocytes compared with podocytes of wild-type littermates (Reiser *et al.* 2005).

Besides *TRPC6*, there are other *TRPC* family members expressed in podocytes. *TRPC1*, *TRPC2*, and *TRPC5* were observed in mouse glomeruli in a pattern consistent with expression in podocytes (Reiser *et al.* 2005). *TRPC3* was also detected in immortalized mouse podocyte cell lines (Kim *et al.* 2009). It is possible that some of the *TRPC6* channels in podocytes interact with other types of ion channels and form heteromeric complexes.

1.4.7 *TRPC6* and FSGS

The link between *TRPC6* and FSGS was first described in 2005 when two independent research groups discovered that mutations in *TRPC6* channels cause familial FSGS (Reiser *et al.* 2005; Winn *et al.* 2005). This finding underscored the potential importance of Ca^{2+} dynamics for podocyte function. Since then, an increasing number of *TRPC6* mutations are identified from patient families with FSGS. To date, all reported *TRPC6* mutations occur either in the cytoplasmic NH_2 or coiled-coil domain in the COOH terminals of the protein (Reiser *et al.* 2005; Winn *et al.* 2005; Heeringa *et al.* 2009; Santin *et al.* 2009; Zhu *et al.* 2009; Buscher *et al.* 2010; Gigante *et al.* 2011; Mir *et al.* 2012). Among them, some are gain-of-function mutations resulting in increased calcium current amplitudes and/or increased intracellular calcium influx. However, there are also some *TRPC6* mutations that did not modify the calcium influx in heterologous expression systems. *TRPC6* mutations in the four ANK repeats and the CC domains play important roles since ANK repeats are common protein-protein interaction motifs thought to be important in protein function, perhaps signifying association with the cytoskeleton (Montell 2005), whereas the two CC domains are

ubiquitous protein motifs commonly used to control oligomerisation (Vazquez *et al.* 2004). However, the precise mechanism of how *TRPC6* mutations cause FSGS is still unclear.

1.5 Research Hypothesis and Scope of Thesis

FSGS is a clinicopathological entity characterized frequently by steroid-resistant nephrotic syndrome and rapid progression to end-stage kidney disease. It accounts for up to 20% of patients on dialysis. In Singapore, 65% of children biopsied for steroid-dependent or steroid-resistant nephrotic syndrome showed FSGS as the underlying histopathology. The treatment for FSGS is currently largely empirical, and response rates are, at best, only moderate. Only a small percentage of affected individuals achieve complete remission. The reason for this lack of effective treatment is that the pathogenesis of FSGS has not been fully elucidated. The molecular studies of familial cases in the last two decades suggest that FSGS is a defect of the podocyte. Several genes encoding for structural proteins of the podocyte, such as *NPHS1*, *NPHS2*, *ACTN4* and *TRPC6* gene have been identified.

Almost 20 *TRPC6* mutations have been reported in adults and children with glomerular disease. Some of these mutations cause disease with variable penetrance, including non-penetrance. The mechanism of this variable penetrance is unknown. We describe a Singapore Chinese index family where 6 members had a novel *TRPC6* p.R68W (c.202C>T) mutation, two of whom had renal failure from FSGS and 1 had proteinuria. Amongst the 3 healthy non-penetrant members, one successfully donated a kidney to her sister with FSGS, and both donor and recipient had remained well after 19 years.

We have found a novel *TRPC6* missense mutation p.R68W in the index family. We also detected single nucleotide polymorphisms (SNPs) in podocin and nephrin genes which seemed to segregate with renal disease in the family. We therefore hypothesized that the

TRPC6 p.R68W mutation interacted with podocin and/or nephrin polymorphisms and therefore resulted in variable phenotypes.

In this thesis, we screened the *TRPC6*, podocin and nephrin genes in the index family and validated the sequence variants in 224 Singapore Chinese controls. The interactions between *TRPC6*, podocin and nephrin variants were studied by co-transfecting these variants into human embryonic kidney cells and measuring *TRPC6* currents using whole-cell patch-clamp method. Immunoblotting, surface biotinylation and mRNA stability assays were also performed to elucidate the mechanisms of the interactions.

CHAPTER 2 MATERIALS & METHODS

2.1 Study Participants

Our study is centred on an index family comprising of 9 members, of which 2 had ESRD from FSGS and one had proteinuria. The other 6 members do not have renal disease. For podocyte gene variations screening, we recruited 97 unrelated Singapore Chinese patients with sporadic steroid-resistant or steroid-dependent NS (SDNS) and/or FSGS (mean age of disease onset 5.7 years, range 0.9 to 19.0 years) (Appendix I-1). Diagnostic criteria for NS and definitions for steroid resistance and dependence were according to standard guidelines (1981). Additionally, we included 128 unrelated Singapore Chinese cord blood controls with no known family history of renal diseases. Moreover, control data from the Singapore Genome Variation Project (Teo *et al.* 2009) (96 Chinese) and local exome sequencing data (200 Chinese) were used. Blood samples were obtained from study participants after informed consent was obtained in accordance with a protocol approved by the National University Hospital. The stored cord blood samples were legacy samples obtained anonymously without consent, and approval has been obtained from the Ethics Committee for this study.

2.2 Mutation Screening of Podocyte Genes

2.2.1 Human Genomic DNA (gDNA) Extraction

Genomic DNA was isolated from peripheral blood leukocytes. Three millilitres (mL) of blood were collected in ethylenediaminetetraacetic acid (EDTA) from the participants. One mL of blood was used for the extraction of gDNA. The red cells were lysed by repeatedly washing the cells with TE10/10 buffer. The white cell pellet was then obtained and incubated in 1 to 3mL of TE10/10 buffer supplemented with 0.5% SDS (1st Base, Singapore) and 300µg of Proteinase K (Promega, USA) overnight at 37°C. Equal volume of phenol (Merck, Germany) was added to the sample and mixed for 7 to 10 minutes before centrifuging at

3000rpm for 10 minutes. The lower organic phase was removed and equal volume of 24:1 (v/v) chloroform-isoamyl alcohol (Merck, Germany) was added. The sample was mixed for 7 to 10 minutes before centrifuging at 3000rpm for 10 minutes. The lower organic phase was removed and gDNA was precipitated using 100% ethanol with 5M of NaCl. The gDNA was washed once with 70% ethanol and once with 100% ethanol. It was air-dried and suspended in nuclease free water. The concentration of the gDNA was measured using the NanoDrop 1000 spectrophotometer (Thermo Scientific, USA). All gDNA were diluted to a working concentration of 100ng/3µL.

2.2.2 Human Total RNA Isolation from Leukocytes

For RNA isolation, 5mL whole blood was diluted and gently mixed with pre-warmed HBSS at a ratio of 1:1, followed by gentle layering of the mixed blood to 4mL Ficoll-paque in 15mL Falcon tube, and centrifugation at 2000rpm for 30 minutes. The ring of PBMC was harvested using a Pasteur Pipette, and transferred to a new 15mL tube followed by topping up with cold HBSS to the brim. This was inverted gently to wash cells and then centrifuged at 1500rpm for 5 minutes. The supernatant was decanted and the cell pellet was washed with cold HBSS. The suspension was again centrifuged cells at 1500rpm for 5 minutes and the supernatant decanted. Subsequently, 8mL of HBSS was added. The number of cells was counted by loading 8uL of the cell suspension into the neubauer chamber. The cell suspension was centrifuged again at 1500rpm for 5 minutes, the supernatant decanted, and 1ml of TRIzol (Invitrogen, USA) added per 10^7 cells. Standard RNA isolation procedures were then performed.

2.2.3 Primers for Podocyte Genes

Primers for mutational screening of all the 13 exons and the flanking intronic sequences of *TRPC6* gene were adopted from published literature (Winn *et al.* 2005). Five additional pairs of primers were designed for the *TRPC6* promoter region and 5' UTR, which is about 1000 bp upstream of the transcriptional start site. Table 2-1 depicts the primer sequences and polymerase chain reaction (PCR) conditions for direct sequencing of *TRPC6*. Similarly, primers for mutation screening of other podocyte genes, namely *NPHS1* (nephrin), *NPHS2* (podocin) and *ACTN4* (alpha-actin 4) were from the literature (Lenkkeri *et al.* 1999; Boute *et al.* 2000; Kaplan *et al.* 2000; Karle *et al.* 2002).

Table 2-1 Primer Sequences and PCR Conditions for Direct Sequencing of *TRPC6*

Promoter /Exons	Forward Primer (5' to 3')	Reverse Primer (5' to 3')	T_{ann} (^{0}C)	Pdt Size (bp)
Promoter	gcattttcccacacttccaac	gacctttaagcagtagtagccaa	57	453
	cctcatctgcttctttgcct	atgttccaaacgccagatgt	58	386
	tctttatcggtatcattggaa	agccaaagcctgtcctgtag	52	387
	cctagttcaggctcataccgcctcctg	acgacggtgaagcaggggtgcaga	69	391
	taagtggtgacttttccccgggccagt	cctaggaggtacacacgcgggttcagg	69	490
5' UTR and 1	cctcctagttcaggctcataccgcctcctg*	acgacggtgaagcaggggtgcaga*	50	391
	taagtggtgacttttccccgggccagt*#	cctaggaggtacacacgcgggttcagg*#	53	490
2	gcaaagtgcttggctttctt	cattctggcccatgtaatcc	60	439
	cgtgagaaggggagaaggtt	attgcttccacaatccgaac	58	323
	agaatgccactcactcaacg	tggagtcacatcatgggaga	58	310
	gttcggattgtggaagcaat	tggagtggctaaacgagtca	60	292
	ctcccatgatgtgactccaa	gcttgtggagggtgaagtct	60	336
	tgactcgtttagccactcca	ctgagcacatgggggaag	60	233
3	tctgaagcatagtaaaacgtggt	ccctttatccttatttagcaccaa	58	313
4	gccatttgtttgttgcctgt	acccaactgtgattccctga	58	427

Promoter /Exons	Forward Primer (5' to 3')	Reverse Primer (5' to 3')	T_{ann} (^{0}C)	Pdt Size (bp)
5	ggagatcattggaatgtgcag	aatgaacccaaggcaactgt	58	490
6	caggctgagacctttcaaaca	tgcagtaaccgaactactactgac	58	406
7	cgcagaaaaagaagttacc*	catggacttacataaacgctg*	55	418
8	ccatccttgcagcaatccta	gaatgaacaaagggcgaaga	55	490
9	cgatcactggg gtctgagag	aaagggatgtggcatagtgg	55	400
10	agggaagaaccccgtaagaa	gcttctgaacatctgtcccttt	56	290
11	ctcagacaacctctaacaaacagc	caaaatgcctggtacatggt	55	457
12	ggctcactacagggaggaag	gctctccaggcactctgc	55	250
13 and 3'UTR	ctgatttcctcctgtccca*	actagggctccagatgatagg*	57	381
	tttgtccacttgaagccat*	atccacagagcaggcaagaa*	55	371
	gtgtctgcctgaaaatgggt*	cgcacacacacaaaactgga*	59	376
	gtttttcctccactgaaccctg*	gtaagtaacaacaacaacctctt*	54	436
	tgttctatccttctacccaaa*	caactgctgattcaaatactg*	53	448

* Primers framing the regions of 5' UTR, exon 1, 7 and 13, and 3'UTR on the *TRPC6* gene were re-designed.
# , Q solution was added to reaction mixture
T_{ann}, annealing temperature; Pdt, Product;; bp, base pairs; UTR, untranslated region.

2.2.4 PCR Amplification for Sequencing

PCR amplification was performed using the GeneAmp 9700 PCR system (Applied Biosystems, USA). For direct sequencing, a reaction mixture (15µL) contained 30 to 100µg of gDNA, 1x PCR buffer, 1.5-2mM of $MgCl_2$, 0.2µM of dNTP (Applied Biosystems, USA), 0.2µM to 0.5µM of each primer (Sigma-Aldrich, USA), 1U of Taq polymerase (QIAGEN, Germany) and nuclease free water. Betaine (Sigma-Aldrich, USA) was added for the amplification of certain regions. The reactions were performed for 30 cycles, with denaturation at 95°C for 1 minute, annealing at 50-60^{0}C for 1 minute according to annealing temperature list in the table 2-1, and extension at 72°C for 1 min. In the first cycle,

denaturation was performed at 95°C for 5 minutes. In the last cycle, the extension lasted for 9 min. Subsequently, 5μL of amplicons were run on a 1.5% gel and visualized under ultraviolet illumination on ChemiDoc XRS (Bio-rad Laboratories, USA) to confirm their specificity.

2.2.5 DNA Sequencing

DNA sequencing is the process of determining the precise order of nucleotides within a DNA molecule. It is the most direct and reliable approach to show whether a gene is mutated or, in gene cloning, to detect whether the correct sequence and direction of interested gene has been cloned into the plasmid DNA.

To detect gene mutations, 2.5μL amplicons obtained from Section 2.2.4 were treated with 5U of Exonuclease I (USB Corporation, USA) and 1 U Shrimp Alkaline Phosphatase (USB Corporation, USA) for 15 minutes at 37°C, followed by inactivation at 80°C for 15 minutes. This step is to remove any leftover primers and dNTPs from the PCR template. The sequencing reaction mix contained 1.5μL of treated PCR template, 0.2μL of either forward or reverse primer (10μM), 5μL of diluted BigDye® Terminator v3.1 Ready Reaction Mix (Applied Biosystems, USA) and 3.3μL of nuclease free water. The reactions were run on the GeneAmp 9700 PCR system (Applied Biosystems, USA) for 25 cycles consisting of denaturation at 96°C for 10 seconds, primer annealing at 50°C for 5 seconds and primer extension at 60°C for 4 minutes. This was followed by sodium acetate-ethanol precipitation (Appendix II-1). The DNA pellet was air-dried and resuspended in 12μL of HiDi-formamide (Applied Biosystems, USA). The dissolved DNA templates were loaded into a MicroAmpTM Optical 96 well reaction plate (Applied Biosystems, USA) and run on the 3100 Genetic analyzer (Applied Biosystems, USA). The sequencing data was analyzed using Sequencher™ v4.7.

Similarly, to validate gene of interest in plasmid vector, the sequencing reaction mix contained 0.3 μL plasmid DNA, 0.2 μL primer (forward or reverse, 10 μM), 5μL of diluted BigDye® Terminator v3.1 Ready Reaction Mix and 4.5μL of nuclease free water. The sequencing reaction was denatured at 96°C for 2 minutes followed by the same 25 sequencing cycles as mentioned before.

2.3 Vector Constructions

2.3.1 pEGFP-*TRPC6*

After total RNA was isolated from human peripheral blood using Trizol reagent (Invitrogen, USA), cDNA were synthesized using SuperScript III Reverse Transcriptase (Invitrogen, USA) and Oligo (dT) 12-18 according to manufacturer's instruction (AppendixII-2). Using human control cDNA as templates, 1uL of cDNA was used to amplify the full length human *TRPC6* cDNA (Genebank Accession Number: AJ006276). The forward and reverse primers were designed and sequences are shown below. Restriction enzyme *EcoRI* (underlined) was added on 5' of both primers to create fusion gene, EGFP-*TRPC6*.

*TRPC6*_F: AAAGAATTCCATGAGCCAGAGCCCGGCGT;

*TRPC6*_R: AAAGAATTCTTATCTATTGGTTTCCTCTTGATTTGG.

The amplification reaction was performed using Elongase enzyme (Invitrogen, USA) according to standard protocols. Denaturation was performed at 94°C for 2 min, followed by 30 cycles of denaturation at 94°C for 30 seconds, annealing at temperatures ranging from 60-55°C for 30 seconds using touchdown PCR technology (Don *et al.* 1991), and extension at 68°C for 4min. The last extension was 72°C for 10 min.

The desired band was excised under UV light and extracted and purified using QIAquick gel extraction kit (QIAGEN, Germany) according to the manufacturer's protocol (Appendix II-3). The purified PCR products were digested by EcoRI. Meanwhile, the mammalian expression vector pEGFP-C1 (Clontech, USA) was digested by EcoRI followed by the treatment of Alkaline Phosphatase (NEB, UK) to remove the 5´ phosphate groups from DNA. Ligation was performed using T4 DNA ligase (NEB, UK) followed by heat-shock transformation using One Shot® TOP10 Chemically Competent E. coli cells (Appendix II-4). Single colonies were picked and plasmid DNA was extracted by Minipre kit (QIAGEN, Germany) (Appendix II-5). The presence of insert of the plasmid DNA was validated by EcoRI digestion. The direction of *TRPC6* cDNA insert and its sequence were then confirmed via direct DNA sequencing using primers listed in Table 2-2.

Table 2-2 Primer Sequences for Validation of *TRPC6, NPHS1*and *NPHS2* cDNA

Genes	*TRPC6* (2,796 bp)	NPHS1 (3,723 bp)	NPHS2 (1,149 bp)
Forward Primers (5'-3')	atgagccagagcccggcgttc tgatcgctccacaagcctat ctgcaagtgcaatgactgca agacaatggcggtcaagttc ctgcccttcctggctctcat ttcattgcgagattcatggc ggacccctctgatcctcaaa ctactttgaggagggcagaac aggcccagatagataaggaga	agctgctcctgctgacccca agagcttggagctgccgtgc acctgacattcctggcgcgg aaggctggacagctcagcgc ttgctgcccgtgtccgtgtc tgccaaactggcccaggctg acgtgtctgccgcccaggat accagctgcccacagagcca gcagggtcggaagaggaccg gcagggtcggaagaggaccg	atggagaggagggcgcgg tgctcttcatcatcatgacc ttgccttggattcagtgacc
Reverse Primers (5'-3')	cattctggcccatgtaatcc ttggagtcacatcatgggaga ggagtccaacaacaaagtct gttttgcattatctgtgctgg ttgactgttcttccaagtga ctggaacagctcagaaatcc gctaggtcttctgtattctg	cttccgaccctgcctctgtc agttgaccacgtactcctgc atggtgcctgcctctggggt aggagctcacggtttcgcgg cttccgaccctgcctctgtc	agaccagggcctttggctct gctggcaacctcacatcttt

2.3.2 pIRES-nephrin and pIRES-podocin

Human cDNA was synthesized from human kidney total RNA (Clontech, USA). The full length human *NPHS1* (Genebank Accession Number: AF035835) was amplified by the

following two primers： *Nephrin*_F (ATGGCCCTGGGGACGAC) and *Nephrin*_R (TTACACCAGAT GTCCCCTCAGC). The purified PCR product (*NPHS1*gene) was first cloned into pGEM®-T-easy vector (Promega, USA) according to the manufacturer's protocol. After chosen the correct construct, the plasmid DNA containing *NPHS1* gene was cut by SphI followed by T4 DNA polymerase (NEB, UK) to generate blunt ends, and then it was digested by SalI. Similarly, the empty vector pIRES2 DsRed-express2 vector (Clontech, USA) was cut by XhoI followed by T4 DNA polymerase (NEB, UK) to generate the blunt ends, and then it was cut by SalI. *NPHS1* was then cloned into pIRES2 vector. The correct construct was confirmed by sequencing primers listed in Table 2-2. Since pIRES2 vector contains red fluorescent protein DsRed-Express coding region for transfection visualization, the co-transfected HEK cells containing both EGFP-*TRPC6* and IRES-*nephrin* constructs would then be yellow or orange in color.

Similarly, full length human *NPHS2* gene (Genebank Accession Number: BC029141) was amplified using two primers: *podocin*_F (ATGGAGAGGAGGGCGCGG); and *podocin*_R (CCTATAACATGGGAGAGTCTTT), and then cloned it into pGEM®-T-easy vector. The generated pGEM-*podocin* vector and pIRES2 vector were digested by EcoRI, and then the *podocin* gene was cloned into pIRES2 vector.

2.3.3 p3XFLAG-nephrin

To add the FLAG tag to the N-terminal of *nephrin* for co-immunoprecipitation study of *TRPC6* and *NPHS1*, *NPHS1* cDNA was amplified from pIRES-*nephrin* plasmid using the following pair of primers which included the sequence specific for the restriction enzyme Hind III (underlined):

*Nephrin*_H3F: GCGAAGCTTATGGCCCTGGGGACGACGCTCA

*Nephrin*_H3R: GCGAAGCTTACACCAGATGTCCCCTCAGCTCGA

The PCR product was then purified and cloned into p3XFLAG vector (Sigma, USA). The sequence of the construct was validated using designed primers listed in Table 2.2.

2.3.4 Large-scale Production of Cloned Plasmid

To obtain highly purified and large amounts of plasmid DNA for transfection, cloned plasmid DNA was transformed again, and single colonies were selected and incubated in a starter culture of 2 mL LB medium containing the appropriate selective antibiotics. The starter culture was diluted 1/500 into 120 mL selective LB medium and cultured overnight at 37^0C with agitation. The bacteria culture was harvested using an ultra-centrifuge (Sorvall RC-6 Plus) at 6,000 x *g* for 15 minutes at 4^0C. After discarding the supernatant, the plasmid DNA was extracted from the bacterial pellet using Plasmid Midi Kit (QIAGEN, Germany) according to the manufacturer's protocol (Appendix II-6). The concentration and purity of the plasmid DNA was determined by NanoDrop 1000 spectrophotometer (Thermo Scientific, USA). The insert sequence of the plasmid DNA was confirmed by sequencing again.

2.4 Site-directed Mutagenesis

Site-directed mutagenesis was performed for *TRPC6*, *NPHS1* or *NPHS2* sequence variants. Pairs of mutagenic oligonucleotide primers containing the desired sequence variants and flanked by unmodified nucleotide sequences were designed for all three genes. Table 2-3 shows the nucleotide positions for the variants (bases in bold). Published *TRPC6* mutations known to have gain of function in vitro, namely P112Q and R895C, were included as well. Mutagenesis was carried out with amplification reactions using *TRPC6*, *nephrin* or *podocin*

cDNA templates, mutagenic primers and *Pfu* DNA polymerase (Stratagene, USA) according to the manufacturer's instructions (Appendix II-7). The clones were then selected and sequenced to identify and verify the sequence variants.

Table 2-3 Primers for Site-directed Mutagenesis of Podocyte Genes

Gene and variant position	Primer sequences (5'-3')
TRPC6 c.202C>T	Forward: CAGACTGGCTCACCGG**T**G GCAGACAGTTCTCCG
	Reverse: CGGAGAACTGTCTGCC**A**CCGGTGAGCCA GTCTG
TRPC6 c.334C>A	Forward: GCTGAATATGGTAACATCC**A**AGTGGTGCGGAAG
	Reverse: CTAACATCTTCCGCACCACT**T**GGATGTTACCATA
*TRPC6*c.2683C>T	Forward: GACATCTCAAGTCTC**T**GCTATGAACTCCTTG
	Reverse: CAAGGAGTTCATAGC**A**GAGACTTGAGATGTC
NPHS1c.294C>T	Forward: GAATTCCACCTGCACAT**T**GAGGCCTGTGACCTCAG
	Reverse: CTGAGGTCACAGGCCTC**A**ATGTGCAGGTGGAATTC
NPHS1c.2289C>T	Forward: CATAGTCTGCACTGT**T**GATGCCAATCCCATC
	Reverse: GATGGGATTGGCATC**A**ACAGTGCAGACTATG
NPHS2c.954T>C	Forward: CAGGCACCCCTGCTGC**T**GTTCAGCTTCGATACC
	Reverse: GGTATCGAAGCTGAAC**A**GCAGCAGGGGTGCCTG

2.5 Cell Cultures and Transfection Experiments

Human embryonic kidney cells stably transfected with M1 muscarinic receptor (HEK293-M1) were kindly provided by Dr. David E Clapham from Harvard University (Reiser *et al.* 2005). The cells were grown at 37^0C in monolayer culture in a humidified air atmosphere with 5% CO_2. The culture medium contained Dulbecco's modified Eagle medium (DMEM), (Gibco, USA), and Ham's F-12 medium (1:1) with 10% heat-inactivated fetal bovine serum (FBS), 100U/ml penicillin, 100μg/ml streptomycin and100μg/ml G418. Similarly, HEK293 cells were cultured in DMEM (Gibco, USA) supplemented with 10% FBS, 100 U/mL penicillin and 100 μg /ml streptomycin (Gibco, USA).

TRPC6 cDNA was transfected into HEK293-M1 cells alone, or in combination with *NPHS1* or *NPHS2* cDNA, using calcium phosphate precipitation method (Liao *et al.* 2007)

(Appendix II-8). One day before transfection, HEK293-M1 cells were plated at low density onto poly-D-lysine coated cover slips in 35-mm Petri dishes. Subsequently, the culture medium was replaced with new medium with antibiotics free, and 1μg of WT or mutant *TRPC6* cDNA was transiently transfected into HEK293-M1 cells with or without 1μg of *NPHS1/NPHS2* variant cDNA. Six hours later, culture medium was replaced without antibiotics. The cells were grown for 24–48h after transfection before whole-cell patch clamp recordings.

2.6 Patch-clamp Electrophysiology

HEK293-M1 cells with EGFP-*TRPC6* alone, or in combination with *NPHS1* or *NPHS2*, were visualized under fluorescence microscope (Olympus, Japan) and currents were recorded using Axopatch 200B amplifier. The pClamp9 software (Axon Instruments, USA) was used to analyze the currents. The borosilicate glass pipettes were pulled using Micropipette horizontal Puller (Sutter Instrument, USA) and polished with fire polisher (Digitimer, UK) to obtain pipette resistances of 1.3–2.5 MΩ. Cells with leak currents lower than 50 pA were selected for recording. In this study, a patch of the membrane was isolated electrically from extracellular solution with a glass electrode. After the glass electrode touches the cell surface, a light suction force was applied to achieve gigaseal. A stronger suction force was then applied to rupture the patch membrane within the glass electrode (Figure 2-1). Whole cell patch clamp technique was then performed to measure the current though *TRPC6* channels. For cells transfected with *TRPC6* alone, we used the voltage-ramp protocol in which voltage ramps from -100 mV to 100 mV over 150 milliseconds were applied to the cells every 3.45 s (Reiser *et al.* 2005). Current traces were recorded from a holding potential of 0 mV. All currents were determined by recording the capacitative current by a voltage clamp, and they were normalized to cell size (Appendix I-2). For cells cotransfected with *TRPC6* and nephrin or podocin, we applied gap-free protocol in which the cells were held at holding potential of 0 mV for the duration of the experiment (Inoue *et al.* 2009). Similarly, the normalized

currents were in Appendix I-3 to I-6.

The bath solution contained 135 mM NaCl, 5 mM CsCl, 2 mM $CaCl_2$, 1 mM $MgCl_2$, 10 mM HEPES and 10 mM glucose (pH 7.4). The pipette solution contained 135 mM CsMES, 10 mM CsCl, 3 mM MgATP, 0.2 mM NaGTP, 0.2 mM EGTA, 0.13 mM $CaCl_2$ and 10 mM HEPES buffer (pH 7.3). Pipette offset function was used to minimize junction potential affection. Whole-cell currents were sampled at 10 kHz and filtered at 1 kHz. All recordings were carried out at room temperature (25^0C).

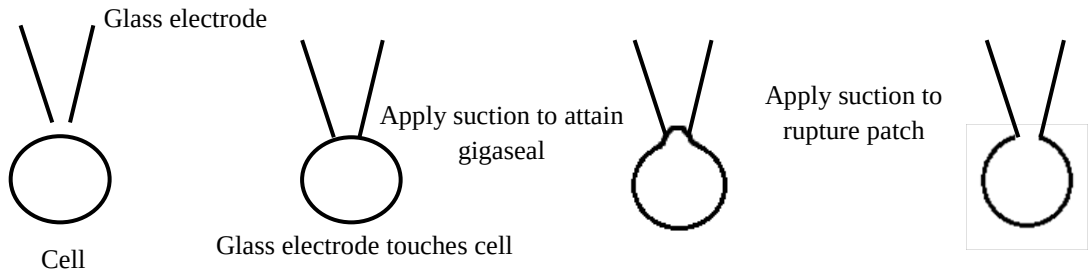

Figure 2-1 Diagram Illustrating Steps to Achieve Whole-cell Patch Clamp.
In this study, whole cell patch clamp method was used to study the overall currents through *TRPC6*.

2.7 Western Blotting and Co-immunoprecipitation

Wild-type *nephrin*, or variants (c.294C>T, c2289C>T), together with pEGFP-C1 vector were transiently transfected into HEK293-M1 cells. At 24 hours, the total protein was extracted by CelLytic M reagent (Sigma, USA). Western blotting methods were performed using anti-*nephrin* antibody (Abcam, UK) according to standard procedures (Appendix II-9). The protein bands were quantified using the Image J software (available at http://rsb.info.nih.gov/ij) and normalized to GFP band densities (Appendix I-7).

Interactions between *TRPC6* and *nephrin* variants were studied by co-immunoprecipitation. This was performed using immunoprecipitation kit (Roche, Switzerland) according to the standard protocols. HEK-M1 cells that were seeded in 10cm petri dish were transiently transfected with 5 μg of each plasmid DNA encoding EGFP-*TRPC6* and FLAG-*nephrin* using Lipofectamine^{2000} reagent according to the manufacturer's protocol. After 24 h incubation, the cells were lysed with 1mL of ice-cold lysis buffer for 30 minutes. They were then scraped form the surface of the petri dish and centrifuges at 12,000 *g* for 15 minutes. To precipitate FLAG-*nephrin* construct, the supernatant was collected and immunoprecipitated with 50 μL of protein G-agarose beads and anti-EGFP (Roche, Switzerland) primary antibody for 4 h. Samples were then centrifuged for 1 min at 800 *g* and washed twice with ice-cold lysis buffer. Similarly, to precipitate EGFP-*TRPC6* construct, anti-FLAG primary antibody (Santa Cruz, USA) was used. Immunoprocipitated protein were dissolved in 40 μL of 2 × Laemmli buffer and boiled for 5 min before western blot analysis of *nephrin* or *TRPC6.*

2.8 Surface Expression of *TRPC6*

HEK293 cells were co-transfected with Fyn and wild-type or mutant *TRPC6* cDNA, as well as the *nephrin* homozygous variants c.294C>T and c.2289C>T. These cells were surface biotinylated with biotin-SS reagent according to the manufacturer's instructions (Pierce, USA), and pulled down with streptavidin agarose beads. Immunoblotting with anti-EGFP was performed on both biotinylated and whole-cell total lysates (Winn *et al.* 2005). The control samples were from cells transfected with EGFP-*TRPC6*^{WT} and harvested without adding biotin-SS reagent. The reported *TRPC6* mutation p.P112Q was used as a positive control. The surface protein was normalized to total protein extracted (Appendix I-7).

2.9 RNA Stability Assay

Transfected cells treatment and RNA extraction. In this experiment, 10^6 HEK293 cells per well were transfected with 1μg wild-type nephrin or its variants (c.294C>T singly, c2289C>T singly, and double SNPs) in 6-well multiple well microplate (Corning®, USA) using calcium phosphate precipitation method. Six hours after transfection, the cell medium was replaced with growth medium containing 5 μg/ml actinomycin D (Sigma, USA) in the absence of antibiotics. The cells were cultured for another 24 hours before being harvested. Total RNA from transfected cells was isolated before and after incubation with actinomycin D using TRIzol reagenet (Invitrogen, USA) following the manufacturer's instructions (Appendix II-10). All transfection experiments were carried out in triplicates.

Quantification of transcripts. Reverse transcription of 1 μg RNA was performed using Maxima First Strand cDNA Synthesis Kit (Thermo Scientific, USA) with a total volume of 20μL according to the manufacturer's instructions. Real-time PCR was carried on LightCycler® 480 (Roche Diagnostic, Switzerland). To amplify *nephrin* cDNA, 2ul of cDNA was used and the primers were *Nephrin*-8F (ACCAGCTGCCCACAGAGCCA) and *Nephrin*9R (CTTCCGACCCTGCCT CTGTC). The housekeeping gene GAPDH was amplified using GAPDH-F (CTGGCATGGCCTTCCGTGTC) and GAPDH-R (GGAGGAGTGGGTGTCGCTGT) primers. PCR reactions were pre-incubated for 10min at 95°C followed by 42 cycles of 5 sec at 95°C, 10 sec at 60°C, and 12 sec at 72°C (Appendix II-11). All PCR assays were performed in duplicates. The fluorescent melting curves acquired were analysed using the LC480 Gene Scanning software v1.5 (Roche Diagnostics, Switzerland). Normalization was performed to adjust the florescent signals of all the samples prior to melting to all the same level. The transfection efficiency of each group is equal confirmed by co-transfected pEGFP-C1 plasmid DNA.

2.10 Statistics Analysis

Data analysis was performed using SPSS 20.0 for Windows (Chicago, IL). Allele frequencies were compared by chi-square test. All variants in the controls were analyzed for Hardy–Weinberg equilibrium using the Pearson Chi-square test. Haplotype analysis using SNPstat software (http://bioinfo.iconcologia.net/SNPStats_web) was performed for variants that fulfilled Hardy–Weinberg equilibrium (Sole *et al.* 2006). Electrophysiological currents in whole-cell patch-clamp were expressed as mean ± SEM and compared using two-tailed unpaired Student's t tests. For multiple comparisons, one-way ANOVA was performed with Bonferroni correction. A p value of less than 0.05 was considered statistically significant.

CHAPTER 3 MUTATIONAL SCREENING OF PODOCYTE GENES IN PATIENTS WITH NEPHROTIC SYNDROME/FSGS

3.1 Introduction

Focal segmental glomerulosclerosis (FSGS) is the most common cause of therapy-resistant nephrotic syndrome in children worldwide. About 10% of children with nephrotic syndrome are steroid-resistant and of these, 70% have FSGS (Cattran and Rao 1998; Mekahli *et al.* 2009). In Singapore, 65% of children biopsied for steroid-dependent or steroid-resistant nephrotic syndrome showed FSGS as the underlying histopathology (unpublished data, Children's Kidney Center, Singapore). In adults, approximately 30–50% of them with FSGS do not respond to steroid therapy (Haas *et al.* 1997).

Typical clinical manifestations of FSGS include proteinuria, hypertension and nephrotic syndrome. FSGS generally has a poor outlook. About 30-40% of children with FSGS progress to end-stage renal disease (ESRD) within ten years (Cattran and Rao 1998; Mekahli *et al.* 2009). In North America, FSGS accounts for 5–20% of all ESRD cases and it is the second leading cause of ESRD in children (Kitiyakara *et al.* 2003; Kitiyakara *et al.* 2004; 2007). FSGS is also an important cause of chronic kidney disease in adults (Schlondorff and Pollak 2006). The global incidence of FSGS has been increasing and the current annual incidence is estimated at 0.8 per 100,000 (Woo *et al.* 2010; McGrogan *et al.* 2011). The proportion of ESRD attributed to FSGS has also increased more than 10-fold between 1980 and 2000, and FSGS now accounts for 12.2% of incident pediatric patients with ESRD in the United States (Kitiyakara *et al.* 2003; Kitiyakara *et al.* 2004; Collins *et al.* 2013).Primary FSGS occurs due to podocyte injury, which can be immune-mediated or as a result of mutations in the podocyte genes (Reiser *et al.* 2005; Winn *et al.* 2005). Recent research has implicated as many as 24 podocyte genes in primary nephrotic syndrome/FSGS (McCarthy *et al.* 2013). Examples of genes implicated in childhood SRNS and FSGS are podocin (*NPHS2),* nephrin (*NPHS1)* and wilms tumor 1 (*WT1)*(McCarthy and Saleem 2011), while examples in

adult-onset nephrotic syndrome include podocin (*NPHS2)*, alpha-actinin 4 (*ACTN4*) and *TRPC6* (McCarthy and Saleem 2011). Among these, mutations in nephrin and podocin are most common. They cause two types of severe nephrotic syndrome presenting in early life, Finnish type congenital nephrotic syndrome (CNF) and a form of autosomal recessive familial FSGS, respectively.

Nephrin is the first podocyte structural protein that is linked to CNF (Kestila *et al.* 1998). Its deficiency was also detected in other forms of NS. Additionally, an overlap in *NPHS1/NPHS2* mutation spectrum was documented in patients with congenital FSGS (Koziell *et al.* 2002). They together cause almost 60% of the cases of nephrotic syndrome (Mucha *et al.* 2006). Table 3-1 provides a summary of the prevalence of *NPHS1*, *NPHS2* and *TRPC6* mutations in childhood and adult-onset SRNS/FSGS. Of note, the prevalence of these mutations is dependent on many factors, such as the family history, age of onset, ethnicity, and histologic lesion. As shown in this table, almost 100% of patients with CNS have a mutation. Podocin mutations have an ethnicity bias. They are most frequently reported in Western European countries, and R138Q mutation is considered a European founder mutation (McKenzie *et al.* 2007; Rood *et al.* 2012).

Table 3-1 Prevalence of *NPHS1, NPHS2,* and *TRPC6* Mutations in SRNS/FSGS

Genes	Age of onset					
	CNS	**Infantile NS**	**Childhood NS**	**Adult FSGS (familial)**	**Adult FSGS (sporadic)**	**Remarks**
NPHS1	34–90% (Kestila *et al.* 1998; Hinkes *et al.* 2007; Buscher *et al.* 2010; Santin *et al.* 2011)	0–2% (Hinkes *et al.* 2007; Buscher *et al.* 2010).	14% (Santin *et al.* 2009)	n.a.	2% (Santin *et al.* 2009)	
NPHS2	0–51% (Kestila *et al.* 1998; Hinkes *et al.* 2007; Buscher *et al.* 2010; Santin *et al.* 2011)	19–41% (Hinkes *et al.* 2007; Buscher *et al.* 2010)	0–18% (Gbadegesin *et al.* 2007; He *et al.* 2007; Cho *et al.* 2008; Hinkes *et al.* 2008; Lowik *et al.* 2008)	4–24% (Tonna *et al.* 2008; Machuca *et al.* 2009)	0–11% (Aucella *et al.* 2005; He *et al.* 2007; McKenzie *et al.* 2007; Tonna *et al.* 2008; Machuca *et al.* 2009)	In Western European adults, adult-onset FSGS is caused by combination of R229Q and one pathogenic NPHS2 mutation. NPHS2 mutation.
TRPC6	n.a.	5% (Buscher *et al.* 2010)	0–6% (Lowik *et al.* 2008; Heeringa *et al.* 2009; Santin *et al.* 2009; Gigante *et al.* 2011)	0–12% (Reiser *et al.* 2005; Heeringa *et al.* 2009)	0–2% (Lowik *et al.* 2008; Santin *et al.* 2009)	Study from Heeringa et al. included patients with age of onset 9–30 years (Heeringa *et al.* 2009)

*: This table is adapted from Rood et al., (Rood *et al.* 2012)

TRPC6 belongs to the transient receptor potential superfamily of cation-selective ion channels. It is a calcium-permeable cation channel important for the increase of intracellular calcium concentration after the engagement of G protein-coupled receptors and receptor tyrosine kinases (Montell 2005). *TRPC6* mutations were first reported to cause FSGS in 2005 by two independent research groups (Reiser *et al.* 2005; Winn *et al.* 2005), and since then, more than 10 *TRPC6* mutations have been identified as a cause of autosomal dominant inherited FSGS in late adolescence and adulthood. However, whether *TRPC6* is mutated in Singapore patients with nephrotic syndrome and/or FSGS is unknown.

Most current treatment strategies for FSGS involve empirical and non-directed use of immunosuppressants including high-dose steroids, calcineurin inhibitors such as cyclosporine A (CSA), mycophenolate mofetil, and even biologicals such as Rituximab. These medications are not only expensive, but also have many side effects including susceptibility to infections and malignancy. More importantly, not all patients will respond to these treatments. Overall, only about 50% of FSGS patients given empirical treatment respond to steroids and/or calcineurin inhibitors(D'Agati *et al.* 2011). In general, patients with immune FSGS are much more likely to respond to immunosuppressants while those with genetic FSGS are less likely to do so, except for those with mutations in certain specific genes such as *WT1*. This is clearly shown in Table 3-2 which summarizes findings in the literature on the response of genetic FSGS patients to CSA. Of the patients in whom genetic mutations have been found, 32% responded to CSA, while 68% did not. This is in contrast to patients in whom no genetic mutation was found, 67% responded to CSA while 32% were resistant. Buscher et al showed that this disparity in CSA response between the two groups was statistically significant.(Buscher *et al.* 2010) It is thought that genetic FSGS patients respond to calcineurin inhibitors due to their direct modulating effects on the podocytes (Faul *et al.*

2008; Schonenberger *et al.* 2011). Interestingly, the response to immunosuppression appears to be gene-dependent. Those with *WT1* or heterozygous *NPHS2* mutations are more likely to respond to CSA compared to those with mutations in other genes (Table 3-2). The exact mechanism of this is unknown.

Table 3-2 Response of Genetic and Non-genetic Primary FSGS Patients to Cyclosporine A

Gene		CSA-resistant (No. of patients)	CSA-esponsive (No. of patients)	Response to CSA	References
NPHS1		3	0	NA	(Buscher *et al.*
		0	1*	Unknown	(Caridi *et al.* 2003)
	Total	**3 (75%)**	**1 (25%)**		
NPHS2 (homozygous or compound heterozygous)		8	0	NA	(Caridi *et al.* 2003)
		4	0	NA	(Buscher *et al.*
		5	0	NA	(Ehrich *et al.* 2007)
		5	0	NA	(Buscher *et al.*
		14	5	Partial	(Ruf *et al.* 2004)
		2	1	Partial	(Megremis *et al.*
		0	1	Partial	(Malina *et al.* 2009)
	Total	**38 (84%)**	**7 ((16%)**		
NPHS2 (Heterozygous)		2	1	Unknown	(Caridi *et al.* 2003)
		2	3	Complete (2),	(Ruf *et al.* 2004)
		1	4	Complete (3),	(Buscher *et al.*
		2	0	NA	#
	Total	**7 (47%)**	**8 (53%)**		
WT1		4	0	NA	(Ehrich *et al.* 2007)
		0	3	Complete (1), Partial (2)	(Gellermann *et al.* 2010) (CR)
		0	2	Partial	(Sinha *et al.* 2010)
		0	2	Partial	(Buscher *et al.*
		0	1	Complete	(Wasilewska *et al.*
	Total	**4 (33%)**	**8 ((66%)**		
TRPC6		2	0	NA	(Buscher *et al.*
		2	0	NA	#
	Total	**4 (100%)**	**0**		
PLCE1		0	2		(Hinkes *et al.* 2006)
Overall	**Total**	**56 (68%)**	**26 (32%)**		
Non-genetic		**10 (32%`)**	**21 (67%)**	Complete	(Buscher *et al.*

Note: All patients are steroid-resistant.CSA: cyclosporine A; NA: not applicable; CR: case report. * concurrent podocin R229Q; # data from preliminary study in our center; † Data collated from the genetic studies listed in this table.

Given the general poor response to immunosuppression in genetic FSGS, it is recommended that all steroid-resistant patients should undergo genetic testing, and if mutations are found, intensified immunosuppression should not be given (Buscher *et al.* 2010; McCarthy and Saleem 2011; Santin *et al.* 2011). This not only avoids the adverse effects, but also the high costs of these drugs. Additionally, genetic screening has implications on donor selection as potential donors with mutations are generally not accepted due to theoretical increased susceptibilities of both donor and recipient towards later development of FSGS (Santin *et al.* 2009).

In this chapter, we attempted to screen podocyte gene mutations, including *NPHS1, NPHS2, TRPC6* from Singapore patients with NS and/or FSGS, and tried to compare the allele and genotype frequencies of the sequence variants found in patients and healthy controls.

3.2 Results

We recruited 97 unrelated Singapore Chinese patients with idiopathic sporadic NS (mean age at disease onset 5.7 years, range 0.9-19.0 years) with steroid-resistant nephrotic syndrome and/or FSGS and 128 unrelated Singapore Chinese cord blood controls with no known family history of renal diseases. Control data from the Singapore Genome Variation Project (96 Singaporean Chinese) (Teo *et al.* 2009) and local exome sequencing data (200 Singaporean Chinese) were also used for comparison. All variants in the controls were analyzed for Hardy–Weinberg equilibrium using the Pearson Chi-square test. Haplotype analysis using SNPstat software (http://bioinfo.iconcologia.net/SNPStats_web) was performed for variants that fulfilled Hardy–Weinberg equilibrium (Sole *et al.* 2006).

3.2.1 Phenotypes in Family

The proband (III.2) (Figure 3-1) presented with non-nephrotic proteinuria, microscopic hematuria and normal renal function at seven years old. Renal biopsy yielded 22 glomeruli, of which one had global sclerosis and another had segmental sclerosis. The remaining glomeruli had mild increase in mesangial matrix with no increase in mesangial cells. Occasional tubules were atrophied. The interstitium had focal lymphocyte collections around the sclerosed glomeruli. Immunofluorescence examination was negative. Electron microscopy was not performed. This histological finding was compatible with FSGS, not otherwise specified. He was initially treated with an angiotensin-converting-enzyme inhibitor, but his proteinuria worsened to nephrotic range three years later. He was started on prednisolone, cyclosporine A and mycophenolate mofetil, which he did not respond. He eventually reached ESRD by 16 years old. He received a deceased-donor renal transplant at 25 years old but died from a bleeding duodenal ulcer one month later. There was no FSGS recurrence post-transplant.

The proband's mother (II.4) developed proteinuria and microscopic hematuria, with normal renal function, at the age of 17 years. Renal biopsy yielded 11 glomeruli, of which two had segmental sclerosis. A few tubules were atrophied within the focally fibrotic interstitium. Immunofluorescence was negative. Electron microscopy was not performed. She did not receive any treatment and was lost to follow-up. She subsequently had two pregnancies at 29 and 31 years old, during which she had pre-eclampsia in the third trimesters. After her second pregnancy, her serum creatinine was 119 μmol/L and urine total protein 0.18 g/day. Two years later, her serum creatinine rose to 146 μmol/L (creatinine clearance 55 ml/min) and urine total protein was 4.7 g/day. She reached ESRD by 35 years of age and received a renal

transplant from II.2. To date at 19 years post-transplant, both donor and recipient had normal renal function and no proteinuria.

The proband's sister (III.3) developed hematuria and proteinuria of 0.74 g/day/1.73m^2 at the age of 12 years. Her proteinuria normalized following treatment with aldosterone receptor blockers. Her renal function had remained normal. No renal biopsy was performed. The youngest brother (III.4) had remained healthy to date.

3.2.2 Genotypes in Family

The human *TRPC6* gene has 13 exons and is 132.37 kb long. Using primers designed (table 2-1), we screened for *TRPC6* sequence variants in its promoter region (1000bp upstream of 5'-UTR), both UTRs, 13 exons and the intron-exon boundaries in this family. Human genomic *TRPC6* sequence was obtained from NCBI database (NG_011476). We found a variant c.−254C>G in 5' UTR which is listed in NCBI SNP database (rs3824934). We also found a heterozygous novel *TRPC6* mutation c.202C>T in exon 2, resulting in the substitution of arginine-68 (positively charged) to tryptophan (hydrophobic), in six members of the family (Figure 3-1). Of these, three (II.4, III.2 and III.3) were penetrant, while the other three (I.1, II.2, III.4) have remained non-penetrant (Figure 3-1). Notably, II.2, who donated a kidney to II.4, has the *TRPC6* mutation. This *TRPC6* p.R68W mutation occurs at an evolutionary highly conserved residue of the protein which is also present in *TRPC3* and *TRPC7* (Figure 3-3). It is just proximal to the first ankyrin repeat which starts from amino acid residue 97 (Figure 3-4). There are no sequence conflicts or putative alternative splicing sites near this mutation. It is found in one out of 256 chromosomes of cord blood controls,

but is not present in the dbSNP (NCBI), 1000genomes and NHLBI exome sequencing (6500 exomes) databases. It is also not present in the exomes of 200 Singapore Chinese controls. No mutations in *ACTN4*, *NPHS2* or *CD2AP* were found in this family.

Meanwhile, two synonymous *NPHS1* polymorphisms, rs2285450 (c.294C>T) and rs437168 (c.2289C>T) and one *NPHS2* polymorphism rs1410592 (c.954T>C) (Figure 3.2), which segregated with renal disease, were identified in this family. These three SNPs were also found in our 97 Singapore Chinese paediatrics patients. The family members with FSGS (II.4 and III.2) were homozygous for both *NPHS1* polymorphisms, while the donor (II.2) did not have any *NPHS1* polymorphisms at the two positions. Interestingly, the proteinuric patient (III.3), together with the two other non-penetrant members (I.1 and III.4), had heterozygous c.294C>T and heterozygous c.2289C>T *NPHS1* polymorphisms.

All three penetrant family members (II.4, III.2 and III.3) and one non-penetrant member III.4 were homozygous for the *NPHS2* c.954T>C polymorphism. One other non-penetrant member I.1 had heterozygous *NPHS2* c.954T>C polymorphism while the donor II.2 did not have the polymorphism.

It appeared that the *NPHS1* c.294C>T and c.2289C>T and *NPHS2* c.954T>C polymorphisms segregated with renal disease in this family, and that the donor II.2 did not have all of these three polymorphisms.

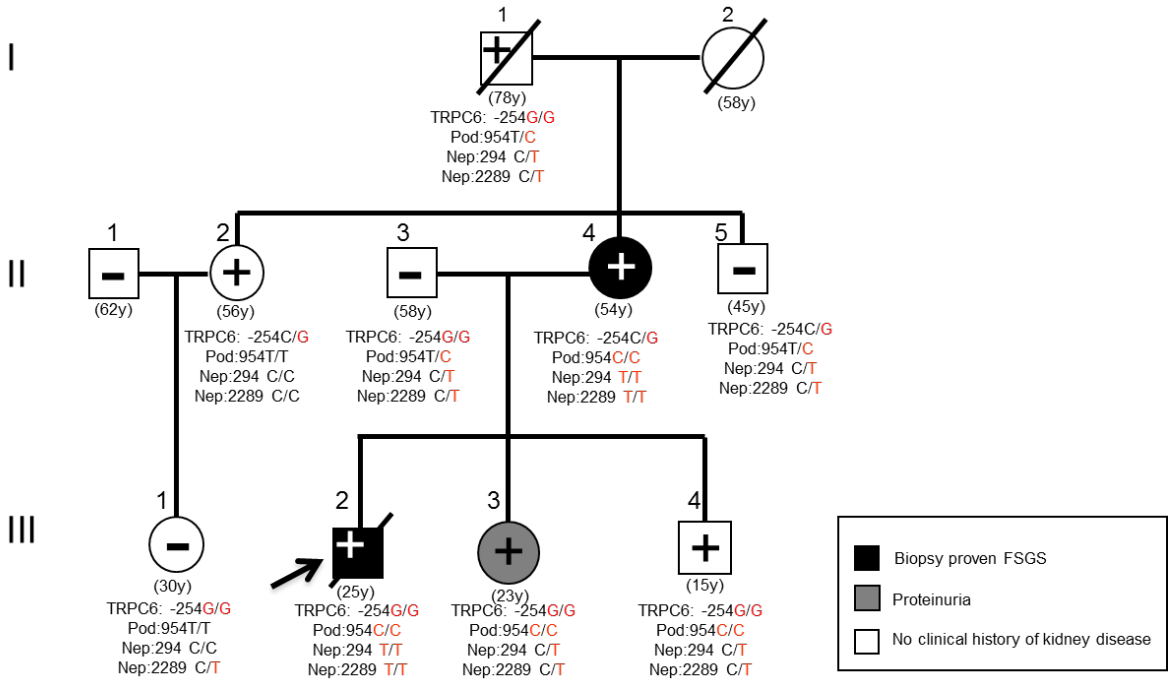

Figure 3-1 Pedigree of the Family with Novel *TRPC6* Mutation and Histological Changes in the Glomeruli.

The proband (III.2) is indicated by the arrow. Squares indicate male family members, circles indicate female family members, black symbols indicate individuals with FSGS and ESRD, grey symbol indicate individual with proteinuria and slashes deceased persons. The plus signs indicate *TRPC6* heterozygous c.202C>T mutation, while the minus signs indicate WT *TRPC6* alleles. Ages (in years) at last observation or at death are shown in brackets. The alleles at coding nucleotide positions 294 and 2289 of the *NPHS1* gene (Nep), 954 of the *NPHS2* gene (Pod), and *TRPC6* promoter polymorphism at -254, are shown below the squares or circles. Alleles in black indicate WT alleles while those in red indicate variant (minor) alleles.

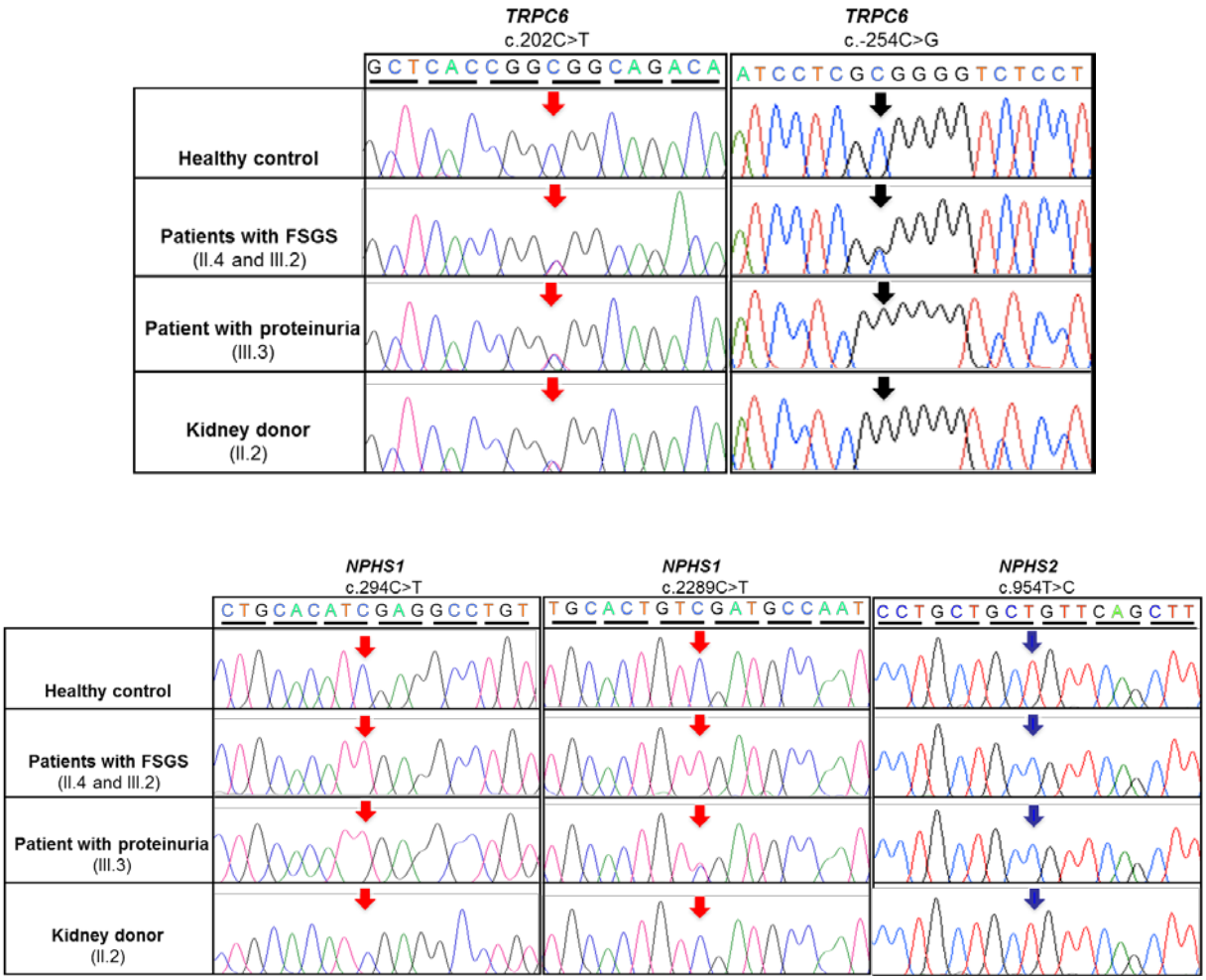

Figure 3-2 Sequencing Electropherograms of Selected Members in the Family.

Five variants were detected in three podocyte genes, *TRPC6*, *NPHS1* and *NPHS2*: *TRPC6* c.202C>T and c.-254C>G; *NPHS1* c.294C>T and c.2289C>T; *NPHS2* c.954T>C. The individuals with renal disease (II.4, III.2, III.3) and the kidney donor (II.2) have the heterozygous *TRPC6* c.202C>T mutation. All of the selected members have either heterozygous or homozygous *TRPC6* c.-254C>G polymorphism. Both II.4 and III.2 have homozygous *NPHS1* c.294C>T and c.2289C>T while III.3 carries heterozygous c.294C>T and heterozygous c.2289C>T polymorphisms. In contrast, kidney donor II.2 has no *NPHS1* and *NPHS2* polymorphisms at the three positions. Patient II.4 and her three children had homozygous *NPHS2* c.954T>C. The uppermost electropherogram is from a healthy control.

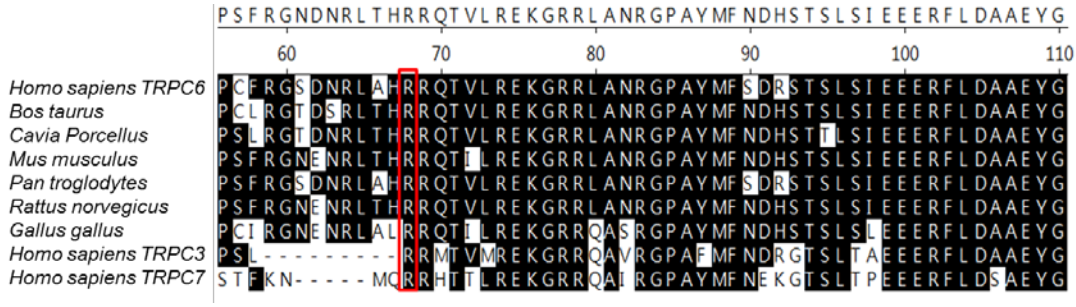

Figure 3-3 Sequence Alignment of *TRPC3, TRPC6* and *TRPC7* in *Homo Sapiens* and *TRPC6* Homologues among Various Species.

Highly conserved amino acid residues are highlighted black. The red box indicates the location of the highly conserved arginine-68 that is changed to tryptophan.

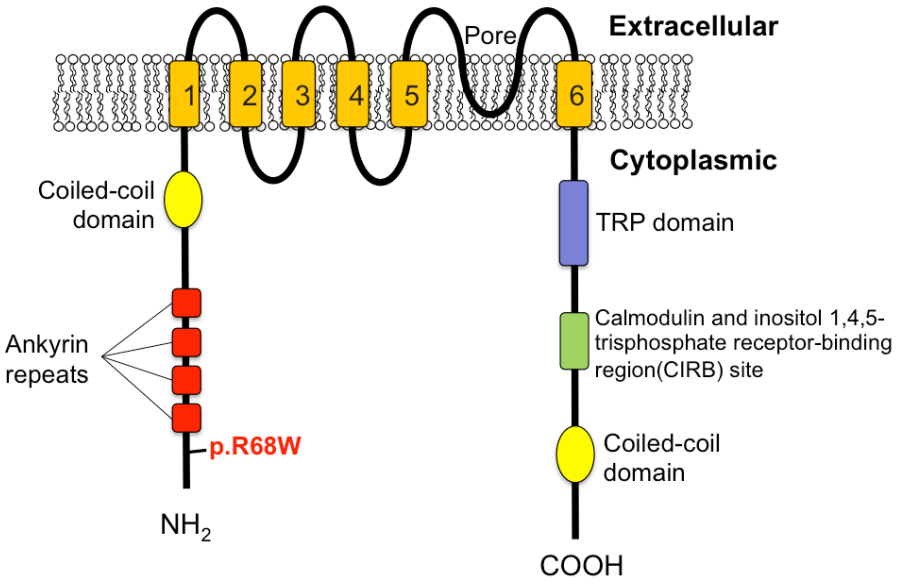

Figure 3-4 Functional Domains of the *TRPC6* Protein.

TRPC6 channels comprise of a membrane domain with six transmembrane segments and the NH_2 and COOH termini are within the cytoplasm. Four ankyrin repeats and a coiled-coil domain are present near the NH_2 terminal. Ankyrin repeats and coiled-coil domains play a role in protein-protein interactions. The p.R68W mutation occurs just proximal to the first ankyrin repeat which starts at amino acid 97.

3.2.3 Genetic Analysis of SRNS/FSGS Patients

3.2.3.1 TRPC6 c.-254C>G polymorphism

It has been reported that the *TRPC6* c.−254C>G polymorphism in idiopathic pulmonary arterial hypertension patients was significantly more common than normal subjects (Yu *et al.* 2009). Hence we tried to compare the allele frequency of this polymorphism in NS/FSGS patients versus healthy subjects. We recruited 88 SRNS/FSGS patients and 91 controls in the Singapore Chinese population.

Our results showed that *TRPC6* c.−254C>G is a common polymorphism. Among the healthy subjects, the G allele frequency (59.1%) was higher than wild-type C allele frequency (40.9%), as shown in Table 3-3. Similarly, among the patients, the G allele frequency (54%) was higher than wild-type C allele frequency (46.0%). There was no statistical difference in the allele frequencies between patients and controls. Genotype analysis showed that for both patients and controls, about one quarter had two wild-type alleles, one quarter had homozygous polymorphism while the rest were heterozygous (Table 3-4). When the genotypes were analyzed using four different models (dominant, co-dominant, over-dominant and recessive models), there was no significant difference among patients and normal subjects, indicating that this *TRPC6* c.954T>C is most likely not a disease-causing polymorphism.

Table 3-3 Allele Frequencies of *TRPC6* c.- 254C>G in Chinese patients and controls

Position (nt.)	SNP	Allele	Controls (n=91), n (%)	NS/FSGS (n=88), n (%)	Odds Ratio (95% CI)	*P*
-254	C to G	C	88 (40.9)	81 (46)	1.10 (0.72 to 1.66)	0.67
		G	94 (59.1)	95 (54)		

P values, odds ratios, and 95% CIs are calculated by X^2 analysis for 2X2 contingency tables.

Table 3-4 Association Study of *TRPC6* c.-254C>G Genotype and its Response Status (crude analysis)

Model	Genotype	Controls (n=91), n (%)	NS/ FSGS (88), n (%)	OR (95% CI)	P
Co-dominant	C/C	19 (20.9)	22 (25)	1.00	0.21
	C/G	50 (55)	37 (42)	0.64 (0.30-1.35)	
	G/G	22 (24.2)	29 (33)	1.14 (0.50-2.60)	
Dominant	C/C	19 (20.9)	22 (25)	1.00	0.51
	C/G-G/G	72 (79.1)	66 (75)	0.79 (0.39-1.59)	
Recessive	C/C-C/G	69 (75.8)	59 (67)	1.00	0.19
	G/G	22 (24.2)	29 (33)	1.54 (0.80-2.97)	
Over-dominant	C/C-G/G	41 (45)	51 (58)	1.00	0.084
	C/G	50 (55)	37 (42)	0.59 (0.33-1.07)	
Log-additive	---	---	---	1.10 (0.73-1.65)	0.66

3.2.3.2 NPHS1 c.294C>T and c.2289C>T polymorphisms

As shown in the family tree in Figure 3-1, the two *NPHS1* SNPs, c.294C>T and c.2289C>T were also detected in the family members. Association analysis of the two SNPs with nephrotic syndrome in Chinese population was performed. For the genotype frequencies of c.294C>T, we found that 75% of healthy controls had wild-type alleles, 25% had heterozygous alleles and none had homozygous T alleles. In contrast, in NS/FSGS patients, 3% of them had homozygous T alleles (Table 3-5). Similarly, for c.2289C>T polymorphism, we found in the Chinese controls, 69% had wild-type alleles, 28% were heterozygous and 3% were homozygous, whereas in patients, 51% had wild-type alleles, 45% were heterozygous, and 4% were homozygous (Table 3-5). Genotypes association analysis of the two *NPHS1*

SNPs with NS showed that, in the Chinese patients, c.294C>T and c.2289C>T were both significantly associated with NS (Table 3-6). We found that c.294C>T was significantly associated with NS under the dominant (OR: 1.74, 95% CI 1.04-2.90, p=0.035), and log-additive (OR: 1.86, 95%CI 1.15-3.02, p=0.012) models. c.2289C>T was significantly associated with NS under the codominant (OR: 2.24, 95%CI 1.47-3.41, p=0.0008), dominant (OR: 2.22, 95%CI 1.47-3.34, p=0.0002), overdominant (OR: 2.16, 95%CI 1.43-3.26, p=0.0003) and log-additive (OR: 1.83, 95%CI: 1.31-2.55, p=0.0006) models.

Table 3-5 Genotype Frequencies of *NPHS1* and *NPHS2* SNPs in Chinese

NPHS1 **c.294C>T**	**Controls (n=221)**	**Patients (n=97)**	***NPHS1*** **c.2289C>T**	**Controls (n=1903)**	**Patients (n=97)**
CC	165 (75%)	61 (63%)	**CC**	1320 (69%)	49 (51%)
CT	56 (25%)	33 (34%)	**CT**	529 (28%)	44 (45%)
TT	0 (0%)	3 (3%)	**TT**	54 (3%)	4 (4%)

Table 3-6 Association Analysis of *NPHS1* Genotypes with NS in Chinese

	c.294C>T		**c.2289C>T**	
	Patients (n=97)	**Controls (n=221)**	**Patient (n=97)**	**Controls (n=1903)**
Patients vs Controls	***Dominant:*** OR: 1.74 (1.04-2.90), **p=0.035** ***Log-additive:*** OR: 1.86 (1.15-3.02), **p=0.012**		***Codominant (C/T):*** OR: 2.24 (1.47-3.41), **p=0.0008** ***Dominant:*** OR: 2.22 (1.47-3.34), **p=0.0002**	

	c.294C>T		c.2289C>T	
	Patients (n=97)	**Controls (n=221)**	**Patient (n=97)**	**Controls (n=1903)**
			Overdominant: OR: 2.16 (1.43-3.26), **p=0.0003** ***Log additive:*** OR: 1.83 (1.31-2.55), **p=0.0006**	

3.2.3.3 NPHS2 c.954T>C Polymorphism

We studied the *NPHS2* c.954T>C polymorphism in the Singapore Chinese population. Table 3-7 showed its genotype and allele frequencies. It was shown that *NPHS2* c.954T>C was a common polymorphism. In both controls and patients, around half of them were heterozygous, and about 30% had homozygous polymorphism. A similar trend was seen in its allele frequencies (Table 3-7). The association study for *NPHS2* c.954T>C polymorphism also showed that there was no statistical difference between controls and patients (data were not shown).

Table 3-7 Genotype and Allele Frequencies of *NPHS2* c.954T>C SNP in Chinese

NPHS2 c.954T>C		Controls (n=125), n (%)	NS/FSGS (n=97), n (%)	p
Genotype frequency	TT	24 (19%)	21 (22%)	0.7369*
	TC	65 (52%)	49 (50%)	
	CC	36 (29%)	27 (28%)	
Allele frequency	T	113 (42%)	91 (47%)	0.77
	C	137 (58%)	103 (53%)	

P values are calculated by X^2 analysis for comparison of the genotype frequencies between patients and controls.

* P value of genotype frequency is calculated by (954 T/C and 954 C/C) vs 954T/T.

3.3 Discussion and Conclusions

FSGS is a common cause of SRNS in children and adults, with an increasing incidence over the past decades. Studies have shown that the incidence of FSGS has increased significantly over the last decades (Haas *et al.* 1997; Barisoni *et al.* 1999). FSGS is considered a podocyte disease with diverse etiology. Hereditary FSGS is associated with poor renal survival and low rates of disease recurrence after renal transplantation (Korbet 2002; Kitiyakara *et al.* 2004). Recently substantial progress has been made in defining the molecular basis of these inherited forms. Many inheritable genetic forms of FSGS caused by mutations in podocyte proteins have been described (shown in table 1.5). These proteins are involved in the development, structural architecture and function of the podocytes. Amongst the major genes implicated in late-onset FSGS are *TRPC6*, *ACTN4*, *CD2AP* and *INF2*. Altered calcium signalling conferred by *TRPC6* mutations are implicated in the disruption of glomerular cell function (Hara *et al.* 2002). Mutations in ACTN4 are associated with dynamic changes of the podocyte actin cytoskeleton (Kaplan *et al.* 2000; Kos *et al.* 2003). *CD2AP* has been implicated in glomerular function on the basis of mouse studies and appears to have important interactions with *nephrin* and *podocin* at the slit diaphragm (Schwarz *et al.* 2001). INF2 encodes a member of the formin family of actin-regulating proteins, and mutations in INF2 have a defect in actin mediated podocyte structural maintenance and repair (Brown *et al.* 2010). The genes *NPHS1*, *NPHS2* and *WT1* are generally associated with onset of NS during childhood, however, distinct sequence variations have been described in patient with late-onset NS/FSGS (Pereira *et al.* 2004; He *et al.* 2007; Benetti *et al.* 2010; Schoeb *et al.* 2010). Furthermore, mutations in these genes are inherited in a dominant manner with incomplete penetrance and a variable expression (Shih *et al.* 1999; Kaplan *et al.* 2000; Kim *et al.* 2003; Reiser *et al.* 2005; Winn *et al.* 2005; Brown *et al.* 2010).

In our study several podocyte gene mutations/polymorphisms were detected. In a Singapore Chinese family with hereditary FSGS, we identified a novel *TRPC6* missense mutation c.202C>T, which resulted in the substitution of arginine (positively charged) to tryptophan (hydrophobic) at position 68 of the protein (p.R68W), and a polymorphism in its promoter region, c.-254C>G.

Mutations in *NPHS1* were originally identified in patients with congenital nephrotic syndrome of the "Finnish type". Recent studies showed that its variants were also associated with late-childhood and adult onset FSGS in familial as well as sporadic cases (Philippe *et al.* 2008; Santin *et al.* 2009). In this study, two reported synonymous polymorphisms, c.294C>T and c.2289C>T were found in *NPHS1* in this family. Meanwhile, we detected one *NPHS2* polymorphism c.954C>T. However, as shown in the genotype of the family (Figure 3.1), the presentation of variations and diseases in the family was not coincident. The three polymorphisms segregated with renal disease.

This novel *TRPC6* missense mutation c.202C>T was only detected in this patient family. It is not present in any public databases. Furthermore, not all *TRPC6* mutation carriers had renal diseases. Three carriers were penetrant, while the other three have remained non-penetrant. Notably, although both the donor and the recipient had this novel mutation, they had normal renal function and no proteinuria at 19 years post-transplant.

Recent study revealed that the allele frequency of the *TRPC6* promoter polymorphism c.−254C>G in idiopathic pulmonary arterial hypertension (IPAH) patients (12%) was

significantly higher than those in normal subjects (6%) analysed from 237 controls and 268 IPAH patients. Subsequently, this SNP was demonstrated to enhance nuclear factor κB–mediated promoter activity and stimulated *TRPC6* expression in pulmonary artery smooth muscle cells (PASMCs) (Yu *et al.* 2009). However, in our association analysis by recruiting 133 NS and/or FSGS patients and 91 healthy controls, we found that c.−254C>G is a very common SNP. Only one-quarter patients and controls had wild-type alleles while the rest (75%) had either homozygous or heterozygous polymorphisms (Table 3-1). We suspect that race may be the main contributor of the status of this *TRPC6* promoter SNP. In Yu's study, all the controls and IPAH patients were white, whereas in our study, controls and patients were all Asian.

CHAPTER 4 ELECTROPHYSIOLOGYCAL CHARACTERIZATION AND SURFACE BIOTINYLATION STUDY OF *TRPC6* CHANNELS WITH NOVEL MUTATION

4.1 Introduction

TRPC6 is a member of transient receptor potential (TRP) superfamily of cation-selective ion channels, which mediate the flux of Na^+ and Ca^{2+} across the plasma membrane and into the cytoplasm, playing important roles in the pathophysiology of many diseases (Nilius *et al.* 2007). The TRP channels, which are divided into seven subfamilies (*TRPC, TRPM, TRPV, TRPA, TRPP*, *TRPML* and *TRPN), TRPC* (*TRPC1-7*), are calcium-permeable cation channels that are widely expressed (Montell 2005). The closely related subgroup comprising *TRPC3*, *TRPC6*, and *TRPC7* channels are important for the increase in intracellular Ca^{2+} concentration.

TRPC6 is expressed in numerous tissues enriched with smooth muscle cells including brain, lung, stomach, colon, kidney, as well as in immune and blood cells (Dietrich and Gudermann 2007). Despite its abundance, the exact physiological role of *TRPC6* has not been fully elucidated. In the kidney, *TRPC6* is expressed in podocyte foot processes in the vicinity of the slit diaphragm (SD) as well as throughout the major foot processes and in the cell body (Reiser *et al.* 2005). Like other TRPC channels, *TRPC6* leads to the influx of calcium in direct or indirect response to phospholipase C (PLC)-mediated signals (Eder *et al.* 2005; Estacion *et al.* 2006). It can also be directly activated by diacylglycerol (DAG) (Hofmann *et al.* 1999; Okada *et al.* 1999). One model of *TRPC6* activation is through M1 muscarinic acetylcholine receptors (M1 mAChR). This can be achieved by addition of Carbachol (CCH) which will cause the M1 mAChR and protein kinase C to form a complex with *TRPC6* channels and activate the channels (Figure 4-1).

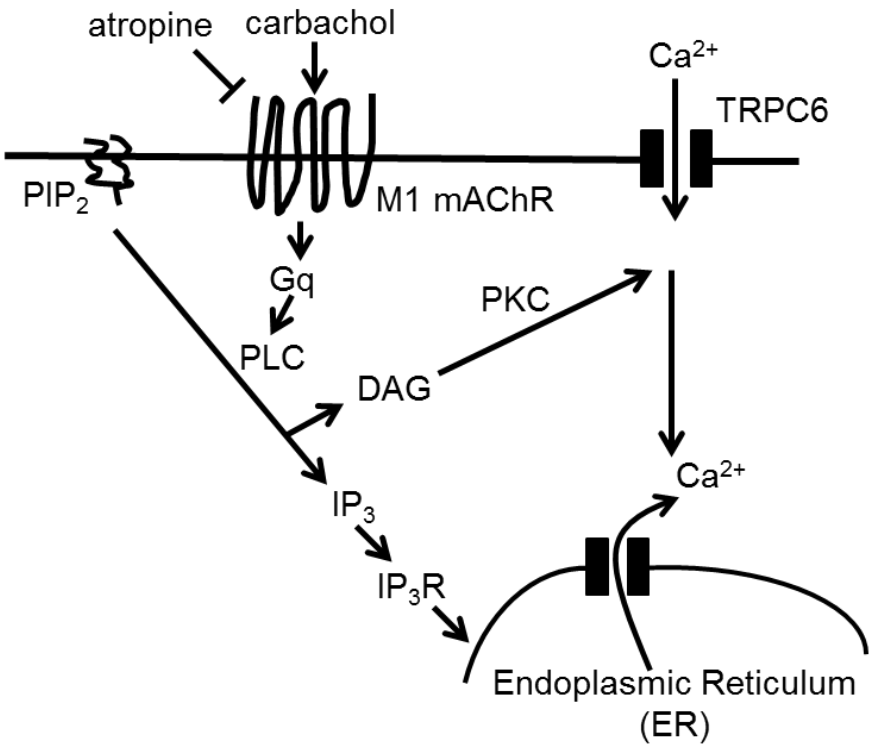

Figure 4-1 Model Depicting for M1 mAChR-regulated *TRPC6* Ca^{2+} Influx Pathway.

Stimulation of M1 mAChRs in HEK cells with carbachol activates PLC, which catalyzes the hydrolysis of PIP_2 into DAG and IP_3. IP_3 in turn activates the IP_3 receptor (IP_3R), causing release of Ca^{2+} from an intracellular Ca^{2+}-containing compartment. Active M1 mAChRs form a complex with *TRPC6* channels and PKC to activate *TRPC6* channels by PKC phosphorylation. The carbachol-stimulated complex formation can be blocked by the mAChR antagonist atropine.

The discovery in 2005 that mutations in *TRPC6* channels cause familial FSGS underscored the potential importance of Ca^{2+} dynamics for podocyte function and opened an entirely new line of investigation (Reiser *et al.* 2005; Winn *et al.* 2005). Since then, several more *TRPC6* mutations were identified from patient families with FSGS. It has been demonstrated that some of these mutations cause gain-of-function resulting in increased calcium current amplitudes and/or increased intracellular calcium concentration, and some even cause increased surface expression. However, there are also several *TRPC6* mutations detected in familial FSGS patients that did not modify the calcium influx in heterologous expression systems. All reported *TRPC6* mutations occur either in the cytoplasmic NH_2 or coiled-coil

domain in the COOH terminals of the protein (Reiser *et al.* 2005; Winn *et al.* 2005; Heeringa *et al.* 2009; Santin *et al.* 2009; Zhu *et al.* 2009; Buscher *et al.* 2010; Gigante *et al.* 2011; Mir *et al.* 2012). The ankyrin repeats consist of 30-34 amino acid residues. They are common protein-protein interaction motifs thought to be important in protein function, perhaps signifying association with the cytoskeleton (Montell 2005). Some of them are even directly involved in the development of human cancer and other diseases (Li *et al.* 2006). The two CC domains in each of the cytosolic N- and C-termini are ubiquitous protein motifs that are commonly used to control oligomerisation (Vazquez *et al.* 2004). However, the precise mechanism of how *TRPC6* mutations cause FSGS is still unclear. Winn and coworkers found that *TRPC6* p.P112Q mutation enhanced its surface expression with greater fraction of the mutant protein associated with the plasma membrane compared with the WT protein, suggesting a mechanism of exaggerated calcium signalling and flux (Winn *et al.* 2005).

In the previous chapter, we reported a novel *TRPC6* mutation p.R68W identified from a Singapore Chinese family with autosomal dominant FSGS. This mutation is the most proximal to the NH_2 terminal among all the reported mutations. Considering the phenotype and genotype of the index family, we hypothesized that this novel *TRPC6* mutation was involved in pathogenesis of FSGS, resulting in gain of function of the mutant *TRPC6* channels. The aim of this chapter is to study the function of p.R68W mutation by whole-cell patch clamp technique, and further explore its surface expression by biotinylation assay.

4.2 Results

4.2.1 *TRPC6*^{R68W} is a Novel Gain-of-function Mutation

To study the effect of the novel missense mutation p.R68W (c.202C>T) on *TRPC6* functions, full length *TRPC6* gene was fused with EGFP in mammalian expression vector pEGFP-C1 (Clontech) for visualization of transfected cells under fluorescence microscope. The mutation c.202C>T was generated using site-directed mutagenesis. Similarly, the published gain-of-function *TRPC6* mutation c.2683C>T (p.R895C) was generated as positive control. Wild-type or mutant *TRPC6*^{R68W} or *TRPC6*^{R895C} cDNA was transfected in HEK293-M1 cells (human embryonic kidney cells stably transfected with the M1 muscarinic receptor) using calcium phosphate methods (Liao *et al.* 2007). At 24-48h after transfection, whole-cell patch clamp was applied to record *TRPC6* current changes before and after the activation of M1 receptors by CCH. The voltage ramped from -100 mV to 100 mV over 150 milliseconds were applied in every 3.45 seconds. More than 10 cells were recorded in each group (wild-type, *TRPC6*^{R68W} or *TRPC6*^{R895C}).

We recorded a typical outward rectifying *TRPC6* current in cells transfected with *TRPC6*. We found that HEK293-M1 cells expressing *TRPC6*^{R68W} channels, compared to those expressing *TRPC6*^{WT} channels, exhibited significantly higher mean inward (-540.9 ± 40.5 pA/pF versus -329.3 ± 30.1 pA/pF, $p<0.001$) and outward (1063.8 ± 113.9 pA/pF versus 622.9 ± 49.5 pA/pF, $p = 0.002$) currents (Figure 4-2 A-G). As expected, the positive control *TRPC6*^{R895C} mutation, compared to *TRPC6*^{WT} channels, had statistically higher mean inward (-1188.0 ± 93.9 pA/pF vs -338.4 ± 32.2 pA/pF, $p <0.0001$, student's t test) and outward (1322.0 ± 142.6 pA/pF vs 619.5 ± 49.4 pA/pF, $p <0.0001$, student's t test) currents. This was consistent with the published data (Reiser *et al.* 2005). The results confirmed that *TRPC6*^{R68W} is a gain-of-

function mutation. Meanwhile, we noticed that the *TRPC6*^{R895C} channels had statistically higher mean inward currents compared to *TRPC6*^{R68W} channels, but there was no statistically significant difference for outward currents.

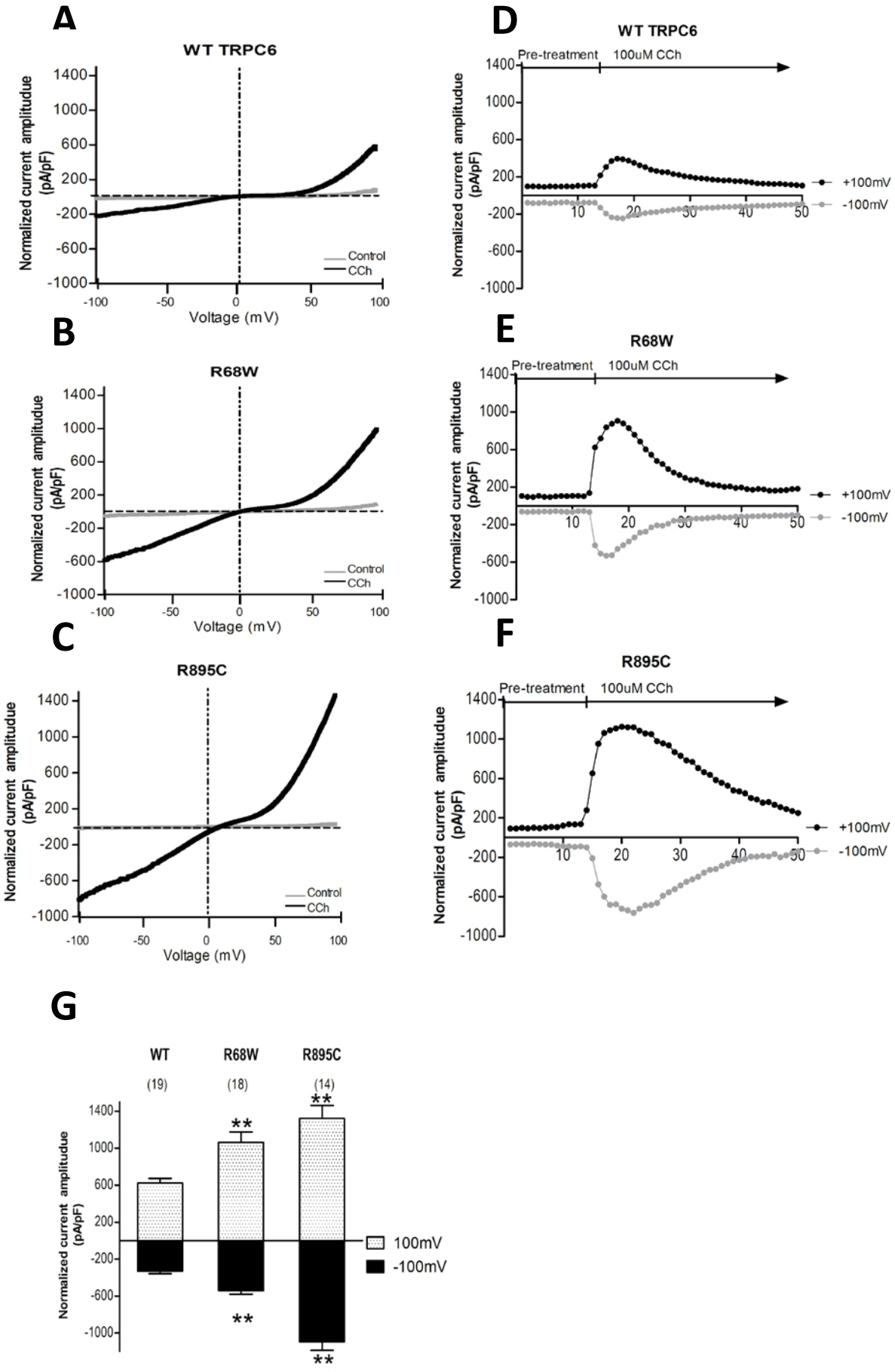
A
WT TRPC6
Normalized current amplitudue (pA/pF)
Voltage (mV)
Control
CCh
B
R68W
C
R895C
D
WT TRPC6
Pre-treatment
100uM CCh
+100mV
-100mV
E
R68W
F
R895C
G
WT
R68W
R895C
(19)
(18)
(14)
100mV
-100mV

Figure 4-2 Electrophysiological Characterizations of *TRPC6*^{R68W} Mutant Channels.

HEK293-M1 cells were transiently transfected with cDNA encoding Wild-type (WT) or mutant TRPC6. The gain-of-function *TRPC6* mutation R895C was used as positive control. Representative whole-cell currents of WT *TRPC6*, R68W and R895C mutant *TRPC6* under both control bath solution (gray traces) or 100 μM Carbachol (CCH, black traces) were shown in (A), (B) and (C), respectively. Voltage ramps from –100 mV to 100 mV over 150 ms were applied every 3.45 s from a holding potential of 0 mV. Current amplitude was normalized for cell capacitance. Similarly, time-dependent normalized current changes of WT *TRPC6* (D) or R68W (E) or R895C (F) were showed before and after activation of *TRPC6* by CCH. (G) Average normalized current amplitude measured at –100mV (dark bars) and 100 mV (light bars) from cells expressing WT *TRPC6* or R68W or R895C mutant *TRPC6*. Current amplitudes from cells expressing R68W and R895C mutant channels were significantly higher at both –100mV and 100 mV than those from cells expressing WT channels (**P < 0.01). The number of experiments for each clone is shown in parentheses, and the error bars show the s.e.m. for each measurement.

4.2.2 Mutation p.R68W Enhanced *TRPC6* Surface Expression

We next evaluated the subcellular localization of mutant *TRPC6* protein by surface biotinylation experiments. Mutant *TRPC6*^{P112Q} was used as a positive control. Cell expressing EGFP-*TRPC6*^{WT} or EGFP-*TRPC6*^{mutant} were incubated with biotin-SS reagent, followed by pull-down with streptavidin agarose beads. Immunoblotting with anti-GFP antibody showed increased biotinylated protein for p.R68W and p.P112Q compared to WT (Figure 4-3 A). The band densities were obtained using ImageJ software, and the ratios of biotinylated cell surface *TRPC6* to total *TRPC6* were normalized with that of *TRPC6*^{WT}. We found that *TRPC6*^{R68W} was significantly increased on cell surface compared with *TRPC6*^{WT} protein (p=0.041) (Figure 4-3 B). The increased surface expression of *TRPC6*^{P112Q} is in accordance with previous report (Winn *et al.* 2005). This enhanced cell surface expression of *TRPC6*^{R68W} protein suggests a mechanism of exaggerated calcium signalling and flux, possibly explaining the increased current amplitudes of *TRPC6*^{R68W} channels.

A

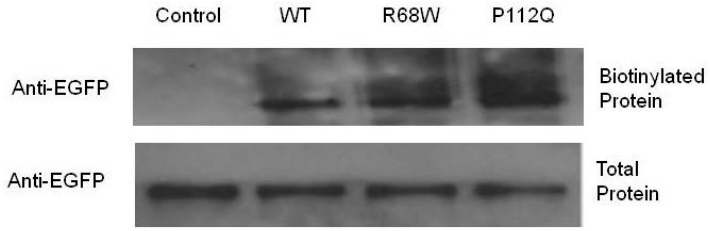

B

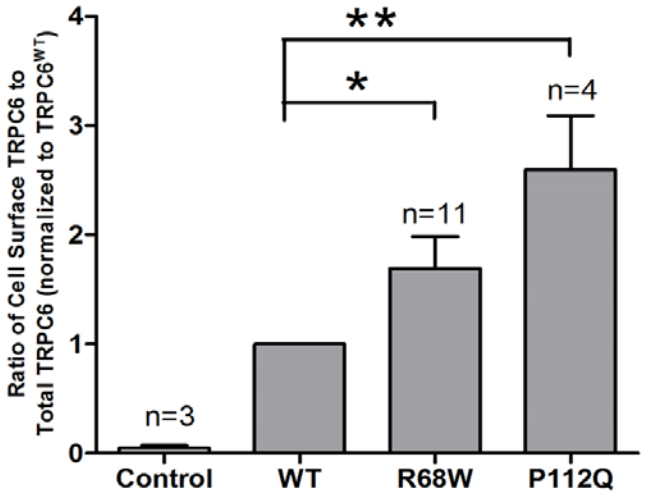

Figure 4-3 *TRPC6* Surface Expression in HEK 293 Cells Transfected with *TRPC6* Protein.

(A) Immunoblot using anti-EGFP antibody on biotinylated and whole-cell total proteins of cells transfected with EGFP-*TRPC6*^{WT}, EGFP-*TRPC6*^{R68W} or EGFP-*TRPC6*^{P112Q} plasmids. (B) Cell surface expression of EGFP-*TRPC6*^{R68W} and EGFP-*TRPC6*^{P112Q} (positive control) were increased compared with *TRPC6*^{WT} channels ($p=0.041$ and $p< 0.01$, respectively). The ratios of cell surface biotinylated *TRPC6* to total *TRPC6* were normalized to that of *TRPC6*^{WT}. The experiment was replicated 11 times for p.R68W and 4 times for p.P112Q with similar results. Densitometry measurement in relative units are depicted in the bar graph next to the immunoblot (the results from all four replicants are quantitated). The error bars represent the standard error and asterisks denote statistically significant comparisons (Student's t-test).

Table 4-1 Summary of Genotype-Phenotype Correlations of Published *TRPC6* Mutations

Mutation	Exon	Location	Ethnicity	Sporadic/ Familial	Age at disease presentation	Change in current amplitude	Intracellular calcium changes	Activation by	Reference
R68W	2	-	Chinese	Familial	7-17	Yes	nd	CCh	Current study
89fsX8 (truncated mutation)	2	Near ANK1	German	Sporadic	7	nd	nd	nd	(Buscher *et al.* 2010)
G109S	2	ANK1	Spanish	Sporadic	21-47	nd	nd	nd	(Santin *et al.* 2009)
P112Q	2	ANK1	NZ/British	Familial	16-61	Yes	Yes	UTP	(Winn *et al.* 2005)
N125S	2	ANK1	Italy/ Spanish	Familial	4-14/42	Yes	Yes	OAG	(Santin *et al.* 2009; Gigante *et al.* 2011)
M132T	2	ANK2	Turkey	Sporadic	9-30	Yes	Yes	CCh	(Heeringa *et al.* 2009)
N143S	2	ANK2	African American	Familial	27-39	No	nd	CCh	(Reiser *et al.* 2005)
R175Q	2	ANK3	Dutch	Familial	27-53	Yes	nd	OAG	(Hofstra *et al.* 2013)
H218L	2	ANK4	Italy	Sporadic	8	Yes	Yes	OAG	(Gigante *et al.* 2011)
S270T	2	TRPII box	Columbian	Familial	17-52	No	nd	CCh	(Reiser *et al.* 2005)
L395A	4	-	Turkish	Sporadic	2.4	nd	nd	nd	(Mir *et al.* 2012)
G757D	9	-	German	Sporadic	1	nd	nd	nd	(Buscher *et al.* 2010)
L780P	9	Near TRP box	Spanish	Sporadic	7	nd	nd	nd	(Santin *et al.* 2009)
K874X	12	CC domain	Polish	Familial	27-57	No	nd	CCh	(Reiser *et al.* 2005)
Q889K	13	CC domain	Chinese	Familial	35-41	Yes	Yes	OAG	(Zhu *et al.* 2009)
R895C	13	CC domain	Mexican	Sporadic	18-46	Yes	nd	CCh	(Reiser *et al.* 2005)
R895L	13	CC domain	Italy	Sporadic	1	Yes	Yes	OAG	(Gigante *et al.* 2011)
E897K	13	CC domain	Irish/German	Familial	24-35	Yes	nd	CCh	(Reiser *et al.* 2005)

nd: not done; ANK: ankyrin repeat; CC: coiled coil; CCh: carbachol; OAG: 1-oleoyl-2-acetyl-sn-glycerol

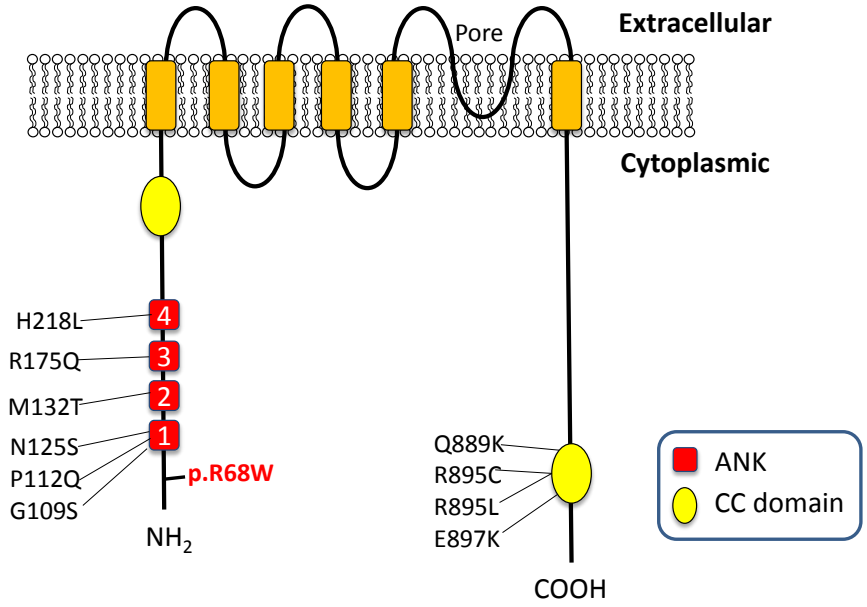

Figure 4-4 Locations of Published Gain-of-function *TRPC6* Mutations on its Topology. Among the 17 reported *TRPC6* mutations to date, 10 had gain of function in heterologous expression systems. All these 10 mutations were mapped to either one of the four ANK domains in the NH2 terminal or the CC domain in the C terminal.

4.3 Discussion and Conclusions

TRPC6 is a calcium-permeable cation channel expressed in many different tissues and organs including the kidneys, where it is specifically expressed in the podocyte cell bodies, major processes in the vicinity of the SD in the foot processes (Reiser *et al.* 2005). The discovery that *TRPC6* mutations cause FSGS underscored the importance of ion channels for podocyte function. Despite its expression in many extra-renal tissues, mutations in *TRPC6* are known to cause glomerular diseases only (Reiser *et al.* 2005; Walz 2005; Mukerji *et al.* 2007). This could be due to the unique role of *TRPC6* in podocytes or the distinct susceptibility of the slit diaphragm to minute changes in calcium dynamics. To date, 17 *TRPC6* mutations have been reported in sporadic or familial glomerular diseases. We summarized these mutations and their genotype-phenotype correlations in Table 4-1. All reported *TRPC6* mutations were mapped to the intracellular NH2-terminal and COOH-terminal domains of the channel

protein. Among these 17 mutations, 10 of them are associated with increase in channel activity in heterologous expression systems, and all of these 10 gain-of-function mutations are located in the either one of four ankrin repeats (ANKs) or the C-terminal cc domain (Figure 4-4).

As shown in Table 4-1, most of the NH_2-terminal missense mutations (89fsX8, G109S, P112Q, N125S, M132T, N143S, R175Q, H218L, and S270T) are located in or near one of the four ankyrin repeats. These mutations may affect the ability of *TRPC6* to oligomerize with other TRPC subunits (Schindl *et al.* 2008) or alter the channel expression at the cell surface (Wedel *et al.* 2003). Among these, p.P112Q mutation causes increased surface expression, and increased angiotensin II-mediated Ca^{2+} influx in heterologous expression systems (Winn *et al.* 2005). NH_2-terminal mutations can also affect *TRPC6* gating properties, as p.N143S and p.S270T mutations result in increased mean open-time compared with wild-type channels (Heeringa *et al.* 2009). The NH_2-terminal mutation with the largest effect on channel currents reported to date is p.M132T. In heterologous expression systems, this mutation results in currents three to five times larger than those of wild-type channels, as well as delayed inactivation in the presence of continuous agonist stimulation (Heeringa *et al.* 2009). Interestingly, this M132T mutation is associated with early age of onset of FSGS in children, suggesting that the current amplitudes correlate with phenotype severity (Heeringa *et al.* 2009).

Among the *TRPC6* mutations at the COOH terminal, the mutation p.L780P is located near the TRP box 1 motif that is conserved in all TRPC channels, whereas the other five mutations (K874*, Q889K, R895C, R895L, and E897K) map to a predicted coiled-coil motif located further downstream. While no study has specifically investigated the importance of the

COOH-terminal coiled-coil motif in *TRPC* channel gating, one study suggests that the COOH-terminal tails of *TRPC4* and *TRPC6* participate in channel oligomerization (Lepage *et al.* 2006). Importantly, most of the mutations (p.Q889K, p.R895C, p.R895L, p.E897K) located in the coiled-coil domain result in increased maximal current amplitudes in heterologous expression systems, effectively resulting in a net gain in function. It is possible that these are caused by increased trafficking to the cell surface (Dryer and Reiser 2010).

We report here a novel gain-of-function *TRPC6* missense mutation, p.R68W. This mutation is the most proximal to the NH_2 terminal among all the reported mutations, and is the first reported mutation located outside a known functional domain or motif. By comparing current changes between positive control $TRPC6^{R895C}$ and $TRPC6^{R68W}$, we noted that $TRPC6^{R895C}$ channels had significantly higher mean inward currents, but not outward currents. In addition, our recording on $TRPC6^{R895C}$ channel showed that it had bigger current changes compared with the result published by Reiser and his coworkers (Reiser *et al.* 2005). This is most likely due to the difference in the conditions of the experimental setup between the reported study and our study.We have also shown p.R68W increased surface expression of the *TRPC6* channels and this could explain the increased *TRPC6* current amplitudes caused by this mutation. This concurred with the study by Winn et al., who showed increased *TRPC6* surface expression due to p.112Q mutation (Winn *et al.* 2005). However, enhanced channel surface expression may not be the only mechanism to explain the increased current amplitudes. It has been reported that the *TRPC6* p.175Q mutation caused increased *TRPC6* current amplitudes but did not result in increased surface expression of the channels (Hofstra *et al.* 2013). Clearly, other mechanisms are involved in causing the increased channel amplitudes.

Studies have suggested that it is the increased *TRPC6* current amplitudes that result in disease, rather than the mutant channels *per se*. Increased $TRPC6^{WT}$ glomerular expression has been shown in acquired human proteinuric diseases and mouse models for human FSGS in the absence of *TRPC6* mutations (Moller *et al.* 2007; Nijenhuis *et al.* 2011). These concurred with studies in cultured podocytes in which overexpression of $TRPC6^{WT}$ resulted in cytoskeleton rearrangement through increase in intracellular calcium and RhoA activation (Jiang *et al.* 2011).

In conclusion, we have shown that p.R68W is a novel gain-of-function mutation that increases *TRPC6* current amplitudes and its surface expression. This is the first gain-of-function mutation located outside a known functional domain.

CHAPTER 5 THE EFFECTS OF *NPHS1* AND *NPHS2* POLYMORPHISMS ON *TRPC6* CHANNELS

5.1 Introduction

The podocyte slit diaphragm (SD) is a critical structure in the glomerular filtration apparatus. It is a cell-cell junction with features of tight and adherens junctions. The SD has a unique multifunctional signaling platform (Wartiovaara *et al.* 2004) involving many important proteins including nephrin (*NPHS1*), podocin (*NPHS2*), NEPH1 and CD2AP (Figure 5-1). The interactions between *TRPC6* and these SD proteins are pivotal in the regulation of cell polarity, cell survival and cytoskeletal organization (Benzing 2004). The two most central proteins in the SD are nephrin and podocin. There has been some evidence suggesting interactions between *TRPC6* and nephrin/podocin.

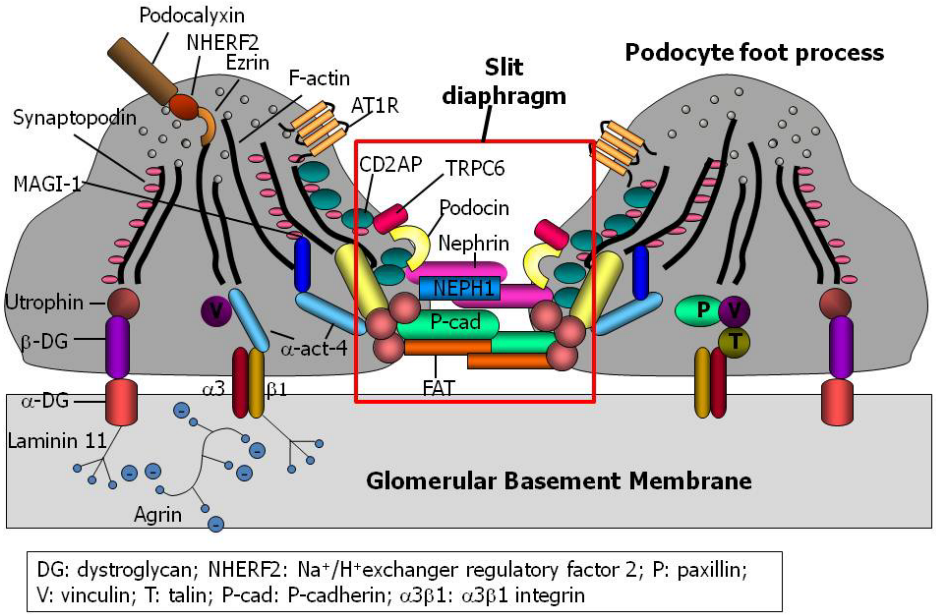

Figure 5-1 Schematic diagram showing cross-sectional views of two adjacent podocyte foot processes and the major proteins in the slit diaphragm between them.

Nephrin belongs to the immunoglobulin superfamily (Kestila *et al.* 1998) and is arguably the most pivotal protein in podocytes (Welsh and Saleem 2010). Of all human podocyte mutations described so far, patients with nephrin mutations have the earliest and most severe clinical phenotype (Kestila *et al.* 1998), suggesting its critical role as a structural and

signalling molecule in the SD. Its cytoplasmic domain has eight tyrosine phosphorylation sites which, upon phosphorylation, act as binding sites for proteins containing SH2 domains, such as phosphatidylinositol- 3-OH kinase and the Src kinase family member *Fyn*. Binding of these proteins are important for the function of nephrin in the regulation of the podocyte actin cytoskeleton. Derangement of the actin cytoskeleton is considered the hallmark in podocyte injury. There has been some evidence to suggest that nephrin affects *TRPC6* function. Reiser et al. have demonstrated enhanced expression and altered cellular localization of *TRPC6* in podocytes of nephrin-deficient mice (Reiser *et al.* 2005), suggesting that nephrin regulates *TRPC6* expression. This is most likely facilitated by Fyn kinase which associates with nephrin (Verma *et al.* 2003) and regulates *TRPC6* channel activation by tyrosine phosphorylation (Hisatsune *et al.* 2004). Tyrosine phosphorylation of *TRPC6* induced a complex formation with PLC-γ1, which is necessary for *TRPC6* surface expression. However, nephrin could inhibit *TRPC6* surface localization activation by binding to phosphorylated *TRPC6* and competitively inhibiting *TRPC6*-PLC-γ1 complex formation (Kanda *et al.* 2011). More interestingly, *TRPC6* disease-causing mutations could render *TRPC6* insensitive to nephrin inhibition, thereby promoting *TRPC6* surface expression and channel activation (Kanda *et al.* 2011).

Podocin is a member of the stomatin protein family exclusively expressed in podocytes of the developing and mature glomeruli (Roselli *et al.* 2002). It is localised at the insertion site of SD between podocyte foot processes (Schwarz *et al.* 2001) and functions as a scaffold protein that links the plasma membrane to the actin cytoskeleton (Machuca *et al.* 2009). Mutations in *NPHS2* gene coding for podocin cause steroid-resistant nephrotic syndrome and FSGS in humans (Boute *et al.* 2000). It was proposed that podocin regulates *TRPC6* by binding to cholesterol, which changes the local lipid environment surrounding the *TRPC6* channel,

thereby altering the ability of *TRPC6* to respond directly to deformation of the plasma membrane (Huber *et al.* 2006). In another study (Fan *et al.* 2009), podocyte injury caused by podocin mutation p.V165X was inhibited by the knockdown of *TRPC6*. In the same study, another podocin mutation p.R168H resulted in abnormal podocin retention in the endoplasmic reticulum and mis-localizations of nephrin and *TRPC6*. These studies suggested that podocin interacts with *TRPC6*. Podocin polymorphisms could therefore possibly play a part in the pathogenesis of FSGS through the interaction with *TRPC6*.

While there have been suggestion for interactions between *TRPC6* and nephrin / podocin, the exact mechanism and how these may affect phenotype is not entirely clear. Considering the novel segregation of *TRPC6*, *NPHS1* and *NPHS2* genotypes to renal disease in the index family, **we** hypothesized that the *NPHS1* and *NPHS2* polymorphisms identified in the index family alter *TRPC6* channel activity, thereby influencing the phenotype and accounting for the variable penetrance and successful renal transplantation in the index family. We therefore aimed to

1) study how the presence of wild-type (WT) nephrin or podocin may influence the current amplitudes of WT or mutant *TRPC6*.

2) study the effects of *NPHS1* polymorphisms (c.294C>T and c.2289C>T) and *NPHS2* polymorphism (c.954T>C) on *TRPC6* channel activity, and how the unique combination of the *NPHS1* polymorphisms, according the genotypes in the index family, may influence *TRPC6* currents.

5.2 Results

In this study, *EGFP-TRPC6* fusion gene was cloned into pEGFP-C1 vector (Clontech) (green fluorescence). In addition, *NPHS1* and *NPHS2* gene was cloned separately into pIRES-DsRed (Clontech) vector (red fluorescence). With the differently coloured fluorescence, co-transfected HEK293-M1 cells with both *TRPC6* and *NPHS1* or *NPHS2* plasmids would be yellow (overlapping green and red fluorescence). This allowed us to select the cells for patch clamp recording which measured the *TRPC6* current changes before and after activation by CCH. We used the gap free protocol in which the cells were held at holding potential of 0 mV for the duration of the patch clamp recording (Inoue *et al.* 2009).

5.2.1 Both Wild-type Nephrin and Podocin Downregulate *TRPC6* Channel Activity

To study the effects of WT *NPHS1* or *NPHS2* on *TRPC6* channels, WT *NPHS1* or *NPHS2* or the empty pIRES2 vector (as negative control) was co-transfected with $TRPC6^{WT}$ or $TRPC6^{R68W}$ into HEK293-M1 cells. CCH-induced currents were recorded using gap-free protocol at the holding potential of 0mV (Inoue *et al.* 2009). As shown in Figure 5-2 A, after exposure to CCH, the *TRPC6* current amplitudes reached the peak in a couple of seconds, and they decreased rapidly even at the presence of CCH. Cells with $TRPC6^{WT}$ and $NPHS1^{WT}$ had significantly lower *TRPC6* currents (21.8 ± 3.8pA/pF) compared to cells with $TRPC6^{WT}$ and empty pIRES2 vector (35.3 ± 4.9pA/pF) (p=0.039) (Figure 5-2 B). Similarly, cells with $TRPC6^{R68W}$ and $NPHS1^{WT}$ had significantly lower *TRPC6* currents (30.2 ± 2.7pA/pF) compared to cells with $TRPC6^{R68W}$ and empty pIRES2 vector (48.5 ± 4.6pA/pF) (p=0.002) (Figure 5-2 B). As a parallel experiment, $NPHS2^{WT}$ or the empty pIRES2 vector was co-transfected with $TRPC6^{WT}$ into HEK293-M1 cells. The results showed that cells with $TRPC6^{WT}$ and $NPHS2^{WT}$ had significantly lower *TRPC6* currents (15.1 ± 1.8pA/pF)

compared to cells with *TRPC6*^{WT} and empty pIRES2 vector (21.6 ± 1.8pA/pF) (p=0.04) (Figure 5-2C). These findings suggested that wild-type *NPHS1* and *NPHS2* downregulate *TRPC6* channel activity.

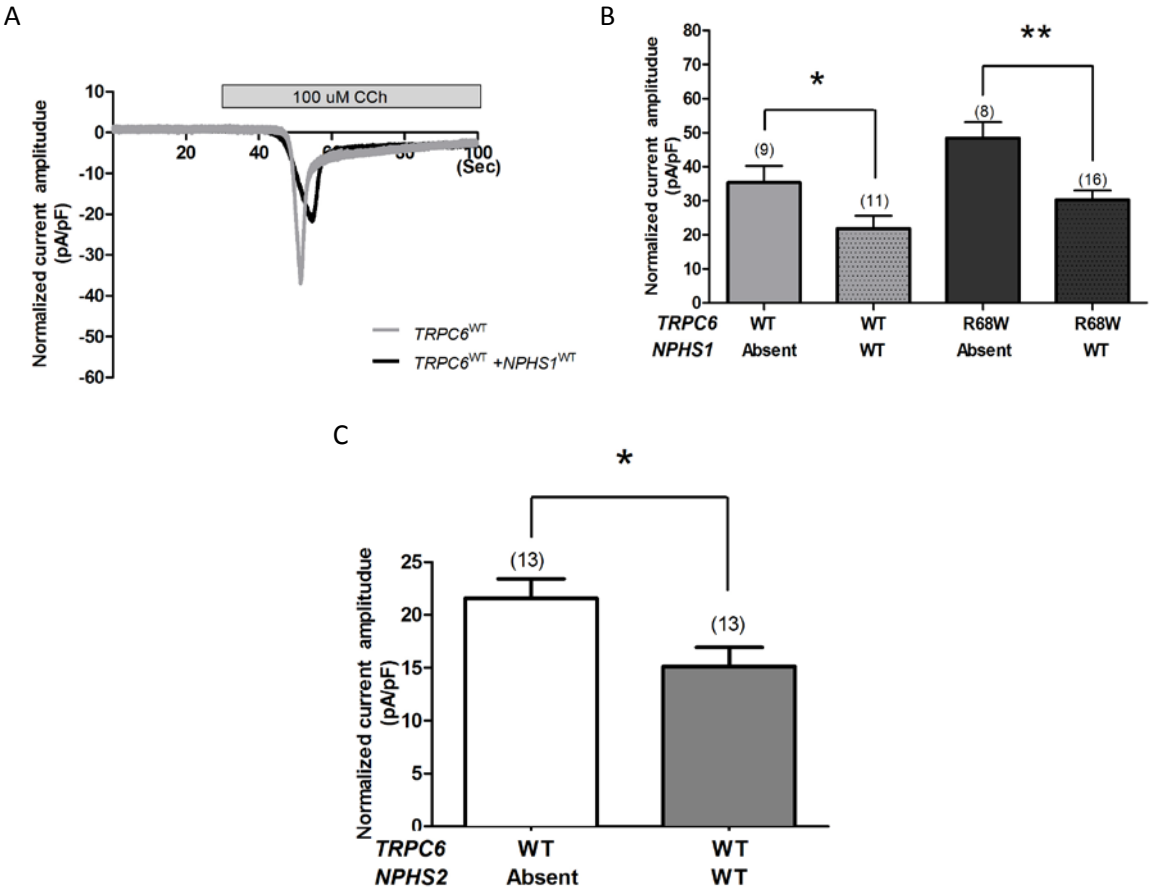

Figure 5-2 Wild-type *NPHS1* and *NPHS2* Downregulate *TRPC6* Channel Activity.

(A) Representative normalized whole-cell currents measured from cells co-transfected *TRPC6*^{WT} with empty vector (grey) o*r* *NPHS1*^{WT} (black). *TRPC6* currents were recorded before and after channel activation by CCH using gap-free protocol with a holding potential of 0mV. (B) *NPHS1*^{WT} downregulated *TRPC6* channel activity. Both *TRPC6*^{WT} and *TRPC6*^{R68W} currents were significantly suppressed by the presence of *NPHS1*. (C) *NPHS2*^{WT} downregulated *TRPC6*^{WT} channel activity. The error bars show the standard errors of the means and asterisks denote statistically significant comparisons (student's t-test). Numbers in parentheses denote the number of cells measured per group.

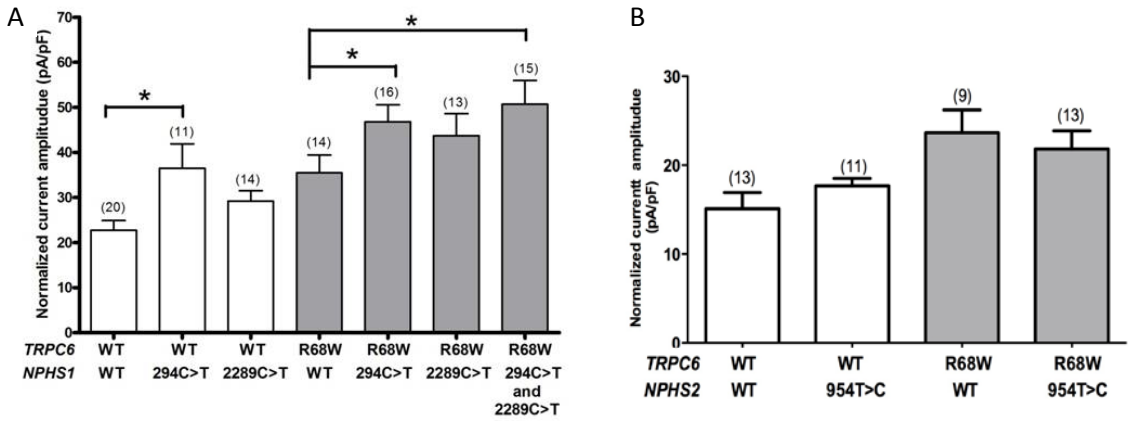

Figure 5-3 Functional Effects of Polymorphisms of *NPHS1* and *NPHS2* on *TRPC6* Channel Activity.

Normalized *TRPC6* current amplitudes of HEK293-M1 cells with $TRPC6^{WT}$ (white bars) or $TRPC6^{R68W}$ (grey bars) in combination with homozygous *NPHS1* or *NPHS2* polymorphisms. (A) Cells with $NPHS1^{294C>T}$ or $NPHS1^{294C>T+2289C>T}$, and not those with $NPHS1^{2289C>T}$, had significantly higher mean $TRPC6^{WT}$ or $TRPC6^{R68W}$ currents compared to those with $NPHS1^{WT}$. (B) Cells with $NPHS2^{954T>C}$ did not alter the currents of $TRPC6^{WT}$ or $TRPC6^{R68W}$ compared to those with $NPHS2^{WT}$. The error bars show the standard errors of the means and asterisks denote statistically significant comparisons (student's t-test). Numbers in parentheses denote the number of cells measured per group.

5.2.2 The Effects of *NPHS1* and *NPHS2* Polymorphisms on *TRPC6* Activity

The effects of *NPHS1* and *NPHS2* polymorphisms on *TRPC6* activity were subsequently studied using gap-free protocol in patch clamp recording.

HEK293-M1 cells were co-transfected with wild-type *NPHS1* ($NPHS1^{WT}$), homozygous c.294C>T ($NPHS1^{294C>T}$), c.2289C>T ($NPHS1^{2289C>T}$) or both polymorphisms ($NPHS1^{294C>T+2289C>T}$), together with $TRPC6^{WT}$ or $TRPC6^{R68W}$. We found that cells with $NPHS1^{294C>T}$ had significantly higher $TRPC6^{WT}$ currents (36.5 ± 5.4pA/pF) compared to those with $NPHS1^{WT}$ (22.7 ± 2.2pA/pF) (p=0.035) (Figure 5-3A). When repeated with $TRPC6^{R68W}$, cells with $NPHS1^{294C>T}$ (46.8 ± 3.7pA/pF) (p=0.047) as well as cells with $NPHS1^{294C>T+2289C>T}$ (50.7 ± 5.2pA/pF) (p=0.029) had higher $TRPC6^{R68W}$ currents than those

with *NPHS1*^{WT} (35.5 ± 4.0pA/pF) (Figure 5-3A). However, there was no significant difference in *TRPC6*^{WT} or *TRPC6*^{R68W} currents when cells were transfected with *NPHS1*$^{2289C>T}$ (Figure 5-3B). These findings suggested that *NPHS1*$^{294C>T}$, but not *NPHS1*$^{2289C>T}$, has decreased ability to inhibit both *TRPC6*^{WT} and *TRPC6*^{R68W}.

Similarly, to study the effects *NPHS2* polymorphism c.954T>C (*NPHS2*$^{954T>C}$) on *TRPC6* activity, HEK293-M1 cells were co-transfected with *NPHS2*^{WT} or homozygous *NPHS2*$^{954T>C}$, together with *TRPC6*^{WT} or *TRPC6*^{R68W} (Figure 5-3B). Cells with *TRPC6*^{WT} and *NPHS2*$^{954T>C}$ (17.7 ± 0.8pA/pF) had slightly increased, but not statistically different, *TRPC6* currents compared with cells with *TRPC6*^{WT} and *NPHS2*^{WT} (15.1 ± 1.8pA/pF) (p=0.27). Cells transfected with *TRPC6*^{R68W} and *NPHS2*$^{954T>C}$ (21.8 ± 2.1pA/pF) had slightly decreased, but not significantly different, *TRPC6* currents compared to cells with *TRPC6*^{R68W} and *NPHS2*^{WT} (23.7 ± 2.6pA/pF) (*p*=0.50). These findings indicated that *NPHS2*$^{954T>C}$ did not affect *TRPC6* channel activity.

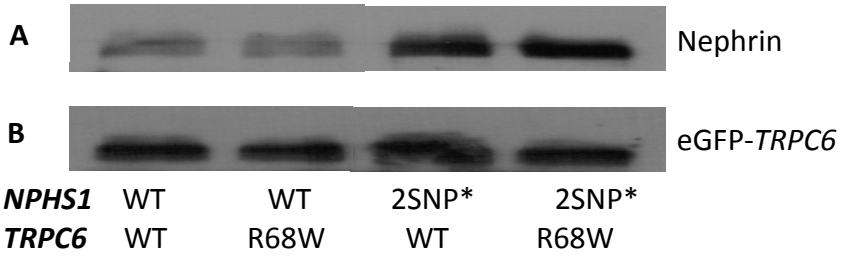

Figure 5-4 The interaction between *TRPC6* and Nephrin was not affected by *NPHS1* SNPs. Co-immunoprecipitation was performed to study the effect of nephrin SNPs on the physical binding between ***TRPC6*** and ***NPHS1***. Anti-FLAG was used to assay the co-precipitated nephrin (Panel A). Anti-EGFP (Roche) was used to precipitate EGFP-*TRPC6* (Panel B). * 2SNP implies the construct had two homozygous nephrin SNPs, c.294C>T and c.2289C>T.

5.2.3 *NPHS1* Polymorphisms, c.294C>T and c.2289C>T Did Not Affect the Interaction between *TRPC6* and *NPHS1*

We next performed co-immunoprecipitation to study the effect of nephrin SNPs on physical binding between *TRPC6* and *NPHS1*. We co-transfected the HEK293 cells with EGFP-*TRPC6* and FLAG-*NPHS1*. The FLAG-NPHS1 construct consists of either wild-type nephrin or the two homozygous nephrin SNPs, c.294C>T and c.2289C>T. We precipitated EGFP-TRPC6 using anti-EGFP (Roche) and the co-precipitated nephrin was assayed using anti-FLAG (Santa Cruz) (Figure 5-4). Our results demonstrated that the two *NPHS1* SNPs did not affect nephrin binding with WT or p.R68W mutant *TRPC6* channels.

5.2.4 The Variable Penetrance of *TRPC6* p.R68W Mutation in the Index Family was Explained by *NPHS1* Polymorphisms

In order to explain the clinical phenotypes, we studied the effects of *NPHS1* variants, c.294C>T and c.2289C>T, on *TRPC6* function based on specific combinations of genotypes in selected members of the index family. *TRPC6*^{WT} or *TRPC6*^{R68W} were co-transfected in various combinations with the *NPHS1* polymorphisms into HEK293-M1 cells, such that each combination represented the combined genotype of a relevant family member (Figure 5-5). Cells representing individuals with *TRPC6*^{WT} (control, III.3 and II.3/II.5) were analyzed as one group in the one-way ANOVA (with Bonferroni correction). As shown in Figure 5-3, there was a trend of increasing current amplitudes with worsening phenotype severity. In particular, cells representing the kidney donor II.2, who had *TRPC6*^{R68W} mutation but no *NPHS1* c.294C>T and c.2289C>T polymorphisms, had currents (35.5 ± 4.0pA/pF) which were not significantly different from cells representing individuals with *TRPC6*^{WT} (24.7 ± 1.4pA/pF), but they were significantly lower than cells representing the individuals with FSGS (II.4 and III.2) who were homozygous for both *NPHS1* polymorphisms (50.7 ±

5.2pA/pF) (p=0.048). These results suggested that the *TRPC6* current increases with the severity of renal phenotypes and proved for the first time, genetic epistasis between *TRPC6* and *NPHS1*.

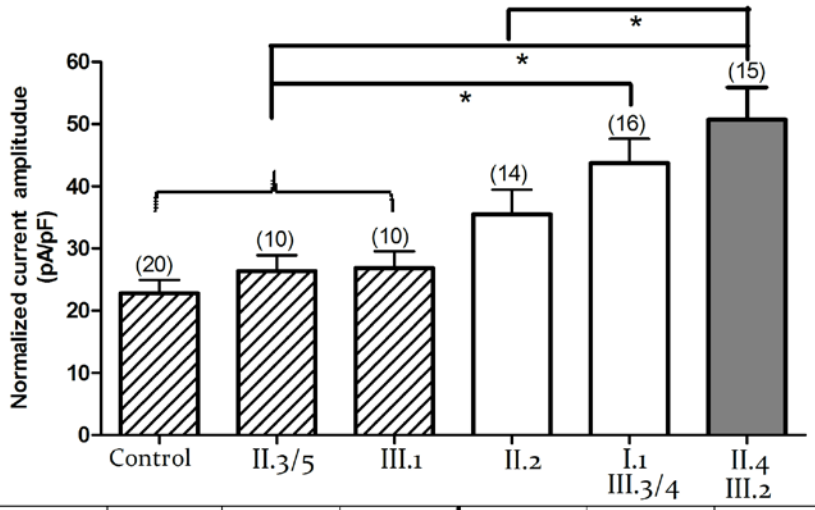

Phenotype	Not applicable	Healthy	Healthy	Healthy kidney donor	Healthy and mild proteinuria	FSGS and ESRD
Genotype						
TRPC6	WT	WT	WT	R68W	R68W	R68W
NPHS1 c.294	C/C	C/C	C/T	C/C	C/T	T/T
NPHS2 c.2289	C/C	C/T	C/T	C/C	C/T	T/T
Mean Current amplitudes ± SE (pA/pF)	22.7 ± 9.7	26.8 ± 8.6	26.4 ± 8.0	35.3 ± 14.8	43.7 ± 15.6	50.7 ± 20.2
p value						
II.2 (Healthy donor)	0.160					
I.1 / III.3/III.4	<0.001**			0.092		
II.4/III.2 (ESRD/FSGS)	<0.001**			0.048*	0.333	

Figure 5-5 Associations between Phenotypes and *TRPC6* Mean Current Amplitudes of Cells Representing Selected Family Members.

HEK293-M1 cells were co-transfected with *TRPC6*^{WT} or *TRPC6*^{R68W} in combination with *NPHS1* polymorphisms according to the genotypes of selected family members. The mean normalized current amplitudes are shown in the bar chart and the corresponding phenotypes and genotypes in the table. Cells representing individuals with *TRPC6*^{WT} (control, III.3 and II.3 / II.5) were analyzed as one group. The p values of the one-way ANOVA (with Bonferroni correction) between the various groups are presented in the table. Cells representing the kidney donor II.2 had significantly lower currents than cells representing II.4 and III.2 with FSGS (p=0.048), but had similar currents compared to cells representing those with *TRPC6*^{WT} (p=0.160). The error bars show the standard errors of the means, numbers in parentheses denote the number of cells measured per group and asterisks denote statistically significant comparisons.

5.3 Discussion and Conclusions

Our study is the first to demonstrate via functional studies the existence of genetic epistasis between *NPHS1* polymorphisms and *TRPC6*, accounting for the variable and non-penetrant expression of a novel mutant *TRPC6* mutation, and the successful kidney transplantation between two individuals with the same mutant *TRPC6* gene.

TRPC6-associated glomerular disease is classically an adult-onset disease occurring as late as the fifth decade of life.(Reiser *et al.* 2005) However, recent reports described early disease onset in children less than ten years old, with the youngest being six months. Moreover, there is a wide spectrum of phenotypes ranging from no renal disease to isolated proteinuria to ESRD.(Heeringa *et al.* 2009; Santin *et al.* 2009; Buscher *et al.* 2010; Gigante *et al.* 2011; Liakopoulos *et al.* 2011; Mir *et al.* 2012; Hofstra *et al.* 2013) Similarly, we observed non-penetrance of the novel *TRPC6*^{R68W} mutation in three family members in the index family and one control. One explanation for the variable penetrance is the multi-hit hypothesis in which other insults and/or genetic variants contribute to disease pathomechanism (Dryer and Reiser 2010). Our findings suggest that the relatively early disease onset in this family could be a result of genetic epistasis between *NPHS1* polymorphisms and *TRPC6*. Interactions between podocyte genes have been thought to be important because concurrent sequence variants have been identified in different podocyte genes, and patients with heterozygous podocin or nephrin mutations are symptomatic even though these are autosomal recessive diseases.(Caridi *et al.* 2003; McCarthy *et al.* 2013) In the kidney, *TRPC6* normally localizes to the slit diaphragm of podocytes, and co-immunoprecipitates with other slit diaphragm proteins like *NPHS1* and *NPHS2*. Other than physical co-localisation, there have been few functional studies confirming the presence of genetic epistasis between different podocyte

genes. Using patch clamp methods, we have shown that *NPHS1*$^{294C>T}$ resulted in the loss of ability of nephrin to suppress *TRPC6* channels. This was not shown for the other polymorphisms *NPHS1 c*.2289C>T and *NPHS2* c.954T>C.

By representing the combined *TRPC6* and *NPHS1* genotypes of selected family members in HEK-M1 cells, we found that there was a trend of increasing current amplitudes with worsening phenotype severity. This concurred with the study by Heeringa et al who found that the *TRPC6* mutation p.M132T, associated with early age of onset of FSGS in children, caused the largest current amplitude changes compared to other mutations which caused later disease onset in adults (Heeringa *et al.* 2009). Studies have suggested that it is the increased *TRPC6* current amplitudes that result in disease, rather than the mutant channels *per se*. Increased *TRPC6*^{WT} glomerular expression has been shown in acquired human proteinuric diseases and mouse models for human FSGS in the absence of *TRPC6* mutations (Moller *et al.* 2007; Nijenhuis *et al.* 2011). These were in accordance with studies in cultured podocytes in which overexpression of *TRPC6*^{WT} resulted in cytoskeleton rearrangement through increase in intracellular calcium and RhoA activation (Jiang *et al.* 2011).

It is noteworthy to mention that although podocin polymorphism c.954T>C did not affect *TRPC6* current amplitudes, whereas wild-type podocin did suppress *TRPC6* activity, similar to wild type nephrin. While it has been shown that wild-type nephrin suppresses *TRPC6* by binding to phosphorylated *TRPC6* and competitively inhibiting *TRPC6*-PLC-γ1 complex formation and therefore inhibiting *TRPC6* surface localization activation (Kanda *et al.* 2011), the exact mechanism of how wild-type podocin may inhibit *TRPC6* is unclear. There have been some suggestion that podocin changes the local lipid environment of the plasma

membrane surrounding *TRPC6*, thus altering the ability of *TRPC6* to respond to deformation of the plasma membrane (Huber *et al.* 2006). Further studies are required to confirm this.

To conclude, this is the first study to demonstrate via functional work the existence of genetic epistasis between NPHS1 polymorphisms and *TRPC6*, accounting for the variable and non-penetrant expression of a novel mutant *TRPC6* mutation.

CHAPTER 6 THE EXPRESSION AND RNA STABILITY OF *NEPHRIN* VARIANTS

6.1 Introduction

Podocytes play a central role in the control of glomerular filtration by collectively maintaining the glomerular architecture and contributing largely to bar the egress of plasma-derived proteins through the slit diaphragm (Haraldsson *et al.* 2008; Meyrier 2011). The slit diaphragm (SD) is a modified adherens junction (Reiser *et al.* 2000) that connects adjacent podocyte foot processes forming a tight interdigitating network to maintain foot processes structure in the glomeruli. Nephrin, being part of the SD, is an essential component of the glomerular filtration barrier. It consists of a large extracellular portion made up of eight IgG-like domains, a fibronectin type-3 motif, a single transmembrane domain and a cytoplasmic domain (Kestila *et al.* 1998).

Mutations of nephrin induce congenital nephrotic syndrome of Finnish type, which is a prototype of congenital nephrotic syndrome. Of all the human podocyte gene mutations, patients with *NPHS1* mutations display the earliest and most severe clinical phenotype with onset of life-threatening proteinuria in utero or within the first 3 months of life (Patrakka *et al.* 2000; Welsh and Saleem 2010). As a key structural and signalling molecule within the SD, nephrin acts as an intracellular signalling scaffold as it recruits other proteins, such as phosphatidylinositol-3-OH kinase, the Src family kinase Fyn and phospholipase Cγ1(PLC-γ1) to its C-terminal domain. It regulates a number of cell signalling pathways including stimulation of members of the MAP kinase family and activation of the phosphoinositide 3-OH kinase–PKB pathway (Huber *et al.* 2003). These effects require interactions with podocin, which targets nephrin to lipid rafts at the plasma membrane and facilitates nephrin signalling (Huber *et al.* 2001; Schwarz *et al.* 2001). In addition, phosphorylation of nephrin at amino acid 1193 leads to the recruitment, phosphorylation and activation of PLC-γ1, which is

known to be involved in a diverse range of cellular functions, including regulation of calcium signalling (Harita *et al.* 2009). Calcium signalling is integral to podocyte homeostasis, supported by the evidence that disease-causing *TRPC6* mutations increase calcium flux (Reiser *et al.* 2005; Winn *et al.* 2005).

Proper localization of nephrin within the specialized lipid micro-domains at the plasma membrane is essential for slit diaphragm signalling (Schermer and Benzing 2009). Studies have demonstrated that plasma from FSGS patients relocalizes nephrin, podocin and CD2AP from the cell surface to the cytoplasm (Coward *et al.* 2005). Nephrin and podocin are localized away from the slit diaphragm in nephrotic syndromes (Luimula *et al.* 2000; Doublier *et al.* 2001). These evidence support the notion that nephrin mislocalization is a key feature of podocyte dysfunction in nephrotic diseases.

In the previous chapter, we concluded that the binding of nephrin and podocin to *TRPC6* downregulates the latter, whereas the presence of nephrin polymorphisms, especially c.294C>T, results in the loss of *TRPC6* downregulation. More importantly, the variable penetrance found in the index family could be explained by interactions between *TRPC6* and *NPHS1* variants. Since single nucleotide polymorphisms (SNPs) represent the most frequent type of sequence variations playing a key role in human phenotypic variability (Johnson *et al.* 2005), we hypothesized that the nephrin polymorphisms c.294C>T and c.2289C>T is functional due to their effects on gene expression, as a consequence to decreased mRNA stability. Therefore, we first aimed to study the effects of nephrin polymorphisms c.294C>T and c.2289C>T on nephrin protein expression by immunoblotting. WT or variant nephrin (*NPHS1*$^{294C>T}$, *NPHS1*$^{2289C>T}$, or the double SNPs, *NPHS1*$^{294C>T+2289C>T}$) was transfected into

HEK293-M1 cells. The same amount of cDNA was used in each group. Total protein was isolated from each group and western blot was performed using appropriate antibodies. The second aim of this chapter is study the effects of these nephrin polymorphisms on mRNA stability, via the use of actinomycin D which is a commonly used transcription inhibitor, followed by real-time polymerase chain reaction to quantify the mRNA. These experiments will help us to understand how these nephrin polymorphisms exert their function.

6.2 Results

6.2.1 *NPHS1*$^{294C>T}$ Decreased Nephrin Protein Expression in HEK293 Cells

We first investigated the effects of *NPHS1* variants on nephrin protein expression by immunoblotting. HEK293 cells were transfected with WT or variant *NPHS1* together with pEGFP-C1 vector. This pEGFP-C1 vector allowed us to compare the transfection efficiency across groups so as to ensure they were identical. 24 h after transfection, total protein was extracted and western blot was performed according to standard protocol using anti-Nephrin antibody (abcam®). We found that cells with *NPHS1*$^{294C>T}$ had significantly lower nephrin expression (densitometry measurements 0.57±0.09) than cells with *NPHS1*^{WT} (1.06±0.10) (p=0.017) (about 2-fold reduction) (Figure 6-1). Similarly, cells with *NPHS1*$^{294C>T+2289C>T}$ had lower expression (0.48±0.09) than cells with *NPHS1*^{WT} (p=0.005). This decrease in nephrin expression was not seen in cells with *NPHS1*$^{2289C>T}$. These findings suggested the decreased ability of *NPHS1*$^{294C>T}$ to inhibit *TRPC6* function could be due to decreased nephrin protein expression.

6.2.2 *NPHS1*$^{294C>T}$ Decreases Nephrin mRNA Stability in HEK Cells

The mRNA stability of the *NPHS1* polymorphisms was then studied. The total RNA of the transfected HEK293 cells was extracted before and after actinomycin D treatment followed by first strand cDNA synthesis. Real-time PCR was performed to record the threshold cycle (C_T) changes of each *NPHS1* variants before and after actinomycin D treatment. The transfection efficiency was identical for the different groups. The data were normalized using housekeeping gene GAPDH and the fold changes were analysed by $2^{-\Delta\Delta C}{}_T$ method (Livak and Schmittgen 2001). We found that the mean mRNA fold change of post-treatment transcripts relative to pre-treatment amounts were significantly lower for *NPHS1*$^{294C>T}$ (0.015±0.011, p=0.002) compared to *NPHS1*^{WT} (0.179±0.030). This showed that the RNA stability of *NPHS1*$^{294C>T}$ decreased more than 10-fold compared with *NPHS1*^{WT}. Similarly, the mRNA stability of *NPHS1*$^{294C>T+2289C>T}$ (0.051±0.027) also significantly decreased by 2.8-fold compared with *NPHS1*^{WT} (0.179±0.030, p=0.019). There was no significant difference for the *NPHS1*$^{2289C>T}$ transcript (0.064±0.048). These finding indicated that nephrin polymorphism c.294C>T altered the rate of mRNA decay resulting in decreased protein expression. The attenuated nephrin expression then resulted in decreased ability of nephrin to inhibit *TRPC6*, hence leading to increased current amplitudes.

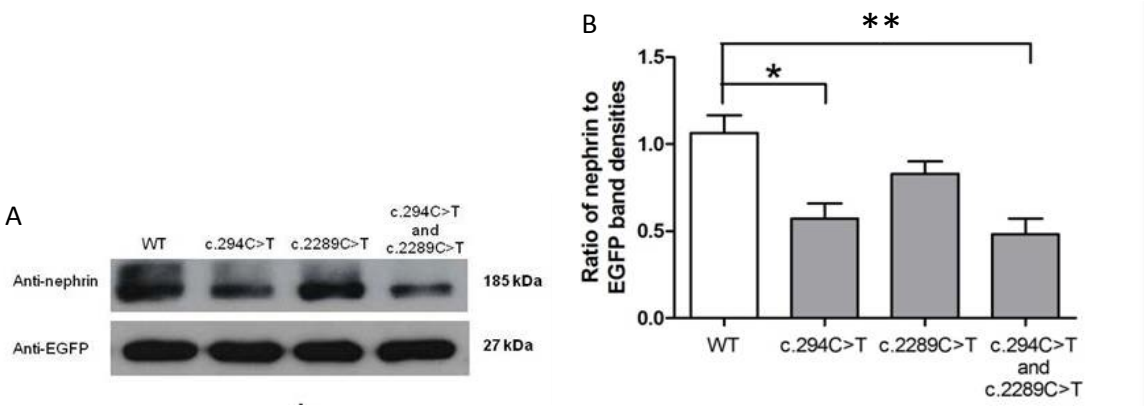

Figure 6-1 Western Blot Analysis for Nephrin Expression in HEK293-M1 Cells Transfected with Nephrin Variants.

(A) Representative western blot analysis. EGFP expression was identical across groups implying equal transfection efficiency. The nephrin band densities were normalized to those of EGFP bands for each group. (B) Bar chart comparing mean ratios of nephrin to EGFP band densities in the different groups. Statistical analysis showed that cells with *NPHS1*$^{294C>T}$ or *NPHS1*$^{294C>T+2289C>T}$ had significantly lower nephrin expression than cells with NPHS1^{WT}. This experiment was performed four times with similar results. The error bars show the standard errors of the means and asterisks denote statistically significant comparisons (student's t-test).

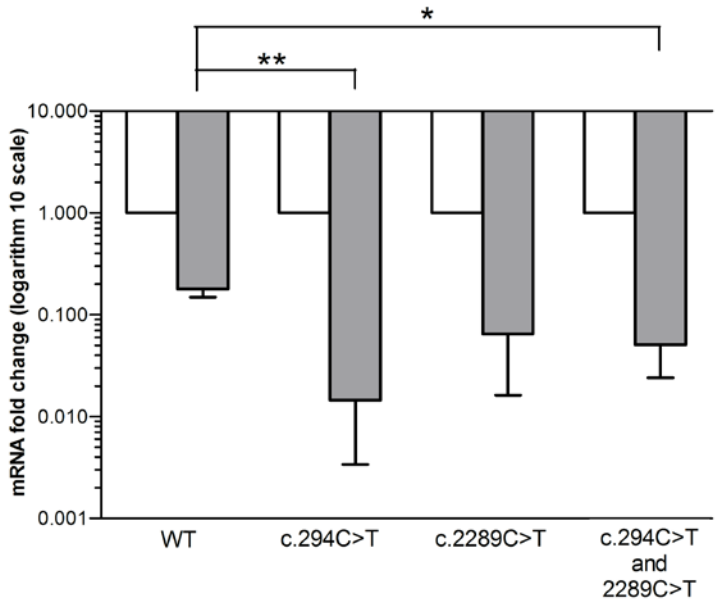

Figure 6-2 Relative mRNA Stability of Nephrin Variants, as Determined by Real-time RT–PCR.

GAPDH was used as the housekeeping gene. The amount of mRNA after actinomycin D treatment (gray bars) in each group were relative to the pre-treatment amount, which were set as 1 (white bars). This experiment was performed four times with similar results. The mean mRNA fold change was significantly lower for *NPHS1*$^{294C>T}$ and *NPHS1*$^{294C>T+2289C>T}$ compared to *NPHS1*^{WT} (p=0.002 and 0.019 respectively). The error bars show the standard errors of the means and asterisks denote statistically significant comparisons (student's t-test).

6.3 Discussion and Conclusions

Genetic factors play an important role in variability of human phenotypes, such as susceptibility to disease and response to therapies. These phenotypic differences may be caused by gene sequence variants via different mechanisms. The most dramatic effects of sequence variants are those involving changes to the encoded protein sequences. However polymorphisms which do not change amino acid sequence can also affect phenotype. There have been several proposed mechanisms (Albert 2011). For example, polymorphisms may occur in non-coding regions, such as the untranslated regions or introns, and affect gene regulation. On the other hand, polymorphisms in coding regions may exert their effects on

mRNA processing (splicing, mRNA modification and turnover), mRNA stability or translation (Johnson *et al.* 2005).

Nephrin is a major component of the glomerular filtration barrier, which was initially identified as the main genetic causes of congenital NS. To date, more than 60 different nephrin mutations, including deletions, insertions, nonsense and missense mutations, and mutations at splice sites and promoters, have been identified (Liu *et al.* 2004). Because these involve changes to the amino acid sequence, they almost invariably result in severe phenotypes, mainly congenital nephrotic syndrome. However, *NPHS1* synonymous polymorphisms have also been associated with renal diseases. For example, from a study of 267 Japanese patients with Ig A nephropathy (IgAN) and 197 healthy controls, *NPHS1* G349A polymorphism was suggested to be associated with heavy proteinuria and a decline in renal function in IgAN (Narita *et al.* 2003). 6 years later this polymorphism was confirmed to be functional by showing that the G allele and AG/GG genotype was associated with the severity of renal function at the time of diagnosis and the GG genotype was an independent risk of the prognosis of IgAN patients (Yu *et al.* 2009). As shown in Chapter 3, our study on 97 unrelated Singapore Chinese patients with idiopathic sporadic NS also indicates that the two *NPHS1* SNPs, c.294C>T and c.2289C>T, are significantly associated with NS. In addition, the study of nephrin expression in non-renal tissues, like human pancreatic islet cells, showed that both synonymous nephrin SNPs c.294C>T and c.2289C>T were associated with type 2 diabetes (Daimon *et al.* 2006).

While there have been reported studies on the association of nephrin polymorphisms with renal disease, there have been none depicting the mechanisms by which these polymorphisms

exert their effects. To our knowledge, we are the first to report the mechanisms by which nephrin polymorphisms interact with *TRPC6* to affect the clinical phenotype. In the current study, we found that c.294C>T nephrin polymorphism decreased mRNA stability which in turn decreased nephrin protein expression. This then led to the loss of ability of nephrin to inhibit *TRPC6* function and therefore increased *TRPC6* current amplitudes.

Decreased nephrin expression has been reported in patients with glomerular diseases and animal models. Huh et al., reported that in patients with membranous glomerulonephritis (GN), the expression of nephrin was lower in regions of effacement of the podoctyte foot processes (Huh *et al.* 2002). Rats with streptozotocin-induced diabetes mellitus showed 45% reduction of nephrin expression in the late proteinuric phase (Kelly *et al.* 2002). More than 60% reduction of nephrin expression was also demonstrated in 17 patients with diabetes and NS (Doublier *et al.* 2003).

Tyrosine phosphorylated *TRPC6* induces a complex formation with PLC-γ1, which is prerequisite for *TRPC6* surface expression. However, this process could be inhibited by WT nephrin, which competitively binds to the phosphorylated *TRPC6*, resulting in decreased surface expression (Kanda *et al.* 2011). Therefore, the decreased nephrin expression in podocytes, or some FSGS-associated *TRPC6* mutations that render the mutant *TRPC6*'s insensitive to nephrin suppression can lead to increased *TRPC6* currents. In addition, it has been shown that increased *TRPC6* currents alone, even in the absence of *TRPC6* mutations, can lead to proteinuric disease. Moller et al., demonstrated that the overexpressed *TRPC6* in cultured differentiated podocytes directly affects cytoskeletal organization. And in mice the transient overexpressed *TRPC6* protein at the slit diaphragm causes proteinuria (Moller *et al.* 2007).

According to data from HapMap and 1000 genomes (references), the TT genotype frequency of c.294C>T nephrin polymorphism ranges from 0% to 6.5% in the different populations in the world. This implies that there are healthy individuals with c.294C>T nephrin polymorphism. Clearly, the presence of c.294C>T polymorphism alone does not result in disease. However, it can act as a "hit" to the development of glomerular disease which has recently been envisaged a disease with "multi-hit" pathomechanism. The c.294C>T nephrin polymorphism therefore increases the genetic predisposition towards renal disease.

In conclusion, we are the first to prove via in-vitro studies that the nephrin polymorphism c.294C>T exerts its functions by decreasing mRNA stability, thereby decreasing nephrin expression, reducing its ability to inhibit *TRPC6* and resulting in increased *TRPC6* current amplitudes. Increased *TRPC6* currents have been shown in glomerular disease. The c.294C>T nephrin polymorphism probably increases the genetic predisposition towards renal disease and is likely not the only factor leading to the development of glomerular disease. We have also shown that c.2289C>T nephrin polymorphism and c.954T>C podocin polymorphism had no effects on mRNA stability or protein expression. These are consistent with our electrophysiological findings. Animal models will be necessary to further elucidate the role of nephrin polymorphisms in the pathomechanism of glomerular diseases.

CHAPTER 7 DISCUSSION AND CONCLUSIONS

7.1 DISCUSSION

Our study is the first to demonstrate via functional studies the existence of genetic epistasis between *NPHS1* polymorphisms and *TRPC6*, accounting for the variable and non-penetrant expression of a novel mutant *TRPC6* mutation, and the successful kidney transplantation between two individuals with the same mutant *TRPC6* gene. Both donor and recipient have remained well with normal renal function and no proteinuria 19 years after transplant. Currently, there is no clear consensus on the suitability of potential kidney donors with podocyte gene mutations and generally, such donors are precluded from donation (Santin *et al.* 2009). Our data, however, have shown that such transplants are possible if there are modifying genes resulting in non-penetrance.

While pathogenic mutations are considered clinically significant, single-nucleotide polymorphisms are rarely regarded as important. In this study, *NPHS1* polymorphisms c.294C>T and c.2289C>T segregated incrementally with severity of renal disease in our index family, and were notably absent in the kidney donor. Using the conservative method of Bonferroni correction for multiple-comparison analysis, cells transfected with mutant *TRPC6* and *NPHS1* variants representing the patients with FSGS had higher *TRPC6* currents compared to cells with $TRPC6^{WT}$. On the other hand, cells with the donor's genotype had lower *TRPC6* currents compared to cells representing those with FSGS, accounting for the lack of FSGS phenotype in the donor kidney. It is interesting that these *NPHS1* polymorphisms had higher allele frequencies in Singapore Chinese patients with SRNS, SDNS and/or FSGS compared to controls, although our experiments on the individual homozygous polymorphsims demonstrated that only $NPHS1^{294C>T}$ and not $NPHS1^{2289C>T}$,

resulted in decreased mRNA stability and nephrin protein expression, with resultant decreased ability to inhibit *TRPC6*^{R68W} compared to *NPHS1*^{WT}.

TRPC6-associated glomerular disease is classically an adult-onset disease occurring as late as the fifth decade of life (Reiser *et al.* 2005). However, recent reports described early disease onset in children less than ten years old, with the youngest being six months. Moreover,there is a wide spectrum of phenotypes ranging from no renal disease to isolated proteinuria to ESRD (Heeringa *et al.* 2009; Santin *et al.* 2009; Buscher *et al.* 2010; Gigante *et al.* 2011; Liakopoulos *et al.* 2011; Mir *et al.* 2012). Similarly, we observed non-penetrance of the novel *TRPC6*^{R68W} mutation in three family members and one control. One explanation for the variable penetrance is the multi-hit hypothesis in which other insults and/or genetic variants contribute to disease pathomechanism (Dryer and Reiser 2010). Our findings suggest that the relatively early disease onset in this family could be a result of genetic epistasis between *NPHS1* polymorphisms and *TRPC6*. Indeed, genetic epistasis has been suggested between a *WT1* polymorphism and a *NPHS1* mutation in patients with SRNS, but no functional validation studies have been performed in previous studies (McCarthy *et al.* 2013).

All 17 *TRPC6* mutations reported to date occur in the cytoplasmic NH_2 or COOH terminals of the protein (Reiser *et al.* 2005; Winn *et al.* 2005; Heeringa *et al.* 2009; Santin *et al.* 2009; Zhu *et al.* 2009; Buscher *et al.* 2010; Gigante *et al.* 2011; Mir *et al.* 2012). Specifically, gain-of-function mutations which increase *TRPC6* currents and/or increase intracellular calcium influx map to either ankyrin repeats in the NH_2 terminal or coiled-coil domain in the COOH terminal (Reiser *et al.* 2005; Winn *et al.* 2005; Heeringa *et al.* 2009; Zhu *et al.* 2009; Gigante *et al.* 2011; Hofstra *et al.* 2013). Ankyrin repeats are common protein-protein interaction

motifs thought to be important in protein function (Montell 2005). The p.R68W mutation occurs proximal to the NH_2 terminal, and is therefore proximal to all the previously reported mutations. It is the first reported mutation located outside a known functional domain or motif that increases *TRPC6* current amplitudes in heterologous expression systems. The gain of function seen with the p.R68W mutation could still be explained by its proximity to the first ankyrin repeat.

We have demonstrated that *TRPC6* current amplitudes increased with worsening phenotype severity in our index family. This concurred with the study by Heeringa et al who found that the *TRPC6* mutation p.M132T, associated with early age of onset of FSGS in children, caused the largest current amplitude changes compared to other mutations which caused later disease onset in adults (Heeringa *et al.* 2009). Studies have suggested that it is the increased *TRPC6* current amplitudes that result in disease, rather than the mutant channels *per se*. Increased $TRPC6^{WT}$ glomerular expression has been shown in acquired human proteinuric diseases and mouse models for human FSGS in the absence of *TRPC6* mutations (Moller *et al.* 2007; Nijenhuis *et al.* 2011). These concurred with studies in cultured podocytes in which overexpression of $TRPC6^{WT}$ resulted in cytoskeleton rearrangement through increase in intracellular calcium and RhoA activation (Jiang *et al.* 2011).

Nephrin is a cell-adhesion protein that interacts with *TRPC6* at the podocyte slit diaphragm (Reiser *et al.* 2005). Mutations in *NPHS1* cause congenital nephrotic syndrome of the Finnish type and other forms of nephrotic syndrome (Kestila *et al.* 1998; Lenkkeri *et al.* 1999). We have shown via patch clamp electrophysiology that $NPHS1^{WT}$ decreases *TRPC6* currents. This explains the finding of enhanced *TRPC6* expression in podocytes of nephrin-deficient

mice (Reiser *et al.* 2005). The mechanism of this interaction was proposed by Kanda et al who demonstrated that phosphorylation of *TRPC6* induced complex formation with phospholipase C-γ1 which in turn led to its surface expression and activation (Kanda *et al.* 2011). This process was inhibited by $NPHS1^{WT}$ which bound to phosphorylated *TRPC6* and competitively inhibited *TRPC6*- phospholipase C-γ1 complex formation. Mutated *TRPC6* channels are insensitive to nephrin suppression, and therefore have enhanced surface expression and increased channel activity (Kanda *et al.* 2011). We have shown that while $NPHS1^{WT}$ can inhibit *TRPC6* p.R68W currents, this ability was lost in the presence of $NPHS1^{c.294C>T}$, the mechanism through which may be decreased nephrin protein expression.

Our work clearly points to the clinical importance of epistasis between genes within the podocyte, and this is probably underestimated in clinical practice. This work provides evidence to the clinician that it may not be sufficient to attribute the disease to one potential disease-causing mutation. This is particularly important in late-onset disease in which variable penetrance has been described, suggesting the importance of other "hits"; as well as in recessive diseases in which only one mutation has been found in the gene of interest. Such consideration is crucial when genetic counselling is offered or when a potential related kidney donor is being considered. As there are so many other genes that may potentially interact with each other and it is often near-impossible to screen every one of them by conventional sequencing, newer techniques such as exome sequencing can definitely play an important role in this disease.

7.2 CONCLUSIONS

We described in a Singapore Chinese index family with hereditary FSGS a successful renal transplant that occurred between a donor and recipient sibling-pair, both of whom carried the same novel *TRPC6* p.R68W missense mutation. To our knowledge, there has been no successful renal transplant described from a donor with a *TRPC6* mutation. This mutation is the most proximal to the NH_2 terminal among all reported *TRPC6* mutations. Unlike previously published gain-of-function *TRPC6* mutations which were all mapped to either ankyrin repeats in the NH_2 terminal or coiled-coil domain in the COOH terminal, the p.R68W mutation is the first gain-of-function mutation which occurs outside of a known functional domain or motif. This mutation increases *TRPC6* current amplitudes and enhanced *TRPC6* surface expression.

We have also found nephrin and podocin polymorphisms which appeared to segregate with renal disease. Among these, we have shown, via electrophysiological methods, how the interactions between the *TRPC6* p.R68W mutation and the nephrin polymorphism c.294C>T could explain the variable penetrance of the *TRPC6* mutation. We showed that this c.294C>T polymorphism decreases mRNA stability and therefore decreases nephrin protein expression. This in turn results in the loss of ability of nephrin to inhibit *TRPC6*, leading to increased *TRPC6* current amplitudes. Increased *TRPC6* current amplitudes *per se* have been associated with glomerular diseases.

In addition, we represented the genotypes of specific family members in HEK cells and further proved that the simultaneous presence of homozygous nephrin c.294C>T and c.2289C>T polymorphisms could explain the differences in phenotype between the donor

and the recipient and therefore the successful renal transplantation that occurred 19 years ago. This work carries important implications in the selection of live related donors in renal transplantation.

7.3 FUTURE DIRECTIONS

The work in this thesis was conducted mainly in HEK293 cells which do not inherently express *TRPC6*, nephrin or podocin. Further studies may involve replication of our work in podocytes as these are the cellular sites of pathology and they natively express these proteins. However, because the *TRPC6* mutations are gain-of-function, we ideally will need to perform these experiments in *TRPC6*-deficient podocytes. Conditionally immortalised podocytes will be required as primary podocyte cultures are notoriously difficult to obtain and maintain.

Additionally, in vivo studies will be necessary to further confirm the interactions of the polymorphisms with *TRPC6*. A *TRPC6* knockout mouse model is available and this has no renal phenotype (Dietrich *et al.* 2005; Quick *et al.* 2012). The *TRPC6* mutation can be introduced by creation of a transgenic mouse and then breeding with the *TRPC6* knockout mouse to remove the effects of the native *TRPC6*. Alternatively, the recently published method of transcription activator-like effector nucleases **(**TALENS) (Cade *et al.* 2012) may be used. Separate mice models with the nephrin polymorphisms will be created and then crossed with the mutated *TRPC6* mice so as to study the effects of genetic epistasis *in vivo*.

REFERENCES

(1981). "Primary nephrotic syndrome in children: clinical significance of histopathologic variants of minimal change and of diffuse mesangial hypercellularity. A Report of the International Study of Kidney Disease in Children." Kidney Int **20**(6): 765-771.

(2007). "U.S. Renal Data System. USRDS 2007 Annual Data Report: Atlas of chronic kidney disease and end-stage renal disease in the United States. National Institutes of Health, National Institute of Diabetes and Digestive and Kidney Diseases, Bethesda, MD."

(2012). U.S. Renal Data System, USRDS 2012 Annual Data Report: Atlas of Chronic Kidney Disease and End-Stage Renal Disease in the United States. . Bethesda, MD, National Institutes of Health, National Institute of Diabetes and Digestive and Kidney Diseases.

Abramowitz, J. and L. Birnbaumer (2009). "Physiology and pathophysiology of canonical transient receptor potential channels." FASEB journal : official publication of the Federation of American Societies for Experimental Biology **23**(2): 297-328.

Akilesh, S., H. Suleiman, et al. (2011). "Arhgap24 inactivates Rac1 in mouse podocytes, and a mutant form is associated with familial focal segmental glomerulosclerosis." The Journal of clinical investigation **121**(10): 4127-4137.

Albert, P. R. (2011). "What is a functional genetic polymorphism? Defining classes of functionality." Journal of psychiatry & neuroscience : JPN **36**(6): 363-365.

Asanuma, K., K. N. Campbell, et al. (2007). "Nuclear relocation of the nephrin and CD2AP-binding protein dendrin promotes apoptosis of podocytes." Proc Natl Acad Sci U S A **104**(24): 10134-10139.

Asanuma, K., E. Yanagida-Asanuma, et al. (2006). "Synaptopodin orchestrates actin organization and cell motility via regulation of RhoA signalling." Nature cell biology **8**(5): 485-491.

Aucella, F., P. De Bonis, et al. (2005). "Molecular analysis of NPHS2 and ACTN4 genes in a series of 33 Italian patients affected by adult-onset nonfamilial focal segmental glomerulosclerosis." Nephron. Clinical practice **99**(2): c31-36.

Avila-Casado Mdel, C., I. Perez-Torres, et al. (2004). "Proteinuria in rats induced by serum from patients with collapsing glomerulopathy." Kidney Int **66**(1): 133-143.

Bandyopadhyay, B. C., W. D. Swaim, et al. (2005). "Apical localization of a functional TRPC3/*TRPC6*-Ca2+-signaling complex in polarized epithelial cells. Role in apical Ca2+ influx." J Biol Chem **280**(13): 12908-12916.

Barisoni, L., W. Kriz, et al. (1999). "The dysregulated podocyte phenotype: a novel concept in the pathogenesis of collapsing idiopathic focal segmental glomerulosclerosis and HIV-associated nephropathy." J Am Soc Nephrol **10**(1): 51-61.

Beaufils, H., J. C. Alphonse, et al. (1978). "Focal glomerulosclerosis: natural history and treatment. A report of 70 cases." Nephron **21**(2): 75-85.

Beltcheva, O., P. Martin, et al. (2001). "Mutation spectrum in the nephrin gene (NPHS1) in congenital nephrotic syndrome." Human mutation **17**(5): 368-373.

Benetti, E., G. Caridi, et al. (2010). "A novel WT1 gene mutation in a three-generation family with progressive isolated focal segmental glomerulosclerosis." Clinical journal of the American Society of Nephrology : CJASN **5**(4): 698-702.

Benzing, T. (2004). "Signaling at the slit diaphragm." Journal of the American Society of Nephrology : JASN **15**(6): 1382-1391.

Berridge, M. J., M. D. Bootman, et al. (2003). "Calcium signalling: dynamics, homeostasis and remodelling." Nature reviews. Molecular cell biology **4**(7): 517-529.

Beskina, O., A. Miller, et al. (2007). "Mechanisms of interleukin-1beta-induced Ca2+ signals in mouse cortical astrocytes: roles of store- and receptor-operated Ca2+ entry." American journal of physiology. Cell physiology **293**(3): C1103-1111.

Bhimma, R., H. M. Coovadia, et al. (1997). "Nephrotic syndrome in South African children: changing perspectives over 20 years." Pediatric nephrology **11**(4): 429-434.
Bidani, A. K., K. D. Mitchell, et al. (1990). "Absence of glomerular injury or nephron loss in a normotensive rat remnant kidney model." Kidney international **38**(1): 28-38.
Bohlen, C. J., A. Priel, et al. (2010). "A bivalent tarantula toxin activates the capsaicin receptor, TRPV1, by targeting the outer pore domain." Cell **141**(5): 834-845.
Bostrom, M. A., P. Perlegas, et al. (2012). "Relevance of the ACTN4 Gene in African-Americans with Non-Diabetic End-Stage Renal Disease." American journal of nephrology **36**(3): 252-260.
Boulay, G. (2002). "Ca(2+)-calmodulin regulates receptor-operated Ca(2+) entry activity of *TRPC6* in HEK-293 cells." Cell Calcium **32**(4): 201-207.
Boute, N., O. Gribouval, et al. (2000). "NPHS2, encoding the glomerular protein podocin, is mutated in autosomal recessive steroid-resistant nephrotic syndrome." Nature genetics **24**(4): 54.
Boute, N., O. Gribouval, et al. (2000). "NPHS2, encoding the glomerular protein podocin, is mutated in autosomal recessive steroid-resistant nephrotic syndrome." Nat Genet **24**(4): 349-354.
Boyer, O., G. Benoit, et al. (2010). "Mutational analysis of the PLCE1 gene in steroid resistant nephrotic syndrome." Journal of medical genetics **47**(7): 445-452.
Boyer, O., G. Benoit, et al. (2011). "Mutations in INF2 are a major cause of autosomal dominant focal segmental glomerulosclerosis." Journal of the American Society of Nephrology : JASN **22**(2): 239-245.
Brown, E. J., J. S. Schlondorff, et al. (2010). "Mutations in the formin gene INF2 cause focal segmental glomerulosclerosis." Nature genetics **42**(1): 72-76.
Buscher, A. K., B. Kranz, et al. (2010). "Immunosuppression and renal outcome in congenital and pediatric steroid-resistant nephrotic syndrome." Clinical journal of the American Society of Nephrology : CJASN **5**(11): 2075-2084.
Buscher, A. K., B. Kranz, et al. (2010). "Immunosuppression and renal outcome in congenital and pediatric steroid-resistant nephrotic syndrome." Clin J Am Soc Nephrol **5**(11): 2075-2084.
Cade, L., D. Reyon, et al. (2012). "Highly efficient generation of heritable zebrafish gene mutations using homo- and heterodimeric TALENs." Nucleic acids research **40**(16): 8001-8010.
Cameron, J. S., D. R. Turner, et al. (1978). "The long-term prognosis of patients with focal segmental glomerulosclerosis." Clinical nephrology **10**(6): 213-218.
Caridi, G., R. Bertelli, et al. (2003). "Broadening the spectrum of diseases related to podocin mutations." J Am Soc Nephrol **14**(5): 1278-1286.
Caterina, M. J., M. A. Schumacher, et al. (1997). "The capsaicin receptor: a heat-activated ion channel in the pain pathway." Nature **389**(6653): 816-824.
Cattran, D. C. and P. Rao (1998). "Long-term outcome in children and adults with classic focal segmental glomerulosclerosis." Am J Kidney Dis **32**(1): 72-79.
Cho, H. Y., J. H. Lee, et al. (2008). "WT1 and NPHS2 mutations in Korean children with steroid-resistant nephrotic syndrome." Pediatr Nephrol **23**(1): 63-70.
Choi, Y. K., Y. J. Kim, et al. (2003). "Suppression of glomerulosclerosis by adenovirus-mediated IL-10 expression in the kidney." Gene therapy **10**(7): 559-568.
Chyb, S., P. Raghu, et al. (1999). "Polyunsaturated fatty acids activate the Drosophila light-sensitive channels TRP and TRPL." Nature **397**(6716): 255-259.
Clapham, D. E. (2003). "TRP channels as cellular sensors." Nature **426**(6966): 517-524.
Cohen, A. H. and C. C. Nast (1988). "HIV-associated nephropathy. A unique combined glomerular, tubular, and interstitial lesion." Modern pathology : an official journal of the United States and Canadian Academy of Pathology, Inc **1**(2): 87-97.
Collins, A. J., R. N. Foley, et al. (2013). "US Renal Data System 2012 Annual Data Report." Am J Kidney Dis **61**(1 Suppl 1): A7, e1-476.
Conlon, P. J., K. Lynn, et al. (1999). "Spectrum of disease in familial focal and segmental glomerulosclerosis." Kidney Int **56**(5): 1863-1871.

Cosens, D. J. and A. Manning (1969). "Abnormal electroretinogram from a Drosophila mutant." Nature **224**(5216): 285-287.

Coward, R. J., R. R. Foster, et al. (2005). "Nephrotic plasma alters slit diaphragm-dependent signaling and translocates nephrin, Podocin, and CD2 associated protein in cultured human podocytes." J Am Soc Nephrol **16**(3): 629-637.

D'Agati, V. (2003). "Pathologic classification of focal segmental glomerulosclerosis." Seminars in nephrology **23**(2): 117-134.

D'Agati, V. D. (2008). "The spectrum of focal segmental glomerulosclerosis: new insights." Current opinion in nephrology and hypertension **17**(3): 271-281.

D'Agati, V. D., F. J. Kaskel, et al. (2011). "Focal segmental glomerulosclerosis." The New England journal of medicine **365**(25): 2398-2411.

D'Agati, V. D., F. J. Kaskel, et al. (2011). "Focal segmental glomerulosclerosis." N Engl J Med **365**(25): 2398-2411.

Daimon, M., G. Ji, et al. (2006). "Association of nephrin gene polymorphisms with type 2 diabetes in a Japanese population: The Funagata study." Diabetes care **29**(5): 1117-1119.

Denis F. Geary and F. Schaefer. (2008). *Comprehensive Pediatric Nephrology*. Philadelphia, First Edition 12: 205-218, Mosby.

Dietrich, A. and T. Gudermann (2007). "*TRPC6*." Handb Exp Pharmacol(179): 125-141.

Dietrich, A., M. Mederos y Schnitzler, et al. (2003). "N-linked protein glycosylation is a major determinant for basal TRPC3 and *TRPC6* channel activity." The Journal of biological chemistry **278**(48): 47842-47852.

Dietrich, A., Y. S. M. Mederos, et al. (2005). "Increased vascular smooth muscle contractility in *TRPC6*-/- mice." Mol Cell Biol **25**(16): 6980-6989.

Don, R. H., P. T. Cox, et al. (1991). "'Touchdown' PCR to circumvent spurious priming during gene amplification." Nucleic acids research **19**(14): 4008.

Donoviel, D. B., D. D. Freed, et al. (2001). "Proteinuria and perinatal lethality in mice lacking NEPH1, a novel protein with homology to NEPHRIN." Molecular and cellular biology **21**(14): 4829-4836.

Doublier, S., V. Ruotsalainen, et al. (2001). "Nephrin redistribution on podocytes is a potential mechanism for proteinuria in patients with primary acquired nephrotic syndrome." The American journal of pathology **158**(5): 1723-1731.

Doublier, S., G. Salvidio, et al. (2003). "Nephrin expression is reduced in human diabetic nephropathy: evidence for a distinct role for glycated albumin and angiotensin II." Diabetes **52**(4): 1023-1030.

Dryer, S. E. and J. Reiser (2010). "*TRPC6* channels and their binding partners in podocytes: role in glomerular filtration and pathophysiology." American journal of physiology. Renal physiology **299**(4): F689-701.

Dryer, S. E. and J. Reiser (2010). "*TRPC6* channels and their binding partners in podocytes: role in glomerular filtration and pathophysiology." Am J Physiol Renal Physiol **299**(4): F689-701.

Dustin, M. L., M. W. Olszowy, et al. (1998). "A novel adaptor protein orchestrates receptor patterning and cytoskeletal polarity in T-cell contacts." Cell **94**(5): 667-677.

Eddy, A. A. and J. M. Symons (2003). "Nephrotic syndrome in childhood." Lancet **362**(9384): 629-639.

Eder, P., M. Poteser, et al. (2005). "Na(+) entry and modulation of Na(+)/Ca(2+) exchange as a key mechanism of TRPC signaling." Pflugers Archiv : European journal of physiology **451**(1): 99-104.

Ehrich, J. H., C. Geerlings, et al. (2007). "Steroid-resistant idiopathic childhood nephrosis: overdiagnosed and undertreated." Nephrol Dial Transplant **22**(8): 2183-2193.

Estacion, M., S. Li, et al. (2004). "Activation of human *TRPC6* channels by receptor stimulation." J Biol Chem **279**(21): 22047-22056.

Estacion, M., W. G. Sinkins, et al. (2006). "Human *TRPC6* expressed in HEK 293 cells forms non-selective cation channels with limited Ca2+ permeability." The Journal of physiology **572**(Pt 2): 359-377.

Faix, J. and R. Grosse (2006). "Staying in shape with formins." Developmental cell **10**(6): 693-706.

Fan, Q., H. Zhang, et al. (2009). "R168H and V165X mutant podocin might induce different degrees of podocyte injury via different molecular mechanisms." Genes to cells : devoted to molecular & cellular mechanisms **14**(9): 1079-1090.

Faubert, P. F. and J. G. Porush (1997). "Familial focal segmental glomerulosclerosis: nine cases in four families and review of the literature." Am J Kidney Dis **30**(2): 265-270.

Faul, C., M. Donnelly, et al. (2008). "The actin cytoskeleton of kidney podocytes is a direct target of the antiproteinuric effect of cyclosporine A." Nat Med **14**(9): 931-938.

Faul, C., M. Donnelly, et al. (2008). "The actin cytoskeleton of kidney podocytes is a direct target of the antiproteinuric effect of cyclosporine A." Nature medicine **14**(9): 931-938.

Filler, G., E. Young, et al. (2003). "Is there really an increase in non-minimal change nephrotic syndrome in children?" Am J Kidney Dis **42**(6): 1107-1113.

Flockerzi, V. (2007). "An introduction on TRP channels." Handbook of experimental pharmacology(179): 1-19.

Fogo, A., E. P. Hawkins, et al. (1990). "Glomerular hypertrophy in minimal change disease predicts subsequent progression to focal glomerular sclerosis." Kidney international **38**(1): 115-123.

Fogo, A. B. (2003). "Animal models of FSGS: lessons for pathogenesis and treatment." Seminars in nephrology **23**(2): 161-171.

Freichel, M., S. H. Suh, et al. (2001). "Lack of an endothelial store-operated Ca2+ current impairs agonist-dependent vasorelaxation in TRP4-/- mice." Nature cell biology **3**(2): 121-127.

Fries, J. W., D. J. Sandstrom, et al. (1989). "Glomerular hypertrophy and epithelial cell injury modulate progressive glomerulosclerosis in the rat." Laboratory investigation; a journal of technical methods and pathology **60**(2): 205-218.

Fuchshuber, A., G. Jean, et al. (1995). "Mapping a gene (SRN1) to chromosome 1q25-q31 in idiopathic nephrotic syndrome confirms a distinct entity of autosomal recessive nephrosis." Human molecular genetics **4**(11): 2155-2158.

Gallon, L., J. Leventhal, et al. (2012). "Resolution of recurrent focal segmental glomerulosclerosis after retransplantation." The New England journal of medicine **366**(17): 1648-1649.

Garg, P., R. Verma, et al. (2007). "Slit diaphragm junctional complex and regulation of the cytoskeleton." Nephron. Experimental nephrology **106**(2): e67-72.

Garg, P., R. Verma, et al. (2007). "Neph1 cooperates with nephrin to transduce a signal that induces actin polymerization." Molecular and cellular biology **27**(24): 8698-8712.

Gbadegesin, R., B. Hinkes, et al. (2007). "Mutational analysis of NPHS2 and WT1 in frequently relapsing and steroid-dependent nephrotic syndrome." Pediatric nephrology **22**(4): 509-513.

Gbadegesin, R., P. Lavin, et al. (2011). "Pathogenesis and therapy of focal segmental glomerulosclerosis: an update." Pediatr Nephrol **26**(7): 1001-1015.

Gellermann, J., C. J. Stefanidis, et al. (2010). "Successful treatment of steroid-resistant nephrotic syndrome associated with WT1 mutations." Pediatr Nephrol **25**(7): 1285-1289.

Gerke, P., T. B. Huber, et al. (2003). "Homodimerization and heterodimerization of the glomerular podocyte proteins nephrin and NEPH1." Journal of the American Society of Nephrology : JASN **14**(4): 918-926.

Gesualdo, L., A. M. Di Palma, et al. (2004). "The Italian experience of the national registry of renal biopsies." Kidney international **66**(3): 890-894.

Gigante, M., G. Caridi, et al. (2011). "*TRPC6* mutations in children with steroid-resistant nephrotic syndrome and atypical phenotype." Clin J Am Soc Nephrol **6**(7): 1626-1634.

Gigante, M., G. Caridi, et al. (2011). "*TRPC6* mutations in children with steroid-resistant nephrotic syndrome and atypical phenotype." Clinical journal of the American Society of Nephrology : CJASN **6**(7): 1626-1634.

Gigante, M., P. Pontrelli, et al. (2009). "CD2AP mutations are associated with sporadic nephrotic syndrome and focal segmental glomerulosclerosis (FSGS)." Nephrology, dialysis, transplantation : official publication of the European Dialysis and Transplant Association - European Renal Association **24**(6): 1858-1864.

Godel, M., B. Hartleben, et al. (2011). "Role of mTOR in podocyte function and diabetic nephropathy in humans and mice." The Journal of clinical investigation **121**(6): 2197-2209.

Goode, B. L. and M. J. Eck (2007). "Mechanism and function of formins in the control of actin assembly." Annual review of biochemistry **76**: 593-627.

Gubler, M. C. (2003). "Podocyte differentiation and hereditary proteinuria/nephrotic syndromes." J Am Soc Nephrol **14 Suppl 1**: S22-26.

Haas, M., S. M. Meehan, et al. (1997). "Changing etiologies of unexplained adult nephrotic syndrome: a comparison of renal biopsy findings from 1976-1979 and 1995-1997." American journal of kidney diseases : the official journal of the National Kidney Foundation **30**(5): 621-631.

Haas, M., B. H. Spargo, et al. (1995). "Increasing incidence of focal-segmental glomerulosclerosis among adult nephropathies: a 20-year renal biopsy study." American journal of kidney diseases : the official journal of the National Kidney Foundation **26**(5): 740-750.

Habib, R. (1973). "Editorial: Focal glomerular sclerosis." Kidney international **4**(6): 355-361.

Hara, Y., M. Wakamori, et al. (2002). "LTRPC2 Ca2+-permeable channel activated by changes in redox status confers susceptibility to cell death." Molecular cell **9**(1): 163-173.

Haraldsson, B., J. Nystrom, et al. (2008). "Properties of the glomerular barrier and mechanisms of proteinuria." Physiological reviews **88**(2): 451-487.

Hardie, R. C. and B. Minke (1992). "The trp gene is essential for a light-activated Ca2+ channel in Drosophila photoreceptors." Neuron **8**(4): 643-651.

Harita, Y., H. Kurihara, et al. (2009). "Phosphorylation of Nephrin Triggers Ca2+ Signaling by Recruitment and Activation of Phospholipase C-{gamma}1." The Journal of biological chemistry **284**(13): 8951-8962.

He, N., A. Zahirieh, et al. (2007). "Recessive NPHS2 (Podocin) mutations are rare in adult-onset idiopathic focal segmental glomerulosclerosis." Clinical journal of the American Society of Nephrology : CJASN **2**(1): 31-37.

Heeringa, S. F., C. C. Moller, et al. (2009). "A novel *TRPC6* mutation that causes childhood FSGS." PloS one **4**(11): e7771.

Hinkes, B., C. Vlangos, et al. (2008). "Specific podocin mutations correlate with age of onset in steroid-resistant nephrotic syndrome." J Am Soc Nephrol **19**(2): 365-371.

Hinkes, B., R. C. Wiggins, et al. (2006). "Positional cloning uncovers mutations in PLCE1 responsible for a nephrotic syndrome variant that may be reversible." Nat Genet **38**(12): 1397-1405.

Hinkes, B., R. C. Wiggins, et al. (2006). "Positional cloning uncovers mutations in PLCE1 responsible for a nephrotic syndrome variant that may be reversible." Nature genetics **38**(12): 1397-1405.

Hinkes, B. G., B. Mucha, et al. (2007). "Nephrotic syndrome in the first year of life: two thirds of cases are caused by mutations in 4 genes (NPHS1, NPHS2, WT1, and LAMB2)." Pediatrics **119**(4): e907-919.

Hisatsune, C., Y. Kuroda, et al. (2004). "Regulation of *TRPC6* channel activity by tyrosine phosphorylation." J Biol Chem **279**(18): 18887-18894.

Hoenderop, J. G., T. Voets, et al. (2003). "Homo- and heterotetrameric architecture of the epithelial Ca2+ channels TRPV5 and TRPV6." The EMBO journal **22**(4): 776-785.

Hofmann, T., A. G. Obukhov, et al. (1999). "Direct activation of human *TRPC6* and TRPC3 channels by diacylglycerol." Nature **397**(6716): 259-263.

Hofmann, T., M. Schaefer, et al. (2002). "Subunit composition of mammalian transient receptor potential channels in living cells." Proc Natl Acad Sci U S A **99**(11): 7461-7466.

Hofstra, J. M., S. Lainez, et al. (2013). "New *TRPC6* gain-of-function mutation in a non-consanguineous Dutch family with late-onset focal segmental glomerulosclerosis." Nephrol Dial Transplant.

Hogg, R. J., R. J. Portman, et al. (2000). "Evaluation and management of proteinuria and nephrotic syndrome in children: recommendations from a pediatric nephrology panel established at the National Kidney Foundation conference on proteinuria, albuminuria, risk, assessment, detection, and elimination (PARADE)." Pediatrics **105**(6): 1242-1249.

Honda, K., T. Yamada, et al. (1998). "Actinin-4, a novel actin-bundling protein associated with cell motility and cancer invasion." The Journal of cell biology **140**(6): 1383-1393.

Horinouchi, I., H. Nakazato, et al. (2003). "In situ evaluation of podocin in normal and glomerular diseases." Kidney Int **64**(6): 2092-2099.

Hostetter, T. H. (2003). "Hyperfiltration and glomerulosclerosis." Seminars in nephrology **23**(2): 194-199.

Hostetter, T. H., J. L. Olson, et al. (1981). "Hyperfiltration in remnant nephrons: a potentially adverse response to renal ablation." The American journal of physiology **241**(1): F85-93.

Huang, J. J., S. C. Hsu, et al. (2001). "Adult-onset minimal change disease among Taiwanese: clinical features, therapeutic response, and prognosis." American journal of nephrology **21**(1): 28-34.

Huber, T. B. and T. Benzing (2005). "The slit diaphragm: a signaling platform to regulate podocyte function." Current opinion in nephrology and hypertension **14**(3): 211-216.

Huber, T. B., B. Hartleben, et al. (2003). "Nephrin and CD2AP associate with phosphoinositide 3-OH kinase and stimulate AKT-dependent signaling." Molecular and cellular biology **23**(14): 4917-4928.

Huber, T. B., B. Hartleben, et al. (2003). "Nephrin and CD2AP associate with phosphoinositide 3-OH kinase and stimulate AKT-dependent signaling." Mol Cell Biol **23**(14): 4917-4928.

Huber, T. B., M. Kottgen, et al. (2001). "Interaction with podocin facilitates nephrin signaling." The Journal of biological chemistry **276**(45): 41543-41546.

Huber, T. B., M. Kottgen, et al. (2001). "Interaction with podocin facilitates nephrin signaling." J Biol Chem **276**(45): 41543-41546.

Huber, T. B., C. Kwoh, et al. (2006). "Bigenic mouse models of focal segmental glomerulosclerosis involving pairwise interaction of CD2AP, Fyn, and synaptopodin." J Clin Invest **116**(5): 45.

Huber, T. B., B. Schermer, et al. (2006). "Podocin and MEC-2 bind cholesterol to regulate the activity of associated ion channels." Proceedings of the National Academy of Sciences of the United States of America **103**(46): 17079-17086.

Huber, T. B., M. Simons, et al. (2003). "Molecular basis of the functional podocin-nephrin complex: mutations in the NPHS2 gene disrupt nephrin targeting to lipid raft microdomains." Hum Mol Genet **12**(24): 3397-3405.

Huh, W., D. J. Kim, et al. (2002). "Expression of nephrin in acquired human glomerular disease." Nephrology, dialysis, transplantation : official publication of the European Dialysis and Transplant Association - European Renal Association **17**(3): 478-484.

Inoki, K., H. Mori, et al. (2011). "mTORC1 activation in podocytes is a critical step in the development of diabetic nephropathy in mice." The Journal of clinical investigation **121**(6): 2181-2196.

Inoue, R., L. J. Jensen, et al. (2009). "Synergistic activation of vascular *TRPC6* channel by receptor and mechanical stimulation via phospholipase C/diacylglycerol and phospholipase A2/omega-hydroxylase/20-HETE pathways." Circulation research **104**(12): 1399-1409.

Inoue, R., L. J. Jensen, et al. (2009). "Synergistic activation of vascular *TRPC6* channel by receptor and mechanical stimulation via phospholipase C/diacylglycerol and phospholipase A2/omega-hydroxylase/20-HETE pathways." Circ Res **104**(12): 1399-1409.

Inoue, R., T. Okada, et al. (2001). "The transient receptor potential protein homologue TRP6 is the essential component of vascular alpha(1)-adrenoceptor-activated Ca(2+)-permeable cation channel." Circulation research **88**(3): 32.

ISKDC (1981). "The primary nephrotic syndrome in children. Identification of patients with minimal change nephrotic syndrome from initial response to prednisone. A report of the International Study of Kidney Disease in Children." J Pediatr **98**(4): 561-564.

Jardin, I., L. J. Gomez, et al. (2009). "Dynamic interaction of h*TRPC6* with the Orai1-STIM1 complex or hTRPC3 mediates its role in capacitative or non-capacitative Ca(2+) entry pathways." The Biochemical journal **420**(2): 267-276.

Jennette, J. C., J. Olson, L., et al. (2007). *Heptinstall's Pathology of the Kidney, Sixth Edition*. Philadephia, PA 19106 USA, Wolters Kluwer.

Jiang, L., J. Ding, et al. (2011). "Over-expressing transient receptor potential cation channel 6 in podocytes induces cytoskeleton rearrangement through increases of intracellular Ca2+ and RhoA activation." Exp Biol Med (Maywood) **236**(2): 184-193.

Johnson, A. D., D. Wang, et al. (2005). "Polymorphisms affecting gene regulation and mRNA processing: broad implications for pharmacogenetics." Pharmacology & therapeutics **106**(1): 19-38.

Julius, D. (2005). "From peppers to peppermints: natural products as probes of the pain pathway." Harvey lectures **101**: 89-115.

Jung, S., A. Muhle, et al. (2003). "Lanthanides potentiate TRPC5 currents by an action at extracellular sites close to the pore mouth." The Journal of biological chemistry **278**(6): 3562-3571.

Kanda, S., Y. Harita, et al. (2011). "Tyrosine phosphorylation-dependent activation of *TRPC6* regulated by PLC-gamma1 and nephrin: effect of mutations associated with focal segmental glomerulosclerosis." Molecular biology of the cell **22**(11): 1824-1835.

Kanda, S., Y. Harita, et al. (2011). "Tyrosine phosphorylation-dependent activation of *TRPC6* regulated by PLC-gamma1 and nephrin: effect of mutations associated with focal segmental glomerulosclerosis." Mol Biol Cell **22**(11): 1824-1835.

Kaplan, J. M., S. H. Kim, et al. (2000). "Mutations in ACTN4, encoding alpha-actinin-4, cause familial focal segmental glomerulosclerosis." Nature genetics **24**(3): 6.

Karle, S. M., B. Uetz, et al. (2002). "Novel mutations in NPHS2 detected in both familial and sporadic steroid-resistant nephrotic syndrome." Journal of the American Society of Nephrology : JASN **13**(2): 388-393.

Kelly, D. J., P. Aaltonen, et al. (2002). "Expression of the slit-diaphragm protein, nephrin, in experimental diabetic nephropathy: differing effects of anti-proteinuric therapies." Nephrology, dialysis, transplantation : official publication of the European Dialysis and Transplant Association - European Renal Association **17**(7): 1327-1332.

Kestila, M., U. Lenkkeri, et al. (1998). "Positionally cloned gene for a novel glomerular protein--nephrin--is mutated in congenital nephrotic syndrome." Molecular cell **1**(4): 575-582.

Kestila, M., U. Lenkkeri, et al. (1998). "Positionally cloned gene for a novel glomerular protein--nephrin--is mutated in congenital nephrotic syndrome." Mol Cell **1**(4): 575-582.

Kestila, M., M. Mannikko, et al. (1994). "Congenital nephrotic syndrome of the Finnish type maps to the long arm of chromosome 19." American journal of human genetics **54**(5): 757-764.

Kim, E. Y., C. P. Alvarez-Baron, et al. (2009). "Canonical transient receptor potential channel (TRPC)3 and *TRPC6* associate with large-conductance Ca2+-activated K+ (BKCa) channels: role in BKCa trafficking to the surface of cultured podocytes." Mol Pharmacol **75**(3): 466-477.

Kim, J. H., B. K. Kim, et al. (2003). "Activation of the TGF-beta/Smad signaling pathway in focal segmental glomerulosclerosis." Kidney international **64**(5): 1715-1721.

Kim, J. M., H. Wu, et al. (2003). "CD2-associated protein haploinsufficiency is linked to glomerular disease susceptibility." Science **300**(5623): 1298-1300.

Kim, J. Y. and D. Saffen (2005). "Activation of M1 muscarinic acetylcholine receptors stimulates the formation of a multiprotein complex centered on *TRPC6* channels." J Biol Chem **280**(36): 32035-32047.

Kirdpon, S., A. Vuttivirojana, et al. (1989). "The primary nephrotic syndrome in children and histopathologic study." Journal of the Medical Association of Thailand = Chotmaihet thangphaet **72 Suppl 1**: 26-31.

Kirsch, K. H., M. M. Georgescu, et al. (1999). "CMS: an adapter molecule involved in cytoskeletal rearrangements." Proceedings of the National Academy of Sciences of the United States of America **96**(11): 6211-6216.

Kitiyakara, C., P. Eggers, et al. (2004). "Twenty-one-year trend in ESRD due to focal segmental glomerulosclerosis in the United States." Am J Kidney Dis **44**(5): 815-825.

Kitiyakara, C., P. Eggers, et al. (2004). "Twenty-one-year trend in ESRD due to focal segmental glomerulosclerosis in the United States." American journal of kidney diseases : the official journal of the National Kidney Foundation **44**(5): 815-825.

Kitiyakara, C., J. B. Kopp, et al. (2003). "Trends in the epidemiology of focal segmental glomerulosclerosis." Seminars in nephrology **23**(2): 172-182.

Kitiyakara, C., J. B. Kopp, et al. (2003). "Trends in the epidemiology of focal segmental glomerulosclerosis." Semin Nephrol **23**(2): 172-182.

Komatsuda, A., H. Wakui, et al. (2003). "Analysis of mutations in alpha-actinin 4 and podocin genes of patients with chronic renal failure due to sporadic focal segmental glomerulosclerosis." Renal failure **25**(1): 87-93.

Korbet, S. M. (1998). "Primary focal segmental glomerulosclerosis." Journal of the American Society of Nephrology : JASN **9**(7): 1333-1340.

Korbet, S. M. (2002). "Treatment of primary focal segmental glomerulosclerosis." Kidney Int **62**(6): 2301-2310.

Korbet, S. M. (2003). "Angiotensin antagonists and steroids in the treatment of focal segmental glomerulosclerosis." Seminars in nephrology **23**(2): 219-228.

Korbet, S. M., R. M. Genchi, et al. (1996). "The racial prevalence of glomerular lesions in nephrotic adults." American journal of kidney diseases : the official journal of the National Kidney Foundation **27**(5): 647-651.

Korbet, S. M., M. M. Schwartz, et al. (1988). "Recurrent nephrotic syndrome in renal allografts." American journal of kidney diseases : the official journal of the National Kidney Foundation **11**(3): 270-276.

Korbet, S. M., M. M. Schwartz, et al. (1994). "Primary focal segmental glomerulosclerosis: clinical course and response to therapy." American journal of kidney diseases : the official journal of the National Kidney Foundation **23**(6): 773-783.

Kos, C. H., T. C. Le, et al. (2003). "Mice deficient in alpha-actinin-4 have severe glomerular disease." The Journal of clinical investigation **111**(11): 1683-1690.

Koziell, A., V. Grech, et al. (2002). "Genotype/phenotype correlations of NPHS1 and NPHS2 mutations in nephrotic syndrome advocate a functional inter-relationship in glomerular filtration." Human molecular genetics **11**(4): 379-388.

Kriz, W. (2005). "*TRPC6* - a new podocyte gene involved in focal segmental glomerulosclerosis." Trends Mol Med **11**(12): 527-530.

Kriz, W., M. Elger, et al. (1995). "Structure-stabilizing forces in the glomerular tuft." Journal of the American Society of Nephrology : JASN **5**(10): 1731-1739.

Kriz, W., E. Hackenthal, et al. (1994). "A role for podocytes to counteract capillary wall distension." Kidney international **45**(2): 369-376.

Kriz, W., M. Kretzler, et al. (1996). "Stability and leakiness: opposing challenges to the glomerulus." Kidney international **49**(6): 1570-1574.

Kwan, H. Y., Y. Huang, et al. (2004). "Regulation of canonical transient receptor potential isoform 3 (TRPC3) channel by protein kinase G." Proceedings of the National Academy of Sciences of the United States of America **101**(8): 2625-2630.

Kwon, Y., T. Hofmann, et al. (2007). "Integration of phosphoinositide- and calmodulin-mediated regulation of *TRPC6*." Molecular cell **25**(4): 491-503.

Lehtonen, S., A. Ora, et al. (2000). "In vivo interaction of the adapter protein CD2-associated protein with the type 2 polycystic kidney disease protein, polycystin-2." The Journal of biological chemistry **275**(42): 32888-32893.

Lenkkeri, U., M. Mannikko, et al. (1999). "Structure of the gene for congenital nephrotic syndrome of the finnish type (NPHS1) and characterization of mutations." American journal of human genetics **64**(1): 51-61.

Lenkkeri, U., M. Mannikko, et al. (1999). "Structure of the gene for congenital nephrotic syndrome of the finnish type (NPHS1) and characterization of mutations." Am J Hum Genet **64**(1): 51-61.

Lepage, P. K., M. P. Lussier, et al. (2006). "Identification of two domains involved in the assembly of transient receptor potential canonical channels." The Journal of biological chemistry **281**(41): 30356-30364.

Li, H., S. Lemay, et al. (2004). "SRC-family kinase Fyn phosphorylates the cytoplasmic domain of nephrin and modulates its interaction with podocin." J Am Soc Nephrol **15**(12): 3006-3015.

Li, J., A. Mahajan, et al. (2006). "Ankyrin repeat: a unique motif mediating protein-protein interactions." Biochemistry **45**(51): 15168-15178.

Liakopoulos, V., A. Huerta, et al. (2011). "Familial collapsing focal segmental glomerulosclerosis." Clin Nephrol **75**(4): 362-368.

Liao, P., D. Yu, et al. (2007). "A smooth muscle Cav1.2 calcium channel splice variant underlies hyperpolarized window current and enhanced state-dependent inhibition by nifedipine." The Journal of biological chemistry **282**(48): 35133-35142.

Liao, Y., C. Erxleben, et al. (2008). "Functional interactions among Orai1, TRPCs, and STIM1 suggest a STIM-regulated heteromeric Orai/TRPC model for SOCE/Icrac channels." Proceedings of the National Academy of Sciences of the United States of America **105**(8): 2895-2900.

Liman, E. R., D. P. Corey, et al. (1999). "TRP2: a candidate transduction channel for mammalian pheromone sensory signaling." Proceedings of the National Academy of Sciences of the United States of America **96**(10): 5791-5796.

Liu, G., B. Kaw, et al. (2003). "Neph1 and nephrin interaction in the slit diaphragm is an important determinant of glomerular permeability." The Journal of clinical investigation **112**(2): 209-221.

Liu, X. L., S. C. Done, et al. (2004). "Defective trafficking of nephrin missense mutants rescued by a chemical chaperone." Journal of the American Society of Nephrology : JASN **15**(7): 1731-1738.

Livak, K. J. and T. D. Schmittgen (2001). "Analysis of relative gene expression data using real-time quantitative PCR and the 2(-Delta Delta C(T)) Method." Methods **25**(4): 402-408.

Lowik, M., E. Levtchenko, et al. (2008). "Bigenic heterozygosity and the development of steroid-resistant focal segmental glomerulosclerosis." Nephrology, dialysis, transplantation : official publication of the European Dialysis and Transplant Association - European Renal Association **23**(10): 3146-3151.

Luimula, P., H. Ahola, et al. (2000). "Nephrin in experimental glomerular disease." Kidney international **58**(4): 1461-1468.

Maas, R. J., J. F. Wetzels, et al. (2012). "Serum-soluble urokinase receptor concentration in primary FSGS." Kidney international **81**(10): 1043-1044.

Machuca, E., G. Benoit, et al. (2009). "Genetics of nephrotic syndrome: connecting molecular genetics to podocyte physiology." Human molecular genetics **18**(R2): R185-194.

Machuca, E., A. Hummel, et al. (2009). "Clinical and epidemiological assessment of steroid-resistant nephrotic syndrome associated with the NPHS2 R229Q variant." Kidney international **75**(7): 727-735.

Malina, M., O. Cinek, et al. (2009). "Partial remission with cyclosporine A in a patient with nephrotic syndrome due to NPHS2 mutation." Pediatr Nephrol **24**(10): 2051-2053.

Mao, J., Y. Zhang, et al. (2006). "Expression profile of nephrin, podocin, and CD2AP in Chinese children with MCNS and IgA nephropathy." Pediatric nephrology **21**(11): 1666-1675.

Maroto, R., A. Raso, et al. (2005). "TRPC1 forms the stretch-activated cation channel in vertebrate cells." Nature cell biology **7**(2): 179-185.
Matsumoto, K., K. Okano, et al. (1988). "Decreased T-colony formation by lymphocytes from patients with focal glomerular sclerosis." International archives of allergy and applied immunology **85**(1): 94-98.
Matsumoto, K., K. Osakabe, et al. (1983). "Impaired cell-mediated immunity in focal glomerular sclerosis." Nephron **34**(4): 220-223.
McCarthy, H. J., A. Bierzynska, et al. (2013). "Simultaneous Sequencing of 24 Genes Associated with Steroid-Resistant Nephrotic Syndrome." Clin J Am Soc Nephrol.
McCarthy, H. J., A. Bierzynska, et al. (2013). "Simultaneous sequencing of 24 genes associated with steroid-resistant nephrotic syndrome." Clin J Am Soc Nephrol **8**(4): 637-648.
McCarthy, H. J. and M. A. Saleem (2011). "Genetics in clinical practice: nephrotic and proteinuric syndromes." Nephron Exp Nephrol **118**(1): e1-8.
McGrogan, A., C. F. Franssen, et al. (2011). "The incidence of primary glomerulonephritis worldwide: a systematic review of the literature." Nephrol Dial Transplant **26**(2): 414-430.
McKenzie, L. M., S. L. Hendrickson, et al. (2007). "NPHS2 variation in sporadic focal segmental glomerulosclerosis." Journal of the American Society of Nephrology : JASN **18**(11): 2987-2995.
Megremis, S., A. Mitsioni, et al. (2009). "Nucleotide variations in the NPHS2 gene in Greek children with steroid-resistant nephrotic syndrome." Genet Test Mol Biomarkers **13**(2): 249-256.
Mekahli, D., A. Liutkus, et al. (2009). "Long-term outcome of idiopathic steroid-resistant nephrotic syndrome: a multicenter study." Pediatr Nephrol **24**(8): 1525-1532.
Mele, C., P. Iatropoulos, et al. (2011). "MYO1E mutations and childhood familial focal segmental glomerulosclerosis." The New England journal of medicine **365**(4): 295-306.
Meyrier, A. (2005). "Mechanisms of disease: focal segmental glomerulosclerosis." Nature clinical practice. Nephrology **1**(1): 44-54.
Meyrier, A. (2011). "Focal and segmental glomerulosclerosis: multiple pathways are involved." Seminars in nephrology **31**(4): 326-332.
Michaud, J. L., K. M. Chaisson, et al. (2006). "FSGS-associated alpha-actinin-4 (K256E) impairs cytoskeletal dynamics in podocytes." Kidney international **70**(6): 1054-1061.
Minke, B. (2010). "The history of the Drosophila TRP channel: the birth of a new channel superfamily." Journal of neurogenetics **24**(4): 216-233.
Minke, B. and B. Cook (2002). "TRP channel proteins and signal transduction." Physiological reviews **82**(2): 429-472.
Mir, S., O. Yavascan, et al. (2012). "*TRPC6* gene variants in Turkish children with steroid-resistant nephrotic syndrome." Nephrol Dial Transplant **27**(1): 205-209.
Mir, S., O. Yavascan, et al. (2012). "*TRPC6* gene variants in Turkish children with steroid-resistant nephrotic syndrome." Nephrology, dialysis, transplantation : official publication of the European Dialysis and Transplant Association - European Renal Association **27**(1): 205-209.
Moller, C. C., C. Wei, et al. (2007). "Induction of *TRPC6* channel in acquired forms of proteinuric kidney disease." J Am Soc Nephrol **18**(1): 29-36.
Mollet, G., J. Ratelade, et al. (2009). "Podocin inactivation in mature kidneys causes focal segmental glomerulosclerosis and nephrotic syndrome." J Am Soc Nephrol **20**(10): 2181-2189.
Montell, C. (2001). "Physiology, phylogeny, and functions of the TRP superfamily of cation channels." Science's STKE : signal transduction knowledge environment **2001**(90): re1.
Montell, C. (2005). "The TRP superfamily of cation channels." Science's STKE : signal transduction knowledge environment **2005**(272): re3.
Montell, C. (2005). "The TRP superfamily of cation channels." Sci STKE **2005**(272): re3.
Montell, C. and G. M. Rubin (1989). "Molecular characterization of the Drosophila trp locus: a putative integral membrane protein required for phototransduction." Neuron **2**(4): 1313-1323.

Mucha, B., F. Ozaltin, et al. (2006). "Mutations in the Wilms' tumor 1 gene cause isolated steroid resistant nephrotic syndrome and occur in exons 8 and 9." Pediatric research **59**(2): 31.

Mukerji, N., T. V. Damodaran, et al. (2007). "*TRPC6* and FSGS: the latest TRP channelopathy." Biochimica et biophysica acta **1772**(8): 68.

Mundel, P. and W. Kriz (1995). "Structure and function of podocytes: an update." Anat Embryol (Berl) **192**(5): 385-397.

Nair, R., J. M. Bell, et al. (2004). "Renal biopsy in patients aged 80 years and older." American journal of kidney diseases : the official journal of the National Kidney Foundation **44**(4): 618-626.

Narita, I., S. Goto, et al. (2003). "Genetic polymorphism of NPHS1 modifies the clinical manifestations of Ig A nephropathy." Laboratory investigation; a journal of technical methods and pathology **83**(8): 1193-1200.

Nasir., H., S. Chaudhry., et al. (2012). "Role of immunoflourescence in the diagnosis of glomerulonephritis." Journal Of Pakistan Medical Association **62**(3): 240-243.

Nijenhuis, T., A. J. Sloan, et al. (2011). "Angiotensin II contributes to podocyte injury by increasing *TRPC6* expression via an NFAT-mediated positive feedback signaling pathway." Am J Pathol **179**(4): 1719-1732.

Nilius, B. and F. Mahieu (2006). "A road map for TR(I)Ps." Molecular cell **22**(3): 297-307.

Nilius, B., G. Owsianik, et al. (2007). "Transient receptor potential cation channels in disease." Physiological reviews **87**(1): 165-217.

Nishida, M., Y. Hara, et al. (2006). "TRP channels: molecular diversity and physiological function." Microcirculation **13**(7): 535-550.

Nyberg, E., S. O. Bohman, et al. (1994). "Glomerular volume and renal function in children with different types of the nephrotic syndrome." Pediatric nephrology **8**(3): 285-289.

Oike, H., M. Wakamori, et al. (2006). "Arachidonic acid can function as a signaling modulator by activating the TRPM5 cation channel in taste receptor cells." Biochimica et biophysica acta **1761**(9): 1078-1084.

Okada, T., R. Inoue, et al. (1999). "Molecular and functional characterization of a novel mouse transient receptor potential protein homologue TRP7. Ca(2+)-permeable cation channel that is constitutively activated and enhanced by stimulation of G protein-coupled receptor." The Journal of biological chemistry **274**(39): 27359-27370.

Orsini, M. and B. Boscherini (1961). "[Corticosteroid therapy of the nephrotic syndrome in children]." Arch Ital Pediatr Pueric **21**: 251-254.

Papeta, N., K. Kiryluk, et al. (2011). "APOL1 variants increase risk for FSGS and HIVAN but not IgA nephropathy." Journal of the American Society of Nephrology : JASN **22**(11): 1991-1996.

Patrakka, J., M. Kestila, et al. (2000). "Congenital nephrotic syndrome (NPHS1): features resulting from different mutations in Finnish patients." Kidney international **58**(3): 972-980.

Patrakka, J., M. Kestila, et al. (2000). "Congenital nephrotic syndrome (NPHS1): features resulting from different mutations in Finnish patients." Kidney Int **58**(3): 972-980.

Pereira, A. C., A. B. Pereira, et al. (2004). "NPHS2 R229Q functional variant is associated with microalbuminuria in the general population." Kidney international **65**(3): 1026-1030.

Petersen, C. C., M. J. Berridge, et al. (1995). "Putative capacitative calcium entry channels: expression of Drosophila trp and evidence for the existence of vertebrate homologues." The Biochemical journal **311 (Pt 1)**: 41-44.

Philippe, A., F. Nevo, et al. (2008). "Nephrin mutations can cause childhood-onset steroid-resistant nephrotic syndrome." Journal of the American Society of Nephrology : JASN **19**(10): 1871-1878.

Phillips, A. M., A. Bull, et al. (1992). "Identification of a Drosophila gene encoding a calmodulin-binding protein with homology to the trp phototransduction gene." Neuron **8**(4): 631-642.

Plant, T. D. and M. Schaefer (2005). "Receptor-operated cation channels formed by TRPC4 and TRPC5." Naunyn-Schmiedeberg's archives of pharmacology **371**(4): 266-276.

Pollak, M. R. (2003). "The genetic basis of FSGS and steroid-resistant nephrosis." Seminars in nephrology **23**(2): 141-146.

Ponticelli, C. and R. J. Glassock (2010). "Posttransplant recurrence of primary glomerulonephritis." Clinical journal of the American Society of Nephrology : CJASN **5**(12): 2363-2372.

Putaala, H., R. Soininen, et al. (2001). "The murine nephrin gene is specifically expressed in kidney, brain and pancreas: inactivation of the gene leads to massive proteinuria and neonatal death." Hum Mol Genet **10**(1): 1-8.

Putaala, H., R. Soininen, et al. (2001). "The murine nephrin gene is specifically expressed in kidney, brain and pancreas: inactivation of the gene leads to massive proteinuria and neonatal death." Human molecular genetics **10**(1): 1-8.

Putney, J. W., Jr. (1977). "Muscarinic, alpha-adrenergic and peptide receptors regulate the same calcium influx sites in the parotid gland." The Journal of physiology **268**(1): 139-149.

Quick, K., J. Zhao, et al. (2012). "TRPC3 and *TRPC6* are essential for normal mechanotransduction in subsets of sensory neurons and cochlear hair cells." Open biology **2**(5): 120068.

Ramsey, I. S., M. Delling, et al. (2006). "An introduction to TRP channels." Annual review of physiology **68**: 619-647.

Reiser, J., W. Kriz, et al. (2000). "The glomerular slit diaphragm is a modified adherens junction." J Am Soc Nephrol **11**(1): 1-8.

Reiser, J., K. R. Polu, et al. (2005). "*TRPC6* is a glomerular slit diaphragm-associated channel required for normal renal function." Nat Genet **37**(7): 44.

Reiser, J., K. R. Polu, et al. (2005). "*TRPC6* is a glomerular slit diaphragm-associated channel required for normal renal function." Nat Genet **37**(7): 739-744.

Rennke, H. G. and P. S. Klein (1989). "Pathogenesis and significance of nonprimary focal and segmental glomerulosclerosis." American journal of kidney diseases : the official journal of the National Kidney Foundation **13**(6): 443-456.

Rood, I. M., J. K. Deegens, et al. (2012). "Genetic causes of focal segmental glomerulosclerosis: implications for clinical practice." Nephrology, dialysis, transplantation : official publication of the European Dialysis and Transplant Association - European Renal Association **27**(3): 882-890.

Roselli, S., O. Gribouval, et al. (2002). "Podocin localizes in the kidney to the slit diaphragm area." The American journal of pathology **160**(1): 131-139.

Ruf, R. G., A. Lichtenberger, et al. (2004). "Patients with mutations in NPHS2 (podocin) do not respond to standard steroid treatment of nephrotic syndrome." J Am Soc Nephrol **15**(3): 722-732.

Ruf, R. G., M. Schultheiss, et al. (2004). "Prevalence of WT1 mutations in a large cohort of patients with steroid-resistant and steroid-sensitive nephrotic syndrome." Kidney international **66**(2): 564-570.

Rydel, J. J., S. M. Korbet, et al. (1995). "Focal segmental glomerular sclerosis in adults: presentation, course, and response to treatment." American journal of kidney diseases : the official journal of the National Kidney Foundation **25**(4): 534-542.

Saimi, Y. and C. Kung (2002). "Calmodulin as an ion channel subunit." Annual review of physiology **64**: 289-311.

Santin, S., E. Ars, et al. (2009). "*TRPC6* mutational analysis in a large cohort of patients with focal segmental glomerulosclerosis." Nephrol Dial Transplant **24**(10): 3089-3096.

Santin, S., E. Ars, et al. (2009). "*TRPC6* mutational analysis in a large cohort of patients with focal segmental glomerulosclerosis." Nephrology, dialysis, transplantation : official publication of the European Dialysis and Transplant Association - European Renal Association **24**(10): 3089-3096.

Santin, S., E. Ars, et al. (2009). "*TRPC6* mutational analysis in a large cohort of patients with focal segmental glomerulosclerosis." Nephrol Dial Transplant.

Santin, S., G. Bullich, et al. (2011). "Clinical utility of genetic testing in children and adults with steroid-resistant nephrotic syndrome." Clin J Am Soc Nephrol **6**(5): 1139-1148.
Santin, S., R. Garcia-Maset, et al. (2009). "Nephrin mutations cause childhood- and adult-onset focal segmental glomerulosclerosis." Kidney international **76**(12): 1268-1276.
Santin, S., B. Tazon-Vega, et al. (2011). "Clinical value of NPHS2 analysis in early- and adult-onset steroid-resistant nephrotic syndrome." Clin J Am Soc Nephrol **6**(2): 344-354.
Savin, V. J., R. Sharma, et al. (1996). "Circulating factor associated with increased glomerular permeability to albumin in recurrent focal segmental glomerulosclerosis." N Engl J Med **334**(14): 878-883.
Schachter, A. D., J. Strehlau, et al. (2000). "Increased nuclear factor-kappaB and angiotensinogen gene expression in posttransplant recurrent focal segmental glomerulosclerosis." Transplantation **70**(7): 1107-1110.
Schell, C. and T. B. Huber (2012). "New players in the pathogenesis of focal segmental glomerulosclerosis." Nephrology, dialysis, transplantation : official publication of the European Dialysis and Transplant Association - European Renal Association **27**(9): 3406-3412.
Schermer, B. and T. Benzing (2009). "Lipid-protein interactions along the slit diaphragm of podocytes." Journal of the American Society of Nephrology : JASN **20**(3): 473-478.
Schiffer, M., M. Bitzer, et al. (2001). "Apoptosis in podocytes induced by TGF-beta and Smad7." The Journal of clinical investigation **108**(6): 807-816.
Schiffer, M., L. E. Schiffer, et al. (2002). "Inhibitory smads and tgf-Beta signaling in glomerular cells." Journal of the American Society of Nephrology : JASN **13**(11): 2657-2666.
Schindl, R., I. Frischauf, et al. (2008). "The first ankyrin-like repeat is the minimum indispensable key structure for functional assembly of homo- and heteromeric TRPC4/TRPC5 channels." Cell Calcium **43**(3): 260-269.
Schlondorff, J. S. and M. R. Pollak (2006). "*TRPC6* in glomerular health and disease: what we know and what we believe." Semin Cell Dev Biol **17**(6): 667-674.
Schnabel, E., J. M. Anderson, et al. (1990). "The tight junction protein ZO-1 is concentrated along slit diaphragms of the glomerular epithelium." J Cell Biol **111**(3): 1255-1263.
Schoeb, D. S., G. Chernin, et al. (2010). "Nineteen novel NPHS1 mutations in a worldwide cohort of patients with congenital nephrotic syndrome (CNS)." Nephrology, dialysis, transplantation : official publication of the European Dialysis and Transplant Association - European Renal Association **25**(9): 2970-2976.
Schonenberger, E., J. H. Ehrich, et al. (2011). "The podocyte as a direct target of immunosuppressive agents." Nephrol Dial Transplant **26**(1): 18-24.
Schwartz, M. M. and A. K. Bidani (1993). "Comparison of glomerular injury in juvenile versus mature rats in a remnant kidney model." The Journal of laboratory and clinical medicine **121**(2): 348-355.
Schwartz, M. M. and S. M. Korbet (1993). "Primary focal segmental glomerulosclerosis: pathology, histological variants, and pathogenesis." American journal of kidney diseases : the official journal of the National Kidney Foundation **22**(6): 874-883.
Schwarz, K., M. Simons, et al. (2001). "Podocin, a raft-associated component of the glomerular slit diaphragm, interacts with CD2AP and nephrin." J Clin Invest **108**(11): 1621-1629.
Schwarz, K., M. Simons, et al. (2001). "Podocin, a raft-associated component of the glomerular slit diaphragm, interacts with CD2AP and nephrin." The Journal of clinical investigation **108**(11): 1621-1629.
Sellin, L., T. B. Huber, et al. (2003). "NEPH1 defines a novel family of podocin interacting proteins." FASEB journal : official publication of the Federation of American Societies for Experimental Biology **17**(1): 115-117.
Shankland, S. J. and M. R. Pollak (2011). "A suPAR circulating factor causes kidney disease." Nature medicine **17**(8): 926-927.

Shao, H., J. H. Wang, et al. (2010). "alpha-actinin-4 is essential for maintaining the spreading, motility and contractility of fibroblasts." PloS one **5**(11): e13921.

Shea, S. M., J. Raskova, et al. (1978). "A stereologic study of glomerular hypertrophy in the subtotally nephrectomized rat." The American journal of pathology **90**(1): 201-210.

Shi, J., E. Mori, et al. (2004). "Multiple regulation by calcium of murine homologues of transient receptor potential proteins *TRPC6* and TRPC7 expressed in HEK293 cells." J Physiol **561**(Pt 2): 415-432.

Shih, N. Y., J. Li, et al. (2001). "CD2AP localizes to the slit diaphragm and binds to nephrin via a novel C-terminal domain." The American journal of pathology **159**(6): 2303-2308.

Shih, N. Y., J. Li, et al. (1999). "Congenital nephrotic syndrome in mice lacking CD2-associated protein." Science **286**(5438): 312-315.

Sinha, A., S. Sharma, et al. (2010). "Frasier syndrome: early gonadoblastoma and cyclosporine responsiveness." Pediatr Nephrol **25**(10): 2171-2174.

Soboloff, J., M. Spassova, et al. (2005). "Role of endogenous *TRPC6* channels in Ca2+ signal generation in A7r5 smooth muscle cells." The Journal of biological chemistry **280**(48): 39786-39794.

Sole, X., E. Guino, et al. (2006). "SNPStats: a web tool for the analysis of association studies." Bioinformatics **22**(15): 1928-1929.

Spassova, M. A., T. Hewavitharana, et al. (2006). "A common mechanism underlies stretch activation and receptor activation of *TRPC6* channels." Proceedings of the National Academy of Sciences of the United States of America **103**(44): 16586-16591.

Srivastava, T., S. D. Simon, et al. (1999). "High incidence of focal segmental glomerulosclerosis in nephrotic syndrome of childhood." Pediatric nephrology **13**(1): 13-18.

Stein-Oakley, A. N., J. A. Maguire, et al. (1997). "Altered expression of fibrogenic growth factors in IgA nephropathy and focal and segmental glomerulosclerosis." Kidney international **51**(1): 195-204.

Stowers, L., T. E. Holy, et al. (2002). "Loss of sex discrimination and male-male aggression in mice deficient for TRP2." Science **295**(5559): 1493-1500.

Strubing, C., G. Krapivinsky, et al. (2003). "Formation of novel TRPC channels by complex subunit interactions in embryonic brain." J Biol Chem **278**(40): 39014-39019.

Suzuki, J., N. Yoshikawa, et al. (1994). "A quantitative analysis of the glomeruli in focal segmental glomerulosclerosis." Pediatric nephrology **8**(4): 416-419.

Tai, Y., S. Feng, et al. (2009). "Functional roles of TRPC channels in the developing brain." Pflugers Archiv : European journal of physiology **458**(2): 283-289.

Tang, J., Y. Lin, et al. (2001). "Identification of common binding sites for calmodulin and inositol 1,4,5-trisphosphate receptors on the carboxyl termini of trp channels." J Biol Chem **276**(24): 21303-21310.

Tejani, A., A. Nicastri, et al. (1983). "Familial focal segmental glomerulosclerosis." Int J Pediatr Nephrol **4**(4): 231-234.

Teo, Y. Y., X. Sim, et al. (2009). "Singapore Genome Variation Project: a haplotype map of three Southeast Asian populations." Genome Res **19**(11): 2154-2162.

Thomas, D. B., N. Franceschini, et al. (2006). "Clinical and pathologic characteristics of focal segmental glomerulosclerosis pathologic variants." Kidney international **69**(5): 920-926.

Tiruppathi, C., M. Freichel, et al. (2002). "Impairment of store-operated Ca2+ entry in TRPC4(-/-) mice interferes with increase in lung microvascular permeability." Circulation research **91**(1): 70-76.

Tonna, S. J., A. Needham, et al. (2008). "NPHS2 variation in focal and segmental glomerulosclerosis." BMC nephrology **9**: 13.

TU, P. (2009). Study of diacylglycerol-activated *TRPC6* channels in murine cortical neurons and their roles in the transport of transition metals PhD, Université Joseph Fourier (Grenoble I).

van den Berg, J. G., M. A. van den Bergh Weerman, et al. (2004). "Podocyte foot process effacement is not correlated with the level of proteinuria in human glomerulopathies." Kidney international **66**(5): 1901-1906.

Vazquez, G., B. J. Wedel, et al. (2004). "The mammalian TRPC cation channels." Biochimica et biophysica acta **1742**(1-3): 21-36.

Vazquez, G., B. J. Wedel, et al. (2004). "Obligatory role of Src kinase in the signaling mechanism for TRPC3 cation channels." The Journal of biological chemistry **279**(39): 40521-40528.

Venkatachalam, K. and C. Montell (2007). "TRP channels." Annual review of biochemistry **76**: 387-417.

Venkatachalam, K., F. Zheng, et al. (2003). "Regulation of canonical transient receptor potential (TRPC) channel function by diacylglycerol and protein kinase C." The Journal of biological chemistry **278**(31): 29031-29040.

Verani, R. R. and E. P. Hawkins (1986). "Recurrent focal segmental glomerulosclerosis. A pathological study of the early lesion." American journal of nephrology **6**(4): 263-270.

Verma, R., I. Kovari, et al. (2006). "Nephrin ectodomain engagement results in Src kinase activation, nephrin phosphorylation, Nck recruitment, and actin polymerization." The Journal of clinical investigation **116**(5): 1346-1359.

Verma, R., B. Wharram, et al. (2003). "Fyn binds to and phosphorylates the kidney slit diaphragm component Nephrin." The Journal of biological chemistry **278**(23): 20716-20723.

Voets, T., A. Janssens, et al. (2004). "Outer pore architecture of a Ca2+-selective TRP channel." The Journal of biological chemistry **279**(15): 15223-15230.

Voets, T., K. Talavera, et al. (2005). "Sensing with TRP channels." Nature chemical biology **1**(2): 85-92.

Walz, G. (2005). "Slit or pore? A mutation of the ion channel *TRPC6* causes FSGS." Nephrol Dial Transplant **20**(9): 9.

Wartiovaara, J., L. G. Ofverstedt, et al. (2004). "Nephrin strands contribute to a porous slit diaphragm scaffold as revealed by electron tomography." The Journal of clinical investigation **114**(10): 1475-1483.

Wartiovaara, J., L. G. Ofverstedt, et al. (2004). "Nephrin strands contribute to a porous slit diaphragm scaffold as revealed by electron tomography." J Clin Invest **114**(10): 1475-1483.

Wasilewska, A. M., E. Kuroczycka-Saniutycz, et al. (2011). "Effect of cyclosporin A on proteinuria in the course of glomerulopathy associated with WT1 mutations." Eur J Pediatr **170**(3): 389-391.

Watanabe, H., M. Murakami, et al. (2009). "The pathological role of transient receptor potential channels in heart disease." Circulation journal : official journal of the Japanese Circulation Society **73**(3): 419-427.

Watanabe, H., J. Vriens, et al. (2003). "Anandamide and arachidonic acid use epoxyeicosatrienoic acids to activate TRPV4 channels." Nature **424**(6947): 434-438.

Wedel, B. J., G. Vazquez, et al. (2003). "A calmodulin/inositol 1,4,5-trisphosphate (IP3) receptor-binding region targets TRPC3 to the plasma membrane in a calmodulin/IP3 receptor-independent process." The Journal of biological chemistry **278**(28): 25758-25765.

Wei, C., S. El Hindi, et al. (2011). "Circulating urokinase receptor as a cause of focal segmental glomerulosclerosis." Nature medicine **17**(8): 952-960.

Wei, C., C. C. Moller, et al. (2008). "Modification of kidney barrier function by the urokinase receptor." Nature medicine **14**(1): 55-63.

Weins, A., P. Kenlan, et al. (2005). "Mutational and Biological Analysis of alpha-actinin-4 in focal segmental glomerulosclerosis." Journal of the American Society of Nephrology : JASN **16**(12): 3694-3701.

Welsh, G. I. and M. A. Saleem (2010). "Nephrin-signature molecule of the glomerular podocyte?" The Journal of pathology **220**(3): 328-337.

Welsh, G. I. and M. A. Saleem (2010). "Nephrin-signature molecule of the glomerular podocyte?" J Pathol **220**(3): 328-337.

Wes, P. D., J. Chevesich, et al. (1995). "TRPC1, a human homolog of a Drosophila store-operated channel." Proceedings of the National Academy of Sciences of the United States of America **92**(21): 9652-9656.

Wing, M. R., D. M. Bourdon, et al. (2003). "PLC-epsilon: a shared effector protein in Ras-, Rho-, and G alpha beta gamma-mediated signaling." Molecular interventions **3**(5): 273-280.

Winn, M. P., P. J. Conlon, et al. (2005). "A mutation in the *TRPC6* cation channel causes familial focal segmental glomerulosclerosis." Science **308**(5729): 4.

Winn, M. P., P. J. Conlon, et al. (2005). "A mutation in the *TRPC6* cation channel causes familial focal segmental glomerulosclerosis." Science **308**(5729): 1801-1804.

Woo, K. T., C. M. Chan, et al. (2010). "Global evolutionary trend of the prevalence of primary glomerulonephritis over the past three decades." Nephron Clin Pract **116**(4): c337-346.

Yanagida-Asanuma, E., K. Asanuma, et al. (2007). "Synaptopodin protects against proteinuria by disrupting Cdc42:IRSp53:Mena signaling complexes in kidney podocytes." The American journal of pathology **171**(2): 415-427.

Yao, J., T. C. Le, et al. (2004). "Alpha-actinin-4-mediated FSGS: an inherited kidney disease caused by an aggregated and rapidly degraded cytoskeletal protein." PLoS Biol **2**(6): e167.

Yap, H.-K. and P. Y.-W. Lau (2008). Hematuria and Proteinuria. Comprehensive Pediatric Nephrology. D. F. Geary and F. Schaefer, Mosby Elsevier**:** 179-193.

Yoshida, Y., A. Fogo, et al. (1989). "Glomerular hemodynamic changes vs. hypertrophy in experimental glomerular sclerosis." Kidney international **35**(2): 654-660.

Yu, L., G. S. Li, et al. (2009). "[Association of NPHS1 gene polymorphism with IgA nephropathy]." Zhonghua yi xue za zhi **89**(13): 881-885.

Yu, Y., S. H. Keller, et al. (2009). "A functional single-nucleotide polymorphism in the *TRPC6* gene promoter associated with idiopathic pulmonary arterial hypertension." Circulation **119**(17): 2313-2322.

Zhang, J., S. L. Xia, et al. (2002). "NO upregulation of a cyclic nucleotide-gated channel contributes to calcium elevation in endothelial cells." American journal of physiology. Cell physiology **283**(4): C1080-1089.

Zhang, L. and D. Saffen (2001). "Muscarinic acetylcholine receptor regulation of TRP6 Ca2+ channel isoforms. Molecular structures and functional characterization." J Biol Chem **276**(16): 13331-13339.

Zhou, W. and F. Hildebrandt (2009). "Molecular cloning and expression of phospholipase C epsilon 1 in zebrafish." Gene Expr Patterns **9**(5): 282-288.

Zhu, B., N. Chen, et al. (2009). "Identification and functional analysis of a novel *TRPC6* mutation associated with late onset familial focal segmental glomerulosclerosis in Chinese patients." Mutat Res **664**(1-2): 84-90.

Zhu, L., R. Jiang, et al. (2011). "Activation of RhoA in podocytes induces focal segmental glomerulosclerosis." Journal of the American Society of Nephrology : JASN **22**(9): 1621-1630.

Zhu, L., L. Yu, et al. (2009). "Genetic effect of the NPHS2 gene variants on proteinuria in minimal change disease and immunoglobulin A nephropathy." Nephrology **14**(8): 728-734.

Zhu, M. X. (2005). "Multiple roles of calmodulin and other Ca(2+)-binding proteins in the functional regulation of TRP channels." Pflugers Archiv : European journal of physiology **451**(1): 105-115.

Zhu, M. X. (2011). TRP Channels

Methods in Signal Transduction. TRP Channels. M. X. Zhu. Boca Raton (FL).

APPENDICES

Appendix I-1 Clinical characteristics and genotypes of selected SNPs of the recruited Chinese patients

Patient no.	Age At Diagnosis	Gender	Renal Biopsy Finding	Poor Prognosis	Steroid Resistant	*TRPC6*	*NPHS1*		*NPHS2*
						c.-254C>G	c.294C>T (I98I)	c.2289C>T (T763T)	c.954T>C (A318A)
10	9.24	M	MCNS	No	No	G/G	C/C	C/T	T/C
11	5.74	M	MCNS	No	Yes	G/G	C/C	C/C	T/C
13	4.58	F	FSGS	Yes	Yes	C/G	C/C	C/C	T/T
14	3.91	F	Not performed	No	No	G/G	C/C	C/C	T/C
16	2.18	F	FGS	Yes	No	G/G	C/C	C/C	T/C
18	5.44	M	MCNS	No	No	G/G	C/T	C/T	T/C
19	2.7	F	MCNS; IgM nephropathy	No	No	C/C	C/T	C/T	T/C
20	16	F	Not performed	No	No	C/G	C/T	C/T	T/C
21	1.67	M	FMPGN	No	No	G/G	C/C	C/T	T/T
22	6.35	M	Minor abnormalities	No	No	C/G	C/T	C/T	T/C
24	1.7	M	Not performed	No	No	G/G	C/C	C/C	T/T
25	2	F	Not performed	No	No	C/G	C/T	C/T	T/C
26	2	M	Not performed	No	No	G/G	C/T	C/T	C/C
27	14.19	F	FMPGN	No	Yes	G/G	C/C	C/T	T/C
28	4	F	Not performed	No	No	G/G	C/C	C/T	T/C
32	1.83	F	FMPGN	No	No	C/C	C/T	C/T	T/C

Patient no.	Age At Diagnosis	Gender	Renal Biopsy Finding	Poor Prognosis	Steroid Resistant	*TRPC6*	*NPHS1*		*NPHS2*
						c.-254C>G	c.294C>T (I98I)	c.2289C>T (T763T)	c.954T>C (A318A)
33	2	F	Minor glomerular abnormalities	No	No	C/G	T/T	T/T	T/C
34	4.78	M	MCNS	No	No	C/C	C/C	C/C	C/C
35	16	F	Minor abnormalities	No	No	C/G	C/C	C/C	C/C
36	6.5	M	Not performed	No	No	C/G	C/C	C/C	C/C
37	6	M	Not performed	No	No	G/G	C/C	C/C	T/C
38	4.41	M	Not performed	No	No	C/G	C/C	C/C	T/T
41	1.11	M	Minor abnormalities	No	Yes	C/G	C/C	C/C	T/T
43	1.88	M	Not performed	No	No	G/G	C/C	C/C	T/C
45	3	M	Not performed	No	No	C/C	C/C	C/C	T/C
46	1.41	F	Minor abnormalities, IgM nephropathy	Yes	No	C/G	C/T	C/T	T/C
50	4	M	Not performed	No	No	C/G	C/C	C/C	T/C
51	3	M	Not performed	No	No	C/C	C/C	C/C	C/C
53	2	F	Not performed	No	No	G/G	C/C	C/C	C/C
54	3	M	Not performed	No	No	C/G	C/T	C/T	T/C
58	11	F	Diffuse mesangial proliferative glomerulonephritis with global and segmental sclerosis	Yes*	Yes	G/G	C/T	C/T	T/C
60	3.5	M	Not performed	No	No	C/C	C/T	C/T	C/C
62	0.9	F	FMPGN	No	Yes	C/C	C/C	C/C	T/T
63	3.53	F	Not performed	No	No	C/C	C/C	C/T	C/C

Patient no.	Age At Diagnosis	Gender	Renal Biopsy Finding	Poor Prognosis	Steroid Resistant	*TRPC6*	*NPHS1*		*NPHS2*
						c.-254C>G	c.294C>T (I98I)	c.2289C>T (T763T)	c.954T>C (A318A)
64	5.77	F	Not performed	No	No	C/G	C/C	C/C	T/C
65	8.99	M	Not performed	No	No	C/C	C/C	C/T	C/C
66	5.01	F	Not performed	No	No	G/G	C/C	C/C	C/C
67	1.9	M	FSGS	Yes*	Yes	C/C	C/C	C/C	C/C
68	1.76	M	FGS	Yes	No	C/C	C/C	C/C	T/C
74	1	F	Not performed	No	No	G/G	C/C	C/C	C/C
75	1.08	F	FSGS	No	Yes	G/G	C/T	C/T	T/T
77		F	Not performed	No	No	C/G	C/C	C/C	T/T
79	6	F	Not performed	No	No	G/G	C/T	C/T	T/C
80	3	F	Mesangial injury, GN w IgM deposits and global sclerosis	No	No	C/G	C/T	C/T	C/C
81	5	M	Not performed	No	No	C/G	C/C	C/C	T/C
82	9.53	M	FSGS	No	No	C/C	C/C	C/C	T/T
83	5.47	M	FGS	Yes	No	C/G	C/T	C/T	T/C
84	4	F	Glomerular minor abnormalities with mesangial IgM IF	No	No	C/G	C/C	C/C	C/C
89	10.85	F	FSGS	No	Yes	G/G	C/C	C/C	T/C
90	10.81	F	MCNS	No	No	C/G	C/C	C/C	T/T
91	7	F	FSGS	Yes	Yes	C/G	C/C	C/C	T/T
93	2.61	M	Not performed	No	No	G/G	C/C	C/C	T/C
94	11.01	M	FSGS	Yes*	Yes	G/G	C/C	C/T	T/C
105	4.79	M	Not performed	No	No	C/G	C/T	C/T	C/C

Patient no.	Age At Diagnosis	Gender	Renal Biopsy Finding	Poor Prognosis	Steroid Resistant	*TRPC6*	*NPHS1*		*NPHS2*
						c.-254C>G	c.294C>T (I98I)	c.2289C>T (T763T)	c.954T>C (A318A)
110	5	F	FSGS with a cellular crescent	Yes*	Yes	C/G	C/T	C/T	C/C
114	0	F	MCNS	No	No	G/G	C/T	C/T	T/C
115	2	M	FGS	No	No	C/C	C/T	T/T	T/C
118	12.33	F	FGS	No	No	G/G	C/T	C/T	T/C
119	4.01	M	Not performed	No	No	C/C	C/C	C/C	C/C
121	10.8	M	Glomerular minor abnormalities	No	No	C/C	C/C	C/T	T/C
127	2	M	MCNS	No	No	C/G	C/C	C/C	C/C
130	7	M	IgM nephropathy, MCNS	No	Yes	C/C	C/T	C/T	T/C
132	1.02	F	Minimal change. Findings compatible with IgM nephropathy	No	No	C/G	C/C	C/C	T/T
137	1.96	M	FSGS	Yes	Yes	C/G	C/T	C/T	T/C
139	19.01	M	FSGS	Yes*	Yes	C/G	C/C	C/C	C/C
140	7	M	FMPGN	No	No	G/G	C/T	C/T	T/T
141	2	F	FGS	No	No	C/C	C/C	C/C	C/C
143	4	M	Not performed	No	No	G/G	C/T	C/T	T/T
144	5	F	Not performed	No	No	C/G	C/T	C/T	T/C
148	3.27	M	FSGS	No	No	C/G	C/C	C/C	T/T
151	10	F	FSGS	Yes*	Yes	C/G	C/C	C/C	T/C
153	11.91	F	Minor abnormalities	No	Yes	G/G	T/T	T/T	C/C
156	2.66	M	FGS	No	No	G/G	C/T	C/T	T/T

Patient no.	Age At Diagnosis	Gender	Renal Biopsy Finding	Poor Prognosis	Steroid Resistant	*TRPC6*	*NPHS1*		*NPHS2*
						c.-254C>G	c.294C>T (I98I)	c.2289C>T (T763T)	c.954T>C (A318A)
159	2	M	Not performed	No	No	C/G	C/T	C/T	C/C
160	1.61	M	FMPGN	No	Yes	C/C	C/C	C/C	C/C
161	2.84	F	FSGS	No	No	C/C	C/C	C/T	T/C
162	5.58	M	Not performed	No	No	C/G	C/T	C/T	T/T
164	3.59	M	FSGS	No	Yes	C/G	C/T	C/T	T/C
169	1.58	M	Mesangial injury GN w IgM deposits and global sclerosis	No	Yes	C/C	C/C	C/C	C/C
170	12.19	M	FSGS	Yes	Yes	C/G	C/C	C/C	T/T
172	4	M	Not performed	No	No	C/G	C/C	C/T	T/T
173	15.25	M	MCNS	No	No	G/G	C/C	C/C	T/C
174	12	F	FSGS	Yes*	Yes	G/G	C/C	C/C	T/C
210	11	F	Diffuse Mesengial Hypercellularity	No	No	C/C	C/C	C/C	T/C
216	8	M	Not performed	No	No	C/G	C/T	C/T	T/T
220	4	M	Not performed	No	No	C/C	C/C	C/C	T/C
223	5	F	Not performed	No	No	C/G	C/T	C/T	C/C
231	9	M	Not performed	No	No	C/G	C/C	C/C	T/C
232	3	M	FSGS	Yes	Yes		C/T	C/T	T/C
235	9	M	FSGS	No	No		C/C	C/T	C/C
236	7	M	FSGS	Yes	No		C/C	C/C	T/C
239	3	M	Not performed	No	No		C/C	C/C	C/C
244	2	M	FSGS	Yes*	Yes		C/C	C/C	T/C
252	17	M	MCNS	No	Yes		C/C	C/T	T/T

Patient no.	Age At Diagnosis	Gender	Renal Biopsy Finding	Poor Prognosis	Steroid Resistant	*TRPC6*	*NPHS1*		*NPHS2*
						c.-254C>G	c.294C>T (I98I)	c.2289C>T (T763T)	c.954T>C (A318A)
253	4	M	MCNS	No	Yes		C/T	C/T	T/C
254	11	M	MCNS	No	Yes		T/T	T/T	T/C
255	11	M	FMPGN	No	No		C/C	C/C	T/C

FGS: Focal global glomerulosclerosis. FMPGN: Focal mesangial proliferative glomerulonephritis.
FSGS: Focal segmental glomerulonephritis.GN: Glomerulonephritis. MCNS: Minimal change nephrotic syndrome.
*Patient progressed to end-stage renal disease. **Patient is resistant to calcineurin inhibitor.

Appendix I-2 Normalized inward and outward currents of cells transfected with WT or mutant *TRPC6

***TRPC6* WT** (19)		**R68W** (18)		**R895C** (14)	
I_{inward}	$I_{outward}$	I_{inward}	$I_{outward}$	I_{inward}	$I_{outward}$
-245.51	397.69	-588.47	714.12	-1384.07	1534.27
-149.19	430.54	-490.07	2417.63	-953.14	1496
-275.65	395.16	-629.14	992.09	-1004.02	970.63
-310.67	692.31	-697.43	1157.27	-1225.96	2073.64
-202.4	396.77	-663.02	1226.33	-963.04	1880.83
-403.99	790.41	-387.36	725.1	-781.13	581.84
-636.28	742.27	-342.49	633.75	-693.17	955.53
-293.01	651.95	-569.3	1097.83	-1165.58	1140.07
-240.89	1074.06	-262.63	586.3	-1454.78	2202.89
-349.4	396.41	-548.18	1430.52	-1091.93	951.35
-298.53	681.1	-771.4	1699.52	-1583.02	960.03
-268.69	974.36	-246.75	497.14	-817.76	2003.48
-544.19	536.5	-687.6	726.2	-501.62	913.99
-594.38	732.81	-576.56	1255.17	-1726.88	838.43
-315.25	435.83	-812.69	545.3		
-251.99	539.69	-323.4	1348.24		
-226.82	361.83	-678.16	844.81		
-277.09	911.87	-460.67	1251.92		
-373.08	693.74				

*: The recording protocol used was voltage-ramp

The numbers in the brackets are the cell numbers recorded.

$I_{inward:}$ the peak of inward current; $I_{outward:}$ the peak of outward current.

Appendix I-3 Normalized current changes of cells transfected with *TRPC6* and/or NPHS1*

TRPC6	WT	WT	R68W	R68W
NPHS1	-	WT	-	WT
	31.53	8.94	32.77	15.49
	21.68	15.01	47.45	36.98
	55.49	17.05	64.3	12.15
	50.54	27.51	29.23	16.55
	19.77	16.81	52.93	32.7
	35.97	15.48	65.4	25.72
	28.13	11.07	50.02	45.8
	20.75	22.55	45.51	32.29
	54.19	31.69		22.81
		54.13		32.54
		19.32		35.58
				47.94
				29.83
				30.9
				20.28
				46.4

*: Current changes are the differences before and after activation of *TRPC6* channels by CCH. The protocol used for this cotransfection and the following cotransfections was gap-free.

Appendix I-4 Normalized current changes for the measurement of the effects of NPHS1 SNPs on *TRPC6*

TRPC6	WT	WT	WT	R68W	R68W	R68W	R68W
NPHS1	WT	294C>T	2289C>T	WT	294C>T	2289C>T	294C>T + 2289C>T
	8.94	15.07	29.83	22.35	51.93	50.44	107.39
	15.01	17.41	25.26	52.28	53.58	53.9	44.82
	17.05	29.65	35.51	28.74	53.28	25.85	42.9
	27.51	37.5	31.77	24.9	68.48	50.53	41.36
	16.81	68.67	34.98	41.66	55.28	77.35	47.08
	15.48	34.61	48.68	21.67	38.74	22.7	26.4
	11.07	49.09	32.39	40.55	84.55	55.13	57.03
	22.55	64.52	31.54	27.17	43	55.35	33.31
	31.69	24.31	24.21	29.71	31.99	29.44	80.59
	54.13	38.86	14.87	24.92	30.17	22.66	43.25
	19.32	21.59	23.94	26.87	33.5	57.72	40.4
	23.73		15.45	71.39	47.81	46.25	51.93
	26.59		30.96	29.42	42.07	21.03	43.68
	32.8		29.99	55.12	35.28		38.9
	22.46				28.07		61.72
	21.89				51.28		
	22.66						
	14.83						
	23.73						
	26.59						

Appendix I-5 Normalized current changes for the measurement of the effects of NPHS2 SNPs on *TRPC6*

TRPC6	WT	WT	WT	R68W	R68W
NPHS2	-	WT	954T>C	WT	954T>C
	31.53	18.30	13.77	18.53	39.53
	21.68	24.57	23.14	17.49	23.12
	19.77	21.59	16.04	13.48	16.35
	35.97	25.43	16.65	20.88	14.01
	28.13	21.51	15.30	39.15	22.89
	20.75	13.88	17.53	29.42	15.94
	15.78	16.04	16.73	21.17	15.14
	15.82	11.64	18.35	27.13	17.48
	16.96	9.72	21.78	25.77	19.78
	17.13	8.16	19.19		19.23
	14.90	10.16	15.94		20.73
	18.49	8.76			27.52
	23.53	6.72			32.15

Appendix I-6 Normalized current changes of selected index family members*

Control	III.3	II.3/5	II.2	I.1/III.4	III.3	II.4/III.2
8.94	28.52	26.79	22.35	30.28	36.32	107.39
15.01	11.95	19.96	52.28	65.5	49.79	44.82
17.05	35.77	25.36	28.74	23.94	66.19	42.9
27.51	27.07	16.31	24.9	28.9	62.85	41.36
16.81	22.38	46.2	41.66	54.51	33.93	47.08
15.48	40.53	25.3	21.67	73.49	23.68	26.4
11.07	22.47	24.7	40.55	61.67	78.28	57.03
22.55	17.19	22.65	27.17	60.94	44.01	33.31
31.69	33.3	25.71	29.71	38.71	31.08	80.59
54.13	29.17	30.87	24.92	23.74	62.57	43.25
19.32			26.87	32.66	43.06	40.4
23.73			71.39	41.61	68.74	51.93
26.59			29.42	29.02	42.53	43.68
32.8			55.12	45.97	31.47	38.9
22.46				42.59	55.53	61.72
21.89				45.61	38	
22.66					28.46	
14.83					34.68	
23.73						
26.59						

*:The genotypes of *TRPC6* and *NPHS1* in the selected index patient family members were represented in HEK-M1 cells by combining equal amount of *NPHS1* cDNA with different *NPHS1* variations. For example, to achieve the genotype of patient III.3, who had proteinuria and had homozygous *NPHS2* c.294TT and heterozygous c.2289CT, one set of *NPHS1* cDNA with single homozygous c.294TT and another set with double homozygous c.294TT and c.2289TT were combined. Currents were then recorded by cotransfection of WT or mutant *TRPC6* and this combined *NPHS1* cDNA.

Appendix I-7 Normalized band densities of nephrin expression and *TRPC6* surface expression

	Gene variations	Band densities			
Nephrin* expression	WT	0.86	1.22	1.25	0.93
	c.294C>T	-	0.61	0.40	0.70
	c.2289C>T	0.72	0.95	0.70	0.95
	double SNPs[#]	0.45	0.32	0.41	0.74
***TRPC6* surface expression^**	negative ctrl	0.01	0.04	0.10	
	WT	1.00	1.00	1.00	
	R68W	2.96	1.83	3.14	
	P112Q	2.99	3.81	-	

*: The band densities were normalized to GFP

^: *TRPC6* surface band densities were normalized to total protein extracted.

#: double SNPs means that the nephrin cDNA contains two homozygous c.294C>T and c.2289C>T SNPs.

Appendix I-8 Sample trace of real-time PCR of nephrin before and after stimulation with actinomycin D

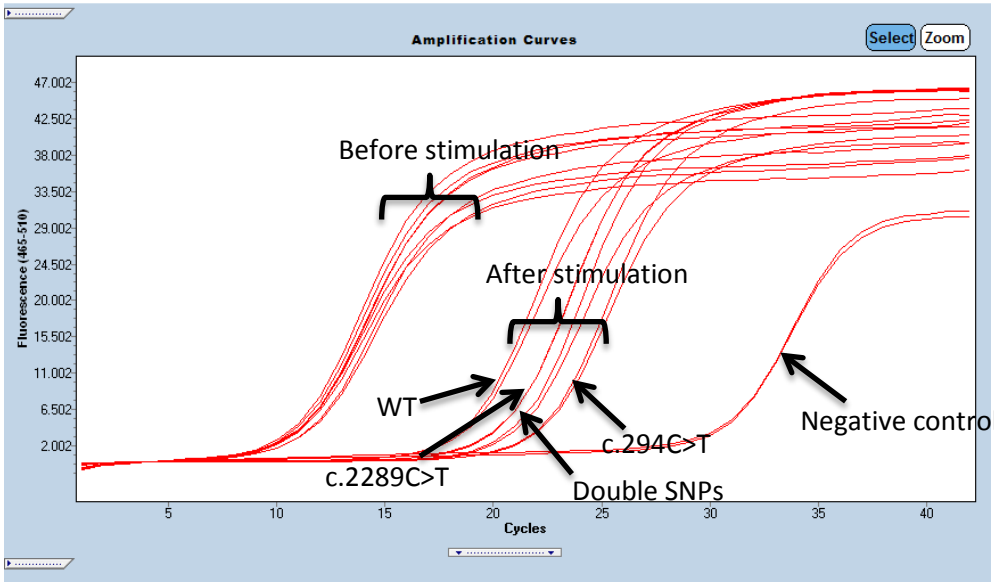

Appendix I-9 Raw data of real-time PCR of nephrin and analysis

Batches	Stimulations	Nephrin variations	GAPDH	Nephrin	ΔCt	ΔΔCt (after-before)	2^(-ΔΔCt)
1	Before stimulation	WT	14.65	10.87	-3.78	0	1.0000
		294	14.84	10.56	-4.28	0	1.0000
		2289	14.89	9.99	-4.9	0	1.0000
		double SNPs	15.05	9.11	-5.94	0	1.0000
	after stimulation	WT	15.23	13.94	-1.29	2.49	**0.1780**
		294	15.38	15.49	0.11	4.39	**0.0477**
		2289	15.26	12.63	-2.63	2.27	**0.2073**
		double SNP	15.2	13.16	-2.04	3.9	**0.0670**
2	Before stimulation	WT	14.76	9.87	-4.89	0	1.0000
		294	14.76	9.97	-4.79	0	1.0000
		2289	14.63	9.71	-4.92	0	1.0000
		double SNP	14.74	9.69	-5.05	0	1.0000
	after stimulation	WT	15.08	12.86	-2.22	2.67	**0.1571**
		294	16.49	21.00	4.51	9.30	**0.0016**
		2289	16.41	19.89	3.48	8.40	**0.0030**
		double SNP	15.73	19.37	3.64	8.69	**0.0024**
3	Before stimulation	WT	15.03	11.32	-3.71	0	1.0000
		294	14.88	9.22	-5.66	0	1.0000
		2289	14.94	9.12	-5.82	0	1.0000
		double SNP	14.96	9.09	-5.87	0	1.0000
	after stimulation	WT	15.06	13.28	-1.78	1.93	**0.2624**

Batches	Stimulations	Nephrin variations	GAPDH	Nephrin	ΔCt	ΔΔCt (after-before)	2^(-ΔΔCt)
		294	15.49	17.48	1.99	7.65	**0.0050**
		2289	14.93	13.61	-1.32	4.50	**0.0442**
		double SNP	15.52	12.73	-2.79	3.08	**0.1183**
4	Before stimulation	WT	15.03	10.47	-4.56	0	1.0000
		294	14.95	10.2	-4.75	0	1.0000
		2289	14.91	10.26	-4.65	0	1.0000
		double SNP	14.83	10.05	-4.78	0	1.0000
	after stimulation	WT	14.92	13.44	-1.48	3.08	**0.1183**
		294	15.81	19.17	3.36	8.11	**0.0036**
		2289	15.48	18.70	3.22	7.87	**0.0043**
		double SNP	15.55	16.85	1.30	6.08	**0.0148**

Appendix II-1 Sodium acetate-ethanol precipitation of DNA after cycle sequencing

Description:

The extension products were precipitated and purified by an ethanol/sodium acetate precipitation procedure.

Procedures:

1. For each sequencing reaction, prepare a 1.5 mL microcentrifuge tube containing 2 μl of 3 M sodium acetate (NaOAc), pH 4.6 and 50 μl of 95% ethanol.
2. Pipette the entire contents of each extension reaction into a tube of sodium acetate/ethanol mixture. Mix thoroughly.
3. Vortex the tubes and place on ice for 10 minutes to precipitate the extension products.
4. Spin the tubes in a microcentrifuge for 20 minutes at 13000 rpm.
5. Carefully aspirate the supernatant with a pipette and discard.
6. Rinse the pellet with 250 μl of 70% ethanol.
7. Spin for five minutes in a microcentrifuge at 13000 rpm.
8. Carefully aspirate the supernatant and discard.
9. Dry the pellet (but not over-dry).

(Reference: PE Applied Biosystems. ABI Prism™ BigDye® v3.1 cycle sequencing kit instruction manual)

Appendix II-2 First strand cDNA synthesis using SuperScript™ III Reverse Transcriptase

Description:

SuperScript™ III Reverse Transcriptase is an engineered version of M-MLV RT with reduced RNase H activity and increased thermal stability. The enzyme can be used to synthesize first-strand cDNA at temperatures up to 55°C, providing increased specificity, higher yields of cDNA, and more fulllength product than other reverse transcriptases.

Procedures:

1. Add the following components to a nuclease-free microcentrifuge tube:

   oligo(dT)20 (50 µM) 1 µL

   total RNA 1µg

   10 mM dNTP Mix 1 µL

   Sterile, distilled water to 13 µL

2. Heat mixture to 65°C for 5 minutes and incubate on ice for at least 1 minute.
3. Collect the contents of the tube by brief centrifugation and add:

   5X First-Strand Buffer 4 µL

   0.1 M DTT 1 µL

   RNaseOUT™ Recombinant RNase Inhibitor 1 µL

   SuperScript™ III RT (200 units/µl) 1 µL

4. Mix by pipetting gently up and down.
5. Incubate at 50°C for 30–60 minutes.
6. Inactivate the reaction by heating at 70°C for 15 minutes.

7. Add 1 µL (2 units) of E. coli RNase H and incubate at 37°C for 20 minutes to remove RNA complementary to the cDNA. The cDNA can thenbe used as a template for amplification in PCR.

(Reference: Invitrogen SuperScript™ III Reverse Transcriptase handbook.)

Appendix II-3 Gel extraction and purification of DNA

Description:

Gel extraction and purification of DNA was carried out using the Qiagen QIAquick gel extraction kit. Protocol of this kit is designed to extract and purify DNA of 70 bp to 10 kb from standard or low-melt agarose gels in TBE buffer. Up to 400 mg agarose can be processed per spin column.

Procedures:

1. Excise the DNA fragment from the agarose gel with a clean, sharp scalpel with the aid of a UV illuminator and weigh the gel slice.
2. Add 3 volumes of buffer QG to 1 volume of gel.
3. Incubate at 50^{o}C for 10 minutes. Mix by vortexing the tube every 2-3 minutes during the incubation until the gel slice has completely dissolved.
4. Add 1 gel volume of isopropanol to the sample and mix.
5. Place a QIAquick spin column in a 2 mL collection tube.
6. To bind DNA, apply the sample to the QIAquick column, and centrifuge for 1 minute.
7. Discard flow-through and place QIAquick column back in the same collection tube.
8. Add 0.5 mL of buffer QG to QIAquick column and centrifuge for 1 minute. Discard flow-through.
9. To wash, add 0.75 mL of buffer PE to QIAquick column and centrifuge for 1 minute.

10. Discard flow-through and centrifuge the QIAquick column for an additional 1 minute at ≥ 10000 x *g* or 13000 rpm.
11. Place the QIAquick column into a clean 1.5 mL microcentrifuge tube.
12. To elute DNA, add 50 µl of buffer EB (10 mM Tris-Cl, pH 8.5) or ddH_2O to the centre of the QIAquick membrane and centrifuge the column for 1 minute at maximum speed.

(Reference: Qiagen QIAquick® spin handbook.)

Appendix II-4 DNA Ligation and Transformation into *E. coli*

Description:

T4 DNA ligase (NEB) Catalyzes the formation of a phosphodiester bond between juxtaposed 5' phosphate and 3' hydroxyl termini in duplex DNA or RNA. This enzyme will join blunt end and cohesive end termini as well as repair single stranded nicks in duplex DNA, RNA or DNA/RNA hybrids. One Shot® TOP10 Chemically Competent E. coli (Invitrogen) are provided at a high transformation efficiency of 1 x 109 cfu/μg supercoiled DNA and are ideal for high-efficiency cloning and plasmid propagation.

Procedures:

1. 10ng of the gel-purified desired PCR fragment (genes of interest) is ligated with commercial vector. The insert to vector molar ratio is 1:3 to 1:5. The DNA ligase reaction is set up in the following mixture:

Purified insert	10 ng
Vector	According to their molar ratio
Ligase 10x buffer	1 μL
T4 DNA ligase (NEB)	1 μL
Nuclease-free water to final volume of	10 μL

2. The ligation mixture is incubated at room temperature for 1-2 hours or 4°C for overnight.
3. Subsequently, 10 μL of the ligation mixture is added to one vial of One Shot® Chemically Competent TOP10 E. coli (Invitrogen) and incubated on ice for 30 minutes.

4. The cells were then subjected to heat shock at 42°C for 30 seconds and incubated on ice for 5 minutes.
5. Add 250 µl of SOC medium to the transformed *E. coli* and incubate for 1 hour at 37^{o}C with shaking at 230 rpm.
6. Spread 100 µl of the incubation mixture onto a LB (Luria-Bertani) plate containing the appropriate selective antibiotics.
7. Incubate the LB plates at 37^{o}C overnight.
8. Single colonies are selected the next day and incubated overnight in 2mL of LB medium with antibiotics at 37^{o}C with agitation at 230 rpm. Plasmid DNA was then extracted using QIAprep Spin Miniprep kit (Qiagen).

Appendix II-5 Extraction and purification of plasmid DNA using Qiagen QIAprep Spin Miniprep kit

Description:

Small scale extraction and purification of plasmid DNA are carried out using the QIAprep Spin Miniprep kit from Qiagen). The QIAprep miniprep procedure is based on alkaline lysis of bacterial cells followed by adsorption of DNA onto silica in the presence of high salt. The procedures consist of three basic steps: preparation and clearing of a bacterial lysate, adsorption of DNA onto the QIAprep membrane, washing and elution of plasmid DNA. The last 2 basic steps are performed on a spin column.

Procedures:

1. Centrifuge overnight bacterial culture at 3500 rpm for 10 minutes.
2. Resuspend pelleted bacterial cells in 250 μL of Buffer P1 and transfer to a microcentrifuge tube. (Ensure that Rnase A has been added to Buffer P1. No cell clumps should be visible after resuspension of the pellet.)
3. Add 250 μL of Buffer P2 and gently invert the tube 4-6 times to mix. (Mix gently by inverting the tube. Do not vortex, as this will result in shearing of genomic DNA. If necessary, continue inverting the tube until the solution becomes viscous and slightly clear. Do not allow the lysis reaction to proceed for more than 5 minutes.)
4. Add 350 μL of Buffer N3 and invert the tube immediately but gently 4-6 times. (To avoid localized precipitation, mix the solution gently but thoroughly, immediately after addition of Buffer N3. The solution should become cloudy.)

5. Centrifuge for 10 minutes. (A compact white pellet will form.) During centrifugation, place a QIAprep spin column in a 2 mL collection tube.
6. Apply the supernatants from step 4 to the QIAprep column by decanting or pipetting.
7. Centrifuge 30-60 seconds. Discard the flow-through.
8. (Optional): Wash QIAprep spin column by adding 0.5 mL of Buffer PB and centrifuging 30-60 seconds. Discard the flow-through. This step is necessary to remove trace nuclease activity when using $endA^+$ strains such as the JM series, HB101 and its derivatives, or any wild-type strain, which have high levels of nuclease activity or high carbohydrate content. Host strains such as XL-1 Blue and DH5α^{TM} do not require this additional wash step.
9. Wash QIAprep spin column by adding 0.75 mL of Buffer PE and centrifuging 30-60 seconds.
10. Discard the flow-through, and centrifuge for an additional 1 minute to remove residual wash buffer.
11. Place QIAprep column in a clean 1.5 mL microcentrifuge tube. To elute DNA, add 50 μL of Buffer EB (10 mM Tris-Cl, pH 8.5) or H_2O to the center of each QIAprep column, let stand for 1 minute, and centrifuge for 1 minute.

(Reference: QIAprep Miniprep Handbook July 1999 page 18-19)

Appendix II-6 Extraction and purification of plasmid DNA using QIAGEN Plasmid Midi kit

Description:

QIAGEN plasmid extraction and purification are based on a modified alkaline lysis procedure, followed by binding of plasmid DNA to QIAGEN resin under appropriate low-salt and pH conditions. RNA, proteins, dyes, and low-molecular–weight impurities are removed by a medium-salt wash. Plasmid DNA is eluted in a high-salt buffer and then concentrated and desalted by isopropanol precipitation.

Procedures:

1. Harvest bacteria by centrifugation at 6000 rpm for 15 minutes at 4^{o}C.
2. Resuspend the bacterial pellet in 8 mL Buffer P1.
3. Add 8 mL Buffer P2, mix thoroughly by vigorously inverting the sealed tube 4–6 times, and incubate at room temperature (15–25°C) for 5 minutes.
4. Add 8 mL of chilled Buffer P3, mix immediately and thoroughly by vigorously inverting 4–6 times, and incubate on ice for 20 minutes.
5. Centrifuge at ≥20,000 x g for 30 minutes at 4°C. Remove supernatant containing plasmid DNA promptly.
6. Centrifuge the supernatant again at ≥20,000 x g for 15 minutes at 4°C. Remove supernatant containing plasmid DNA promptly.
7. Equilibrate a QIAGEN-tip 100 by applying 10 mL Buffer QBT, and allow the column to empty by gravity flow.
8. Apply the supernatant from step 6 to the QIAGEN-tip and allow it to enter the resin by gravity flow.

9. Wash the QIAGEN-tip with 2 x 10 mL Buffer QC.
10. Elute DNA with 5 mL Buffer QF.
11. Precipitate DNA by adding 3.5 mL (0.7 volumes) room-temperature isopropanol to the eluted DNA. Mix and centrifuge immediately at ≥15,000 x g for 30 minutes at 4°C. Carefully decant the supernatant.
12. Wash DNA pellet with 2 mL of room-temperature 70% ethanol, and centrifuge at ≥15,000 x g for 10 minutes. Carefully decant the supernatant without disturbing the pellet.
13. Air-dry the pellet for 5–10minutes, and redissolve the DNA in a suitable volume of buffer (e.g., TE buffer, pH 8.0, or 10 mM Tris·Cl, pH 8.5).

(Reference: QIAGEN® Plasmid Purification Handbook April 2012 page 17-21)

Appendix II-7 QuikChange Site-Directed Mutagenesis Kit

Description:

The QuikChange site-directed mutagenesis kit is used to make point mutations, switch amino acids, and delete or insert single or multiple amino acids. This rapid four-step procedure generates mutants with greater than 80% efficiency.

Procedures:

1. Design forward and reverse mutagenic primers according to the guidelines. 1) Both primers must contain the desired mutation and anneal to the same sequence on opposite strands of the plasmid. 2) Primers should be between 25 and 45 bases in length, with a melting temperature (*T*m) of ≥78°C. 3) The desired mutation (deletion or insertion) should be in the middle of the primer with ~10–15 bases of correct sequence on both sides. 4) The primers optimally should have a minimum GC content of 40% and should terminate in one or more C or G bases.
2. Prepare the mutant Strand Synthesis reaction using *PfuTurbo* DNA polymerase as follows:

   5 μL of 10× reaction buffer
   X μL (5–50 ng) of dsDNA template
   X μL (125 ng) of oligonucleotide primer #1
   X μL (125 ng) of oligonucleotide primer #2
   1 μL of dNTP mix
   ddH_2O to a final volume of 50 μL
   Then add
   1 μL of *PfuTurbo* DNA polymerase (2.5 U/μL)

And perform amplification using the following Cycling Parameters:

Segment	Cycles	Temperature	Time
1	1	95^0C	30 seconds
2	16	95^0C	30 seconds
		55^0C	1 minute
		68^0C	1 minute/kb of plasmid length

3. Take 10 μL of the PCR production to check by electrophoresis.
4. Add 1 μL of the *Dpn* I restriction enzyme (10 U/μl) directly to the amplification reaction (40 μL) below the mineral oil overlay using a small, pointed pipet tip.
5. Gently and thoroughly mix each reaction mixture by pipetting the solution up and down several times. Spin down the reaction mixtures in a microcentrifuge for 1 minute and immediately incubate each reaction at 37°C for 1 hour to digest the parental (i.e., the nonmutated) supercoiled dsDNA.
6. Transfer 1 μL of the *Dpn* I-treated DNA to separate aliquots of the supercompetent cells followed by heat-shock transformation.

(Reference: QuikChange Site-Directed Mutagenesis Kit Instruction Manual, 200518-12)

Appendix II-8 DNA transfection using calcium phosphate precipitation method

Description:

The Calcium Phosphate Transfection method for introducing DNA into mammalian cells is based on forming a calcium phosphate-DNA precipitate. Calcium phosphate facilitates the binding of the DNA to the cell surface. DNA then enters the cell by endocytosis. The procedure is routinely used to transfect a wide variety of cell types for transient expression or for producing stable transformants.

Procedures:

(1) One day before transfection (Day 0), split HEK293 cells into 35mm petri dishes with 2 mL DMEM growth medium containing 10% FBS and 1% pen-strep.

(2) The next day (Day 1), aspirate all growth medium from Petri dish with cells, replace with new DMEM with 10% FBS. Do not include antibiotics in the medium.

(3) Pipette 75 µl 1M $CaCl_2$ in 1.5mL tube.

(4) Add 1 ug plasmid DNA. Mix gently.

(5) Add 75 µL 2× 2X Hepes Buffered Saline (HBS) (Appendix III) drop by drop. Mix gently.

(6) Incubate the transfection complexes 20 minutes.

(7) Add transfection complexes into the Petri dish drop by drop. Mix gently by rocking the dish back and forth.

(8) 4-6 hours later, remove and discard the medium containing calcium phosphate-DNA complexes and replace it with 2 mL of growth medium without pen-strep.

Incubate the cells for 24-48 hours at 37^0C in a humidified 5% CO_2 until they are ready for further analysis (for example, patch clamp recording).

Appendix II-9 Western blot

Description:

Western blot is an extremely useful analytical technique used to detect specific proteins in cell lysate, tissue homogenate or extract. It uses gel electrophoresis to separate native or denatured proteins. The proteins are then transferred to a membrane (typically nitrocellulose or PVDF), where they are detected using antibodies specific to the target protein.

Procedures:

A. Preparation of polyacrylamide gel

1. Clean the spacer glass plate, short glass plate and combs with 70% ethanol and allow them to dry completely. Assemble the gel preparation glass plates as instructed (Figure 1).
2. Prepare the resolving gel mixture according to the table below.
3. Pipette the resolving gel mixture immediately into the space formed by the glass plates.
4. Add 200 µL of distilled water slowly along the side of the glass plate to avoid exposure to air and create a smooth edge.
5. Allow the gel to polymerize for 30 minutes at room temperature.
6. Prepare the stacking gel mixture according to the table below.
7. When the polymerization of the resolving gel is completed, remove the water. Use Kim wipes to absorb. Take care not to touch the surface of the resolving gel.
8. Pipette the stacking gel mixture immediately onto the resolving gel.

9. Carefully place a comb between the glass plates. Do not allow bubbles trapped between the comb and the stacking gel.
10. Allow the stacking gel to polymerize for at least 15 minutes.
11. Remove the comb carefully after the stacking gel is set.

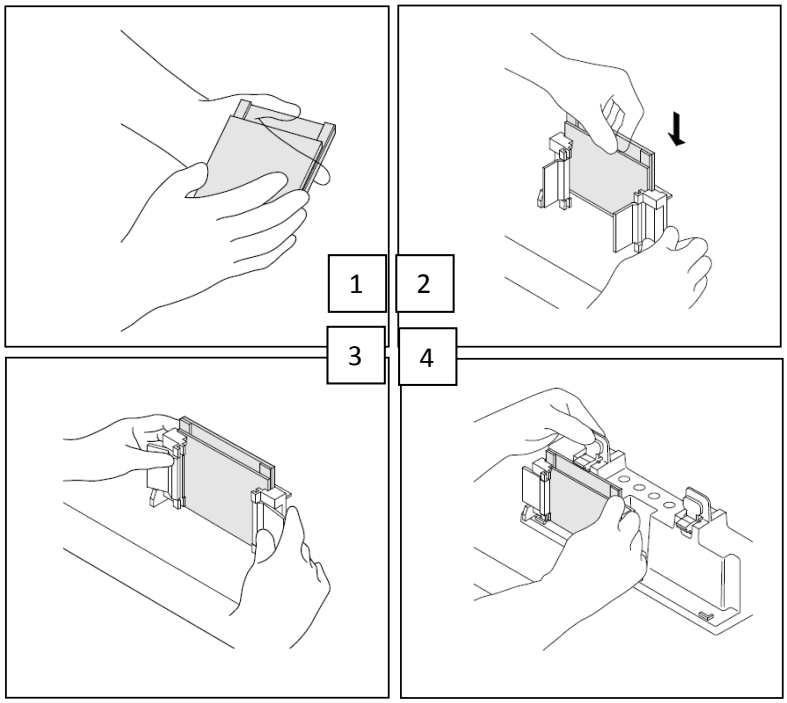

Figure 1 Gel cassette preparation and assembly. A. Place a Short Plate on top of the Spacer Plate. B. Slide the two plates into the Casting Frame, keeping the Short Plate facing front. Insure both plates are flush at the bottom on a level surface. C. Lock the pressure cams to secure the glass plates. D. Engage the spring loaded lever and place the gel cassette assembly on the gray casting stand gasket. Insure the horizontal ribs on the back of the Casting Frame are flush against the face of the Casting Stand and the glass

Table 1 Prepare resolving (10%) and stacking gel (5%).

Components	Resolving gel (10%)	Stacking gel (5%)
30% Acrlymide / Bis Solution	1.67 mL	0.42 mL
1.5M Tris pH 8.8	1.25 mL	
0.5M Tris pH 6.8		0.31 mL
Water	1.98 mL	1.70 mL
10% SDS	50 µL	25 µL
10% Ammonium persulfate	50 µL	25 µL
TEMED	2 µL	2.5 µL
Total volume	5 mL	2.4825 mL

B. Sample preparation and electrophoresis

1. Mini Protean 3 Electrophoresis Assembly (Figure 2).
2. Dilute protein samples (20 µg) 1:1 with Laemmli Sample buffer (add 50 µl of β-mercaptoethanol to 950 µl of Laemmli Sample Buffer).
3. Heat the samples at 95^{o}C for 20 minutes in a pre-heated heating block. Put back into ice.
4. Carefully load the sample into the wells of the polyacrylamide gel. Include protein marker if necessary.
5. Run the gel in 1X SDS/glycine electrophoresis buffer at 100V for 2 hours or until the dye front reaches the bottom of the gel.

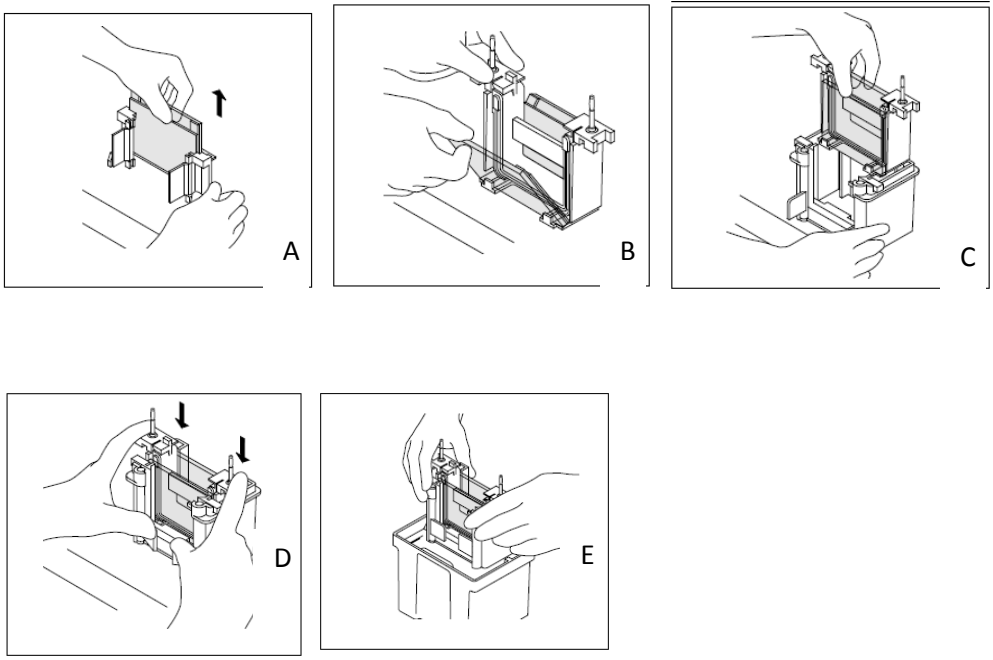

Figure 2 Gel cassette preparation and assembly. A. Remove the Gel Cassette Sandwich from the Casting Frame. B. Place the Gel Cassette Sandwich into the Electrode Assembly with the Short Plate facing inward. C. Slide Gel Cassette Sandwiches and Electrode Assembly into the clamping frame. D. Press down the Electrode Assembly while closing the two cam levers of the Clamping Frame. E. Lower the Inner Chamber into the Mini Tank. (Adapted from MINI-PROTEAN® 3 Electrophoresis Module Assembly)

C. Gel Removal

1. After electrophoresis is completed, pour out the running buffer and open the cams of the clamping frame. Pull out the electrode assembly out of the clamping frame and remove the gel cassette sandwiches.
2. Using the gel releaser, pry the glass plates apart. Run the gel releaser on each side of the spacer plate to separate the gel form the spacer plate.
3. Remove the gel by floating it off the glass plate by inverting the plate and gel onto a filter paper that was soaked in transfer buffer.

D. Assembly of gel/blot transfer

1. Using forceps overlay a piece of membrane (nitrocellulose / PVDF) onto the gel taking care not to trap any bubbles. Ensure the membrane get wet completely.
2. Overlay membrane with a piece of filter paper and using a roller, run it gently across the filter paper top to remove any bubbles that are trapped inside the sandwich.
3. Place a cassette with the black side down on a clean surface.
4. Place a fiber pad (pre-soaked in transfer buffer) onto the black side of the cassette.
5. Place the gel membrane sandwich (from step 7.6.2) onto the fiber pad.
6. Place another fiber pad onto of the sandwich and close the cassette firmly being careful not to move the gel membrane sandwich.
7. Lock the close cassette with the white latch. Slide the cassette into the electrode module with the black side of the cassette facing the red side on module.
8. Place the electrode module into a blotting tank and fill the tank up with chilled transfer buffer.
9. Place a stirrer bar into the tank and placed blotting tank onto a stirrer plate. Set the speed at high so as to maintain even buffer temperature and ion distribution in the tank.
10. Put the lid on, plug cables to the power supply and run the blot. Transfer at 100V for 2 hours or 30V overnight at 4^{o}C with stirring.
11. Refer to Figure 3 for setup diagram.

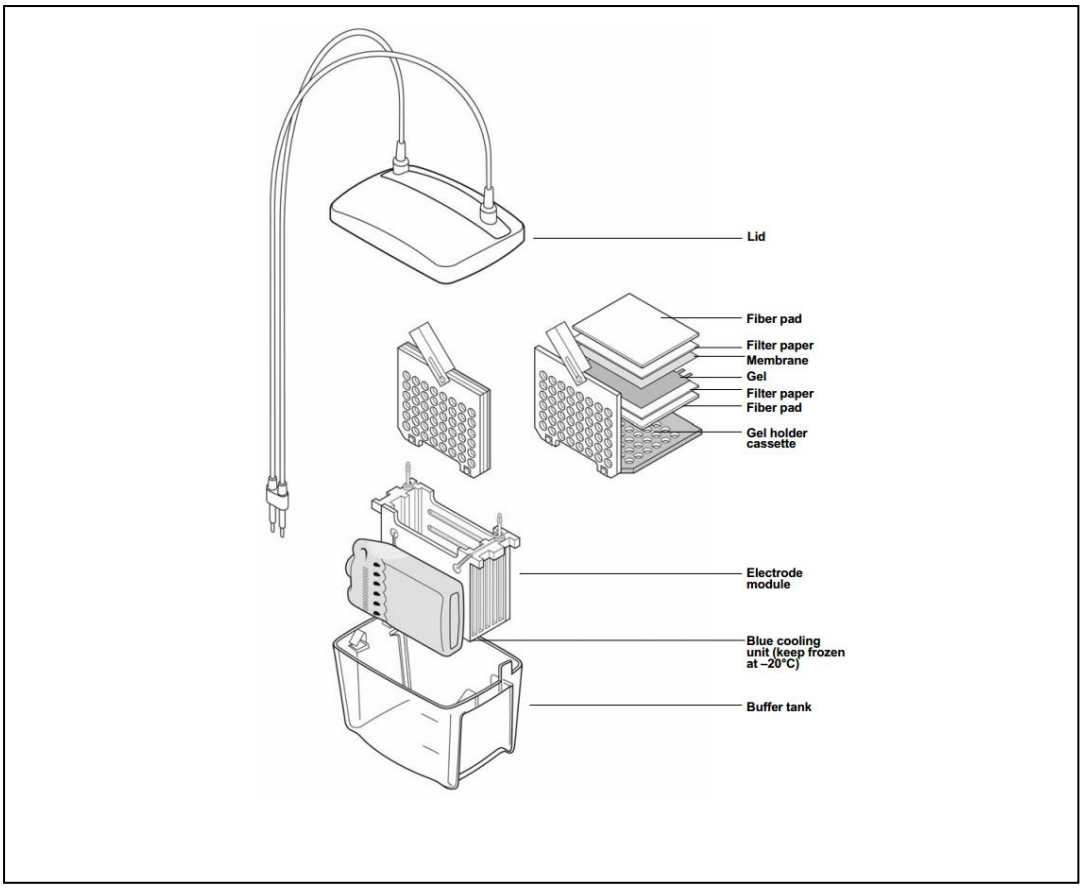

E. Blot Development

1. Stain the membrane with Ponceus S solution for 5 minutes to detect transferred protein on the membrane. Also mark the individual lanes.
2. De-stain the membrane in water for 5 minutes.
3. Wash the membrane in TBS for 5 minutes.
4. Block the membrane in 5% milk for 1 hour with gentle rocking on the labnet rocker.
5. After blocking, wash the membrane 3X in TBS-T, 10 minutes per wash.
6. Dilute primary antibodies in TBS with 0.5 % BSA. Refer to table 1 in Annex A for working dilutions.
7. Add primary antibody to membrane and allow to rock for 30 minutes. Then Incubate membrane overnight at 4^{o}C.
8. Wash membrane 2 X in TBS-T, 10 minutes per wash.

9. Wash membrane 1X with TBS before adding in secondary antibody.
10. Dilute the secondary antibody in 2.5% milk and add to the membrane. Refer to table 2 in Annex A for working dilutions.
11. Incubate the membrane with secondary antibody for 1 hour with gentle rocking.
12. After secondary antibody incubation, wash membrane 6X with TBS-T, 10 minutes per wash.
13. Wash membrane 1X in TBS for 10 minutes.
14. Transfer membrane to 5 ml of Luminata™ Forte Western HRP Substrate and incubate for 3-5 minutes in the dark.
15. Remove membrane from HRP substrate, drain off excess solution. Cover membrane in clear plastic sheet protector.
16. Expose membrane to X-ray film with the required exposure timing.

(Reference: Bio-Rad Mini Protean 3 Instruction Manual
Mini Trans-Blot Electrophoretic Transfer Cell Instruction Manual)

Appendix II-10 Total RNA extraction from HEK cells by TRIzol® reagent

Description:

Total RNA from transfected or untransfected HEK cells was extracted using TRIzol® reagent (Invitrogen). During sample homogenization or lysis, TRIzol® reagent maintains the integrity of the RNA, while disrupting cells and dissolving cell components. Addition of chloroform followed by centrifugation separates the solution into an aqueous phase and an organic phase. RNA remains exclusively in the aqueous phase. After transfer of the aqueous phase, the RNA is recovered by precipitation with isopropyl alcohol. Specifically, the following steps were carried out for 6-well multiple well microplate.

Procedures:

1. Cells are washed once with cold 1 X PBS. Lyse cells directly in the wells by adding 0.5 mL of TRIzol® reagent, and passing the cell lysate several times through a pipette. The amount of TRIzol® reagent added is based on the area of the culture dish (1 mL per 10 cm^2) and not on the number of cells present. An insufficient amount of TRIzol® reagent may result in contamination of the isolated RNA with DNA.
2. Transfer cell lysis to DEPC-treated 1.5mL tubes and store in -80^oC freezer if not immediately isolate total RNA.
3. Before isolation, take out samples that were suspended in TRIzol reagent from -80^oC freezer. Allow them to thaw to room temperature.
4. Add 100 µL of chloroform. Cap and shake vigorously for 15 seconds. Incubate tubes for 5 minutes at room temperature.

5. Centrifuge samples at a 12,000g (7500 rpm) for 15 minutes at 4^{o}C.

6. After centrifugation, samples should separate into a lower red phase (phenol-chloroform), a white interphase (DNA), and a clear top phase. RNA will be contained in the colorless aqueous phase.
7. Transfer this aqueous phase to a new DEPC-tube. Add 250µl of isopropyl alcohol (to precipitate the RNA). Mix well and incubate at room temp for 10 minutes.
8. Centrifuge samples at 12,000g (7500 rpm) for 10 minutes at 4^{o}C, to pellet the precipitated RNA.
9. Carefully remove supernatant and add 0.5 mL of 75% cold ethanol (diluted with DEPC water) to wash the RNA.
10. Centrifuge samples at 7500g (5800 rpm) for 5 minutes at 4^{o}C.
11. Carefully remove supernatant with a pipette and air dry pellet for 5-10 minutes. Do not allow pellet to dry completely or else the RNA will be less soluble.
12. Re-suspend RNA in 35 µL nuclease free water and store at -80^{o}C.

Appendix II-11 Real-time PCR reaction on LightCycler® 480

Description:

Real-time PCR, also called quantitative real time polymerase chain reaction (qPCR) is used to amplify and simultaneously quantify a targeted DNA molecule through measuring the Cp (Crossing point) value of the PCR reaction. Cp value is measured during the exponential growth phase of a typical PCR reaction and is directly related to the amount of target in the sample.

Roche LightCycler supports two fluorescence-based methods for the detection of amplification products: DNA binding dye SYBR Green I and hybridization probes. The fluorescent dye SYBR Green I is the simplest and cheapest chemistry. It binds to the minor groove of the DNA double helix and fluoresces 1000 times brighter when bound than when unbound. The DNA binding results in a dramatic increase of the SYBR Green I molecules to emit light upon excitation. Fluorescence measurement was made at the end of the elongation step of every PCR cycle to monitor the increasing amount of amplified DNA. Therefore, comparing with traditional agarose gel electrophoresis, Real-time PCR need shorter time and the results are much more reliable and reproducible.

Procedures:

A. **Real-time PCR primer design**

   Designing primers is one of the most important steps of a real-time PCR experiment. There are several considerations when designing real-time PCR primers. The product should be short (200 to 300 bp is ideal for SYBR Green),

the two primers should have similar T_m, and the primers should have low or no self complementarity (to avoid primer dimers).

B. Setup of real-time PCR reaction

1. Prepare the reaction mixture for real-time PCR reaction on ice as follows:

Reaction Mixture	Stock concentration	Volume for 1 reaction
Roche Master	X2	5 µL
Forward Primer	10 µM	1 µL
Reverse Primer	10 µM	1 µL
PCR grade water		1µL
Template		2 µL
Total		10 µL

1. Prepare (n+1) numbers of master mix reactions. Pipette 8 µl of the reaction mixture into each well of a FrameStar® plate.
2. Add 2 µl of cDNA template sample.
3. Seal the plate with a PlateMax Ultra Clear permanent heat sealing film.
4. Centrifuge at 1000 rpm for 30 seconds.
5. Put the plate into the LightCycler PCR machine.
6. Run real-time PCR according to the following table.

Steps	Analysis mode	Cycles	Segment	Target temperature	Ramp rate (°C/s)	Hold time
Pre-incubation	None	1		95°C	4.4	10 min
Amplification	Quantification	42	Denaturation	95°C	4.4	5 s
			Annealing	60°C	2.2	10 s
			Extension	72°C	4.4	12s
Melting curve analysis	Melting curves	1	Denaturation	95°C	4.4	10 s
			Annealing	58°C	2.2	15 s
			Melting	95°C	0.11	0 s
Cooling	none	1		40°C	2.2	30 s

Appendix III Common reagent and buffers preparation

(1) LB(Luria-Bertani) Medium

Tryptone	10g
Yeast extract	5g
NaCl	10g
ddH2O	950mL

Adjust the pH of the solution to 7.0 with NaOH and bring volume to 1 liter.

Aotuclave at 121^0C for 20minutes at 15 psi.

(2) LB agar plates

LB medium	1L
Agar	15g

Autoclave at 121^0C for 20minutes at 15 psi.

After autoclaving, cool to about 56^0C, add antibiotics (ampicillin or Kanamycin) and pour into sterile petric dishes.

Let harden, then invert and store at 4^0C in dark.

(3) 1% agarose gel

Nusieve 3:1 ® agarose	1g
TBE buffer	100mL

Heat in microwave for 2 minutes to dissolve all powder.

Cool to 57^0C before casting gel.

Store at 4^0C.

(4) 10x Phosphate buffered saline (PBS)

NaCl	80 g
KCl	2 g
Na_2HPO_4	14.4 g
KH_2PO_4	2.4 g

Dissolve in 800 ml of double distilled water (ddH_2O), adjust pH to 7.4.

Adjust volume to 1 liter with ddH_2O.

Autoclave at 121^0C for 15 minutes.

(5) 1x PBS

10x PBS stock solution	100 ml
ddH_2O	900 ml

Sterile filter with 0.2 µm filter or autoclave if necessary.

(6) 0.1% diethyl pyrocarbonate (DEPC) treated H_2O

DEPC	1mL
ddH_2O	999mL

Shake vigorously to thoroughly mix the DEPC with solution.

Incubate overnight, autoclave at 121^0C for 15 minutes to destroy residual DEPC by causing hydrolysis of DEPC.

(7) 75% ethanol

Absolute ethanol	75mL

Make up with DEPC treated water to 100mL.

(8) Fetal Calf Serum

Heat inactivate at 56^0C for 30 minutes in a water bath.

Aliquot into 50mL tubes.

Store at -70^0C.

(9) TBE buffer (5X)

Tris base	10.8g
Boric acid	5.5g
0.5 M EDTA pH8.0	4mL

Make up to 1 liter with ddH_2O

Store at room temperature.

(10) Loading Dye

Bromophenol Blue	0.25g
Ficoll Type 400	25g

Reconstitute with 100 mL of sterile water.

Stir to dissolve.

Filter with 0.45 µm membrane.

Store at room temperature.

(11) 1XHanks' Balanced Salt solution (HBSS)

10X HBSS(Gibco BRL, cat.#14065-056)	10 mL
1 M Herpes	1 mL
Sodium bicarbonate solution (7.5% w/v)	5drops

Top up with sterile ddH_2O to 100 mL. Mix well and store at 4^0C.